Attenuation of VEGFR3 activity by intracellular versus extracellular mechanisms

Inaugural-Dissertation

zur Erlangung des Doktorgrades
der Mathematisch-Naturwissenschaftlichen Fakultät
der Heinrich-Heine-Universität Düsseldorf

vorgelegt von

Laura Sophie Hilger
aus Herdecke

Düsseldorf, November 2020

aus dem Institut für Stoffwechselphysiologie
der Heinrich-Heine-Universität Düsseldorf

Gedruckt mit der Genehmigung der
Mathematisch-Naturwissenschaftlichen Fakultät der
Heinrich-Heine-Universität Düsseldorf

Berichterstatter:

1. Prof. Dr. Eckhard Lammert

2. Prof. Dr. Axel Gödecke

Tag der mündlichen Prüfung: 15.03.2021

Table of content

I. Annotations to this thesis

Parts of this thesis have been published in ‘Identification of ILK as a critical regulator of VEGFR3 signalling and lymphatic vascular growth’ by Dr. Sofia Urner, Dr. Lara Planas-Paz, Laura Sophie Hilger et al. (Urner et al. 2019). Some figures in this thesis were adapted from and some of the presented experiments were performed by different authors of the mentioned article. Therefore, some results of this thesis are also to be found in Dr. Sofia Urner’s Dissertation with the title ‘Role of integrin-linked kinase (ILK) in VEGFR3 signaling and lymphatic vascular growth’ (Urner 2018a).

Parts of this thesis were adapted from results of the Master’s thesis presented by Laura Sophie Hilger, which was performed from 2016-2017 in the Institute of Metabolic Physiology under supervision by Prof. Dr. Eckhard Lammert.

The specific contributions to each figure are indicated in the respective figure legends.

II. List of abbreviations

A

AD	Alzheimer's disease
AF	Alexa Fluor
ANOVA	Analysis of variance
APP	Amyloid precursor protein

B

B2M	Beta-2-microglobulin
BACE	β-site of APP cleaving enzyme or β-secretase
BCA	Bicinchoninic acid
BrdU	5-bromo-2'-deoxyuridine
BSA	Bovine serum albumin

C

C3	β-Secretase Inhibitor IV
Ca^{2+}	Calcium
cDNA	Complementary DNA
CNS	Central nervous system
CSF	Cerebrospinal fluid
CO_2	Carbon dioxide

D

DAPI	4',6-Diamidino-2-Phenylindole
DMSO	Dimethyl sulfoxide
DNA	Deoxyribonucleic acid
DNER	Delta and notch-like epidermal growth factor-related receptor

E

E	Embryonic day
EBM-2	Endothelial cell basal medium
ECL	Enhanced Chemiluminescence
ECM	Extracellular matrix
EGM-2 MV	Endothelial cell growth factor medium MV2

F

FGFR1	Fibroblast growth factor receptor 1
Flk1	Fetal liver kinase 1
Flt1	Fms-like tyrosine kinase 1
Flt4	Fms-like tyrosine kinase 4
Fwd	Forward

G

GAPDH	Glyceraldehyde 3-phosphate dehydrogenase

H

h	Hour
H_2O	Water
HCl	Hydrogen chloride
HDLEC	Human dermal lymphatic endothelial cell
HEPES	4-(2-hydroxyethyl)-1-piperazineethanesulfonic acid
HEV	High endothelial venule
HMVEC-dLyAd	Human microvascular endothelial cell – dermal, lymphatic, adult
HPRT1	Hypoxanthine phosphoribosyltransferase
HRP	Horseradish peroxidase

I

IAPP	Islet amyloid polypeptide
IgG	Immunoglobulin G
ILK	Integrin-linked kinase
IPP	ILK/PINCH/parvin
ISF	Interstitial fluid

J

JH	Juxtamembrane helix
jls	Jugular lymph sac

K

K.D.	Knockdown
K.O.	Knockout

L

LECs	Lymphatic vascular endothelial cells
LEZ	Lymphatische Endothelzelle(n)
LSM	Laser scan microscopy

M

M	Molar
µg	Microgram
Mg^{2+}	Magnesium
Min	Minute
µM	Micromolar
mM	Millimolar
MOPS	3-(N-morpholino)propanesulfonic acid
mRNA	Messenger RNA

N

NaCl	Sodium chloride
NaF	Sodium fluoride
Na_3VO_4	Sodium orthovanadate
NDS	Normal donkey serum
ng	Nanogram
nM	Nanomolar

O

o/n	Over night

P

PBS	Phosphate-buffered saline
PCR	Polymerase chain reaction
PFA	Paraformaldehyde
PINCH	Particularly interesting new cysteine-histidine-rich protein
PLA	Proximity ligation assay
PLXDC2	Plexin domain containing 2
pTD	Primordial thoracic duct
p-Tyr	Phosphorylated tyrosine

R

rcf	Relative centrifugal force
Rev	Reverse
RNA	Ribonucleic acid
ROS	Reactive oxygen species
RPLP0	Ribosomal phosphoprotein P0
rpm	Revolutions per minute
RT	Room temperature
RTK	Receptor tyrosine kinase

S

Sec	Seconds
SEM	Standard error of the mean
siRNA	Silencing interfering RNA
SMCs	Smooth muscle cells

T

Tyr	Tyrosine

V

V	Volt
VCAM1	Vascular cell adhesion molecule 1
VEGF-C	Vascular Endothelial Growth Factor-C
VEGF-D	Vascular Endothelial Growth Factor-D
VEGFR2	Vascular Endothelial Growth Factor Receptor 2
VEGFR3	Vascular Endothelial Growth Factor Receptor 3
Vol	Volume

1. Summary

The lymphatic vascular system maintains the body's fluid homeostasis and accounts for brain drainage and detoxification. Due to its multiple functions, the lymphatic system is associated to pathologic conditions like lymphedema and cancer, but also to neurodegenerative diseases like Alzheimer's disease. Regardless of the state of health, lymphangiogenesis – the formation and growth of lymphatic vessels from preexisting ones – is required in both the embryonic and the adult body. Lymphangiogenesis is mainly driven by phosphorylation and signaling of the vascular endothelial growth factor receptor 3 (VEGFR3) in lymphatic endothelial cells (LECs). VEGFR3 phosphorylation can be activated by ligand binding of vascular endothelial growth factors C and D (VEGF-C and -D), as well as via mechanical stimulation sensed and translated by e.g. β1 integrin. Since excessive VEGFR3 signaling might cause non-physiologic LEC proliferation and lymphatic overgrowth, it requires strict regulation.

This study focused on the identification of mechanisms facilitating the attenuation of VEGFR3 activity in quiescent adult human LECs and thereby uncovered both extracellular and intracellular ones. In detail, the ILK-PINCH-parvin (IPP) complex proved to be an intracellular regulator of VEGFR3 signaling as it binds to β1 integrin and thereby attenuates interactions between β1 integrin and VEGFR3. Silencing of the *integrin-linked kinase (ILK)* as the central part of the IPP complex significantly stimulated interactions between β1 integrin and VEGFR3, followed by significantly increased VEGFR3 phosphorylation and LEC proliferation. In addition, silencing of *ILK* significantly decreased the protein levels of its complex partner α-parvin. Supporting these results, mechanical stimulation of adult human LECs decreased the interactions between ILK and β1 integrin and further caused a significant decrease in α-parvin protein levels. Notably, silencing of *PARVA* in adult human LECs also resulted in slightly increased VEGFR3 phosphorylation and increased LEC proliferation, supporting the role of α-parvin in this intracellular mechanism for attenuation of VEGFR3 signaling in quiescent adult human LECs.

The β-site of amyloid precursor protein cleaving enzyme 2 (BACE2) on the other hand transpired to be a potential extracellular regulator of VEGFR3 signaling. BACE proteases are required for amyloid production, which forms oligomers or plaques involved in the development and worsening of Alzheimer's disease and type 2 diabetes mellitus. The unspecific pharmaceutical inhibition of BACE proteases in adult human LECs increased total

VEGFR3 levels, as well as VEGFR3 phosphorylation and LEC proliferation. More selective inhibition of BACE1, as well as *BACE1* silencing via siRNAs did not lead to the described effects. In comparison, *BACE2* silencing was sufficient to increase VEGFR3 phosphorylation and LEC proliferation. Thus, rather BACE2 than BACE1 might be part of an extracellular mechanism causing attenuation of VEGFR3 signaling in quiescent adult human LECs.

In summary, my thesis describes ILK and α-parvin as parts of an intracellular mechanism, and BACE2 as a potential part of an extracellular mechanism which both attenuate VEGFR3 activity in quiescent adult human LECs. Thereby, the named candidates prevent LECs from non-physiologic proliferation. The obtained results are linked to pathological conditions such as lymphedema and Alzheimer's disease. The results obtained from silencing of *BACE2* further point to potential adverse effects of unselective BACE1 inhibition, unintentionally affecting BACE2 during the treatment of Alzheimer's disease. The results point into the direction that BACE2 inhibition might impact the functionality of lymphatic vessels, which is especially important for brain drainage and detoxification.

2. Zusammenfassung

Lymphgefäße regulieren und stabilisieren den körpereigenen Wasserhaushalt und tragen zur Drainage und Entgiftung des Gehirns bei. Durch ihre vielschichtigen Aufgaben sind Krankheitszustände wie Lymphödeme, Krebs und neurodegenerative Erkrankungen wie Morbus Alzheimer mit der Funktionalität der Lymphgefäße assoziiert. Die Entstehung und das Wachstum der Lymphgefäße (Lymphangiogenese) ist – unabhängig von Gesundheitszustand und Alter – ein wichtiger Prozess, um die Funktionalität der Lymphgefäße zu gewährleisten. Kontrolliert wird dieser Vorgang hauptsächlich über den vaskulären endothelialen Wachstumsrezeptor 3 (VEGFR3). Dieser ist hauptsächlich auf lymphatischen Endothelzellen (LEZ) exprimiert und induziert nach seiner Aktivierung und Phosphorylierung die Proliferation der LEZ. Die Phosphorylierung des VEGFR3 kann sowohl durch die Bindung der vaskulären endothelialen Wachstumsfaktoren C und D (VEGF-C und VEGF-D) als Liganden an den VEGFR3, als auch durch mechanische Reize aktiviert werden. Letztere werden durch Mechanorezeptoren wie β1 Integrin empfangen und über entsprechende Interaktionen an den VEGFR3 weitergeleitet. Um ein übermäßiges Wachstum der Lymphgefäße aufgrund von unkontrollierten Signalen durch den VEGFR3 zu vermeiden, muss die Aktivität des Rezeptors kontrolliert werden.

Diese Arbeit zielte auf die Identifikation von Mechanismen ab, welche die Signalaktivität des VEGFR3 im physiologischen Zustand abschwächen und somit regulieren. Dabei konnte sowohl ein intrazellulärer, als auch ein möglicher extrazellulärer Mechanismus aufgedeckt werden. Auf intrazellulärer Seite ist der sogenannte IPP Komplex, bestehend aus der ‚integrin-linked kinase' (ILK), dem ‚particularly interesting new cystein-rich protein' (PINCH) und parvin, besonders interessant. Im IPP Komplex bildet ILK das Zentrum und bindet an den Mechanorezeptor β1 Integrin. Die Reduktion des Proteingehalts von ILK, durch den Einsatz von siRNAs in adulten humanen LEZ, resultierte sowohl in signifikant erhöhten Interaktionen zwischen β1 Integrin und VEGFR3, als auch in stark erhöhter VEGFR3 Phosphorylierung. Als Folge dessen, konnte auch eine stark erhöhte Proliferationsrate der LEZ beobachtet werden, welche mit sehr wenig ILK Protein auskommen mussten. Vergleichbare Effekte wurden durch das mechanische Strecken der LEZ erzielt, wobei nicht nur erhöhte Interaktionen zwischen β1 Integrin und VEGFR3, sondern auch signifikant verringerte Interaktionen zwischen ILK und β1 Integrin beobachtet werden konnten. Während bei diesem Prozess die Gesamtproteinmenge von ILK nahezu unverändert blieb, sank der Proteingehalt von ILKs Komplexpartner α-parvin jedoch signifikant ab. Da die Gesamtproteinmenge von α-parvin auch in den LEZ reduziert wurde, welche mit siRNAs gegen ILK behandelt wurden, wurde

anschließend eine Beteiligung von α-parvin an der Regulation der VEGFR3 Signalwege geprüft. Auch die Reduktion der α-parvin Proteinmenge durch den Einsatz von siRNAs löste einen leichten Anstieg der VEGFR3 Phosphorylierung, sowie einen signifikanten Anstieg der LEZ Proliferation aus. Somit konnten sowohl ILK, als auch α-parvin als Teil eines intrazellulären Mechanismus für die Abschwächung der VEGFR3 Signalaktivität in adulten, humanen LEZ identifiziert werden.

Auf der anderen Seite konnte in dieser Thesis das sogenannte ‚β-site of amyloid precursor protein cleaving enzyme 2' (BACE2) als Teil eines möglichen extrazellulären Mechanismus der Abschwächung der VEGFR3 Signalaktivität in LEZ identifiziert werden. Die Aktivität der BACE Proteasen wurde als einflussnehmend auf die Entwicklung von Morbus Alzheimer und Typ 2 Diabetes mellitus beschrieben. Der erste Hinweis auf eine mögliche Beteiligung von BACE2 an der Regulation der VEGFR3 Signalaktivität wurde durch die unspezifische pharmakologische Inhibition der BACE Proteasen in adulten humanen LEZ erhalten. Diese resultierte in einer gesteigerten VEGFR3 Gesamtproteinmenge, sowie einer signifikant erhöhten VEGFR3 Phosphorylierung und LEZ Proliferation. Sowohl die selektivere pharmakologische BACE1 Inhibition, als auch die Reduktion der BACE1 Proteinmenge mittels des Einsatzes von siRNAs, zeigten jedoch keinen Effekt auf VEGFR3 oder die LEZ Proliferation. Im Gegensatz dazu, resultierte die gezielte Reduktion der BACE2 Proteinmenge über den Einsatz von siRNAs in einer gesteigerten VEGFR3 Phosphorylierung und LEZ Proliferation. Diese Ergebnisse deuten auf eine Beteiligung von BACE2, nicht aber BACE1, am Mechanismus der extrazellulären Abschwächung von VEGFR3 Signalen hin.

Zusammenfassend beschreibt meine Thesis, wie ILK und α-parvin Teil eines intrazellulären Mechanismus und BACE2 Teil eines extrazellulären Mechanismus für die Abschwächung der VEGFR3 Signalaktivität sind. Auf diesem Weg nehmen beide Mechanismen Einfluss auf die Proliferation humaner LEZ und somit möglicher Weise auch auf die humane Lymphangiogenese. Darüber hinaus konnte diese Arbeit auf mögliche Nebenwirkungen der gegen Morbus Alzheimer entwickelten BACE1 Inhibitoren hinweisen, welche bislang auch BACE2 inhibieren. Somit ist es möglich, dass der Einsatz dieser Inhibitoren Einfluss auf die Funktionalität der Lymphgefäße nimmt, welche wichtig für die Drainage und Entgiftung des Gehirns und somit auch für dessen Funktionalität sind.

3. Introduction

3.1 The lymphatic vasculature has essential functions

3.1.1 Fluid homeostasis, immunity and uptake of dietary lipids

The human body's vascular systems are named the blood and lymphatic vasculature and complement each other because of their synchronized functions (Pepper and Skobe 2003). The closed and circulatory system of blood vessels serves for the provision of all tissues with oxygen, heat, hormones and nutrients, while removing waste products from their origin and transporting them to places of disposal (Potente and Makinen 2017). In order to fulfil these functions, there needs to be an exchange between blood capillaries and the surrounding tissues. During this exchange phase, a small amount of fluids and solved molecules remain in extracellular spaces, which are also called the interstitium (reviewed in (Wiig and Swartz 2012)). To counteract this constant lack of water, which would otherwise increase the blood viscosity and reduce the blood volume dramatically, the blind-ended lymphatic system steadily takes up interstitial fluid (ISF) and transports it back to the blood vasculature (Figure 1A). Together with immune cells, this solution of ISF, antigens, proteins and small cells is collectively called 'lymph' (Mayerson 1963; Schulte-Merker et al. 2011). Due to this function, the lymphatic system is essential for the body's fluid homeostasis.

The lymphatic system is also relevant for the body's immunity (Forster et al. 1999). During its unidirectional transport, the lymph is filtered in interconnected lymph nodes and cleaned from potentially harmful particles. Lymph nodes are secondary lymphoid organs as e.g. also the spleen (Figure 1B) (Randall et al. 2008). Lymph nodes consist of a fibrous capsule and the medulla, and further contain several immune cells and their germinal centers. The transported lymph of several afferent lymph vessels intermingles inside of one lymph node, where its antigens are concurrently presented to immune cells (reviewed in (Drayton et al. 2006)). The immune cells can subsequently activate reactions of the adaptive immune system and are further able to interchange between lymph flow and blood stream via high endothelial venules. This location of exchange also enables fluid to pass from the lymph into the blood stream, which also gives the lymph nodes a role in maintenance of the body's fluid homeostasis. After passing these different segments, the lymph leaves the lymph node via one efferent lymphatic vessel (Girard et al. 2012; Randolph et al. 2017) (Figure 1C).

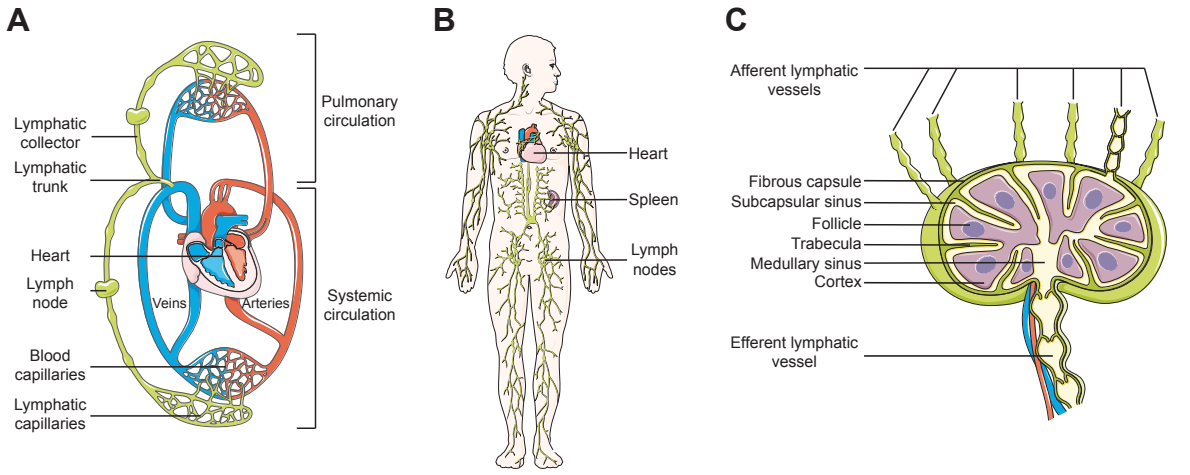

Figure 1: The lymphatic vascular system maintains the body's fluid homeostasis and includes secondary lymphoid organs.
(**A**) Lymphatic capillaries take up interstitial fluid (ISF) which remains in the interstitium around blood capillaries during their exchange phase. Lymphatic collectors transport the lymph from both the systemic and the pulmonary circulation through the interconnected lymph nodes towards lymphatic trunks. The latter drain the filtered lymph back into the blood circulation. (**B**) The network of blind-ending lymphatic vessels collects ISF from all over the body and transports it back to the blood vasculature in order to maintain the body's fluid homeostasis. The lymphatic vascular system further includes secondary lymphoid organs and tissues such as lymph nodes and the spleen. (**C**) Lymph nodes and their enclosed immune cells filter the lymph from potentially harmful particles before the lymph is drained into the blood circulation. The fibrous capsule of lymph nodes is enlarged via trabeculae into the cortex and thereby divides the lymph nodes into nodules. Lymph nodes are connected to several afferent lymphatic vessels which drain the lymph into the subcapsular sinus. From there, the lymph moves towards the medullary sinuses and thereby passes the T cells of the cortex. B cell follicles contain inactivated B cells as a part of the adaptive immune response. Modified from Servier Medical Art by Servier, licensed under a Creative Commons Attribution 3.0 Unported License.

Interestingly, lymphatic vessels are also included into the villi of the small intestine where they are named lacteals. Those specialized lymphatic structures are able to take up dietary lipids and fat-soluble vitamins in the form of chyle from the gut, which is then drained with the rest of the lymph into the blood circulation (Choe et al. 2015). Due to their important functions, lymphatic vessels can be found in most of the human tissues, except from avascular tissues like the cornea (Figure 1B). Even in the retina (Nakao et al. 2012) and parts of the central nervous system (CNS) lymphatic vessels can be found (Aspelund et al. 2015; Louveau et al. 2015).

3.1.2 The glymphatic system and meningeal lymphatic vessels drain the brain

The CNS is known to be a very sensitive organ, which is protected by its tight blood brain barrier (BBB). Hence, it was assumed for a long time that the brain would not be drained by lymphatic vessels (Iliff and Nedergaard 2013). Nevertheless, cerebrospinal fluid (CSF), produced by the choroid plexus before moving to the subarachnoid space, was known to be drained from the CNS. From the subarachnoid space, CSF would for example be absorbed by arachnoid granulation villi for the final transport via cerebral venous sinuses (Figure 2) (Pollay 2010). Later, a so called 'glial' lymphatic system (the glymphatic system) was identified, which is an additional, but paravascular way to drain the CNS (Iliff et al. 2012; Xie et al. 2013). It is built up by perivascular tunnels formed by astroglial cells in the brain parenchyma and both removes waste products from the CNS and distributes several compounds to it. Interestingly, it only works during sleep, which makes sleep essential for the prevention of neurological diseases (reviewed in (Jessen et al. 2015)).

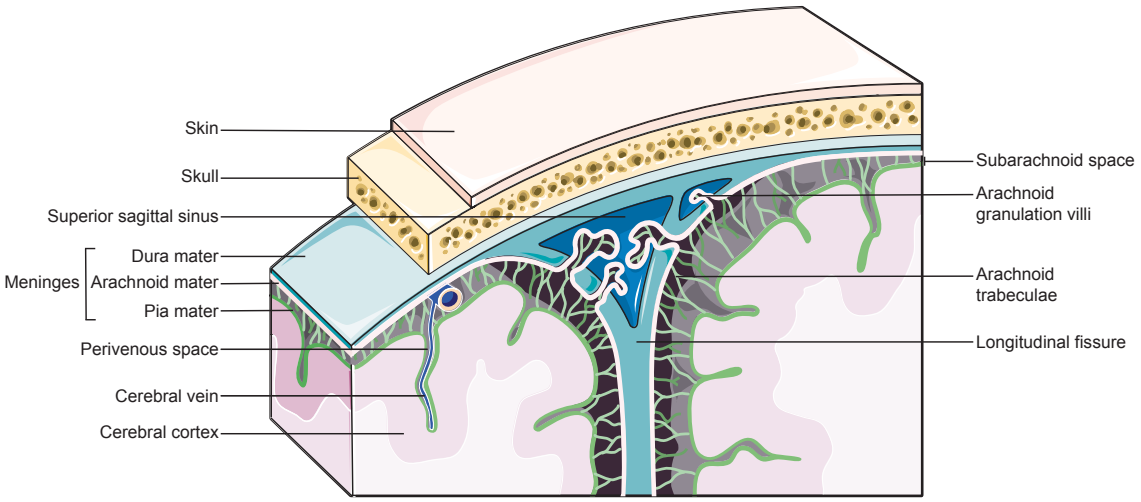

Figure 2: Anatomy of the meninges and their contribution to the glymphatic drainage system. Closely attached to the skin covered skull one finds the meninges. The meninges consist of three layers; the *dura mater*, *arachnoid mater* and *pia mater*. The *dura mater* is attached to the skull and contains a number of lymphatic and blood vessels, while the *arachnoid mater* is avascular. The *arachnoid mater* spans the subarachnoid space which is streaked by arachnoid trabeculae. Arachnoid granulation villi grow from the arachnoid space into the superior sagittal sinus, allowing the diffusion of fluids between the two spaces. The meninges additionally form the longitudinal fissure, which separates the two brain hemispheres. Cerebral veins and arteries are located in the subarachnoid space and further grow directly into the cerebral cortex. They are surrounded by a small perivascular space, from and into which cerebrospinal fluids (CSF) and also interstitial fluids (ISF) diffuse from the cerebral cortex. Those fluids move into the subarachnoid space and via the arachnoid granulation villi into the superior sagittal sinus. Modified from Servier Medical Art and used under the free-to-use Creative Commons Attribution 3.0 Unported License.

Additionally, a part of the CSF was also shown to be drained into cervical lymph nodes, but the exact mechanism remained unclear (Koh et al. 2005; Weller et al. 2009). Recently it could be shown that functional lymphatics in the meninges drain the CNS into deep cervical lymph nodes, a finding which emphasizes the essential functions of lymphatic vessels (Aspelund et al. 2015; Louveau et al. 2015). The meninges consist of three layers; while the *pia mater* is closely attached to the surface of the brain, the avascular *arachnoid mater* is overlying the subarachnoid space. The highly vascularized *dura mater* is attached to the cranial bones or the skull (Figure 2) (Ghannam and Al Kharazi 2019) and contains a significant number of lymphatic vessels. The latter complement ways of major blood vessels and form an extensive network at the base of the skull. Meningeal lymphatic vessels absorb brain ISF and CSF, as well as macromolecules from the subarachnoid space and transport them into deep cervical lymph nodes (Aspelund et al. 2015).

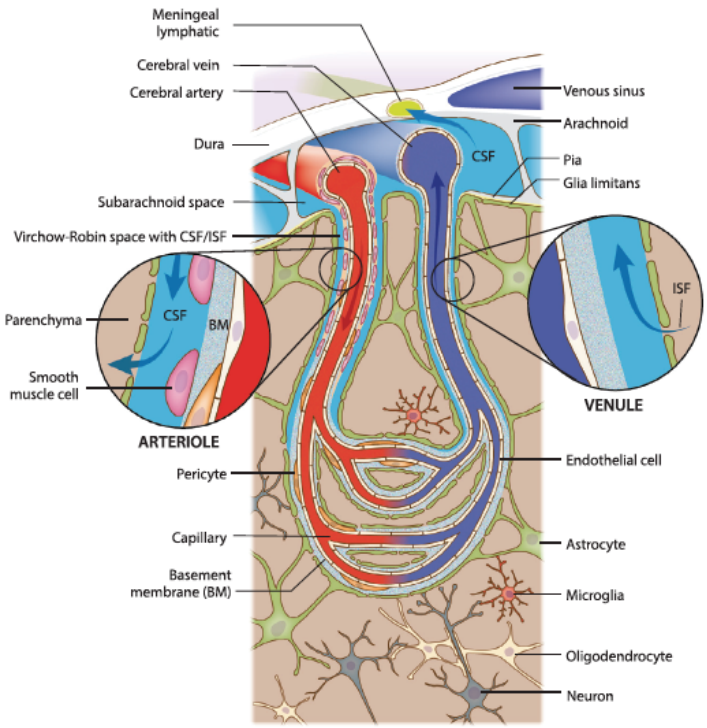

Figure 3: Meningeal lymphatics drain CSF from the subarachnoid space.
The meninges consist of three layers; the *dura mater*, *arachnoid mater* and *pia mater*. The *dura mater* is attached to the skull and contains a number of lymphatic vessels, while the *arachnoid mater* is avascular. The *arachnoid mater* spans the subarachnoid space in which cerebral veins and arteries are located. Those grow directly into the parenchyma containing astrocytes, microglia, oligodendrocytes and neurons. The arterioles and venules are surrounded by a small perivascular space (Virchow-Robin space) and a discontinuous basement membrane, draining cerebrospinal fluids (CSF) from the arterial side towards the parenchyma and taking up interstitial fluids (ISF) from the parenchyma on the venous side. This circular flow of CSF and ISF moves through the subarachnoid space from which it is drained by meningeal lymphatics in the *dura mater*. Reprinted from Da Mesquita, Fu and Kipnis 2018 with permission from Elsevier, provided by Rightslink® Copyright Clearance Center (License Number 4900080146144).

3.2 The hierarchic network of differently specialized lymph vessels

In the peripheral lymphatic vasculature, three different vessel types can be found that form a hierarchical network. Those vessel types are subdivided into lymphatic capillaries or initial lymphatics, pre-collectors and collectors which are all adapted to their respective functions (Schulte-Merker et al. 2011). The different lymphatic vessels all share the feature of lymphatic endothelial cells (LECs) facing the lymphatic lumen, while functional segments of the lymphatic system are divided by lymphatic valves into so called lymphangions (Figure 4) (Mislin 1976).

The smallest of all lymphatic vessel types are the lymphatic capillaries, which are also called lymphatic initials. Initial lymphatics are morphologically specialized for the uptake of ISF. Therefore, they end blindly within the interstitium and reveal a single layer of LECs surrounded by a discontinuous basement membrane (Leak 1970). The discontinuity of this basement membrane is important for the uptake of ISF, because it leaves the cell edges of adjacent LECs uncovered. In addition to this feature, LECs of the lymphatic capillaries are oak leaf like shaped and connected to each other loosely via button-like junctions (Murfee et al. 2007; Baluk et al. 2007). Those junctions enable the overlapping cell edges to build valve like structures which open towards the lumen of lymphatic capillaries. Accordingly, ISF flows unidirectionally from the interstitium into the vessel and backflow is impeded. For the opening of those valve-like structures, there needs to be a certain pressure of ISF working on the endothelial cells (Pepper and Skobe 2003). In order to prevent the vessel from collapsing due to this pressure, the LECs are connected to the extracellular matrix (ECM) via anchoring filaments (Leak and Burke 1968) and integrins (Gerli et al. 2000). The pressure gradient between interstitium and lumen of the lymphatic capillary guides the way for the ISF influx (Breslin 2014) and the lymph is further transported into pre-collecting lymphatic vessels. This vessel type combines the features of small lymphatic capillaries and the bigger lymphatic collectors (Figure 4) (Sacchi et al. 1997). Big collecting lymphatic vessels converge the transported lymph of several pre-collectors. On its way towards the abdomen, lymph has to pass multiple lymphatic valves, which are preventing lymphatic backflow and support lymphatic propulsion (Sabine et al. 2012).

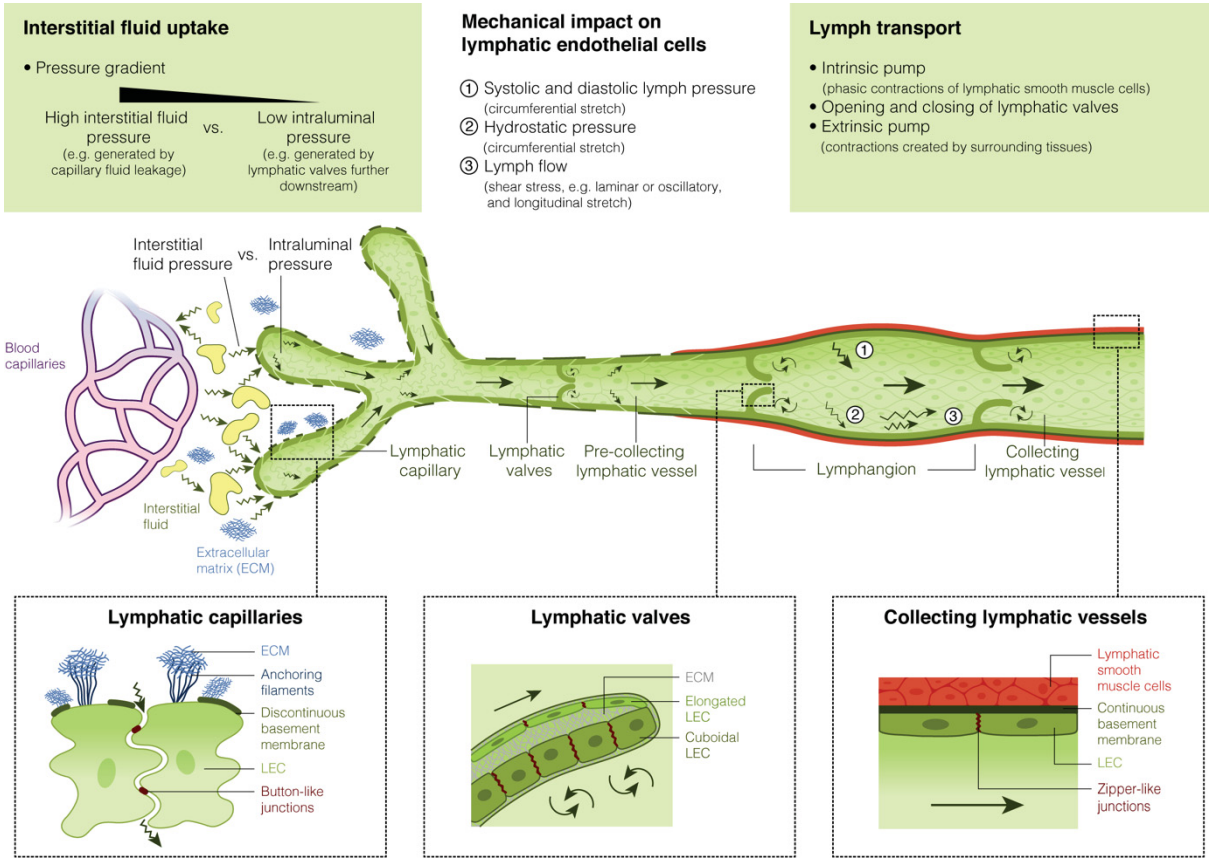

Figure 4: Lymphatic vessels are adapted to their functions and LECs face several mechanical forces.
During the exchange phase of blood capillaries some fluid remains in the interstitium (Interstitial fluid, ISF) and needs to be taken up by lymphatic capillaries. (**A**) Lymphatic capillaries are built by oak-leaf like shaped LECs interconnected by button-like junctions and covered by a discontinuous basement membrane to allow influx of ISF into the vessel. To prevent the lymphatic capillary from collapsing due to the ISF pressure, LECs are connected to the extracellular matrix (ECM) via anchoring filaments and integrins. The pressure of ISF is higher than the intraluminal pressure of lymphatic capillaries, which is generated by lymphatic valves further downstream. Therefore, the ISF uptake works along a pressure gradient towards the lumen of lymphatic capillaries. Lymphatic valves separate the lymphatic vessels into so called lymphangions and impede backflow of the entered fluid. This fluid, referred to as lymph, is transported from lymphatic capillaries through pre-collecting and collecting lymphatic vessels, and finally returns to the blood vasculature. (**B**) LECs of lymphatic valves are heterogeneous in their morphology. Depending on their site at the valve and the respective lymph flow pattern they are exposed to, LECs can either appear to be elongated or cuboidal. (**C**) In collecting lymphatic vessels, LECs are tightly connected to each other via zipper-like junctions and are surrounded by a continuous basement membrane to prevent lymphatic leakage. Collecting lymphatic vessels are further equipped with a thick layer of lymphatic smooth muscle cells, which enforce lymphatic flow via phasic contractions and are therefore named the intrinsic pump of the lymphatic system. The intrinsic pump is supported by extrinsic pump forces generated by surrounding tissues and by opening and closing of lymphatic valves. LECs experience circumferential stretch created by systolic and diastolic lymph pressure (1) and hydrostatic pressure (2) as well as shear stress and longitudinal stretch created by lymph flow (3) in the region of collecting lymphatic vessels. Modified from Urner et al. 2018b with permission from Elsevier, provided by Rightslink® Copyright Clearance Center (License Number 4893661328147).

Lymphatic collectors are characterized by a large vessel diameter and elongated LECs. They are further equipped with zipper-like LEC junctions, a continuous basement membrane and additional mural cells to prevent lymphatic leakage (Baluk et al. 2007; Yao et al. 2012). The thick layer of lymphatic SMCs surrounding lymphatic collectors serves as an intrinsic pump (Benoit et al. 1989; von der Weid and Zawieja 2004) and is supported by contractions and movements of the surrounding organs and muscles, referred to as the extrinsic pump (Figure 4) (Zawieja 2009). A pump like this is necessary for the lymphatic collectors to be compressed and thus for the transport of lymph back into the abdomen, where the largest lymphatic vessels are to be found. Those are the thoracic duct and the right lymphatic trunk which drain the lymph into the blood vasculature via the subclavian veins. The latter are separated from the lymphatic trunks by specialized lymphovenous valves (Yang and Oliver 2014).

3.3 LECs face different mechanical forces

As the human body moves constantly due to the necessity of breathing, heartbeat, gut peristalsis as well as blood and lymph flow (Zawieja 2009), cells are always facing diverse mechanical forces. The lymphatic vasculature is highly sensitive towards mechanical forces, because it needs to adapt to changes in their environment to maintain the body's fluid homeostasis. Consequently, lymphatic vessels are able to sense mechanical changes such as ISF pressure and fluid flow to adjust their function, as it already happens during embryonic development (Daems et al. 2020). On LECs, mechanoreceptors such as β1 integrins play an important role for both sensing of and adaption to changes in mechanical forces (Planas-Paz et al. 2012). Possible ways of adaption are either vessel growth or lymphangiogenesis, adjusted ISF uptake via lymphatic capillaries or adjustments in the lymph transport by collecting lymphatic vessels (reviewed in (Urner et al. 2018b) and (Hilger and Lammert 2019)).

LECs of lymphatic capillaries are directly confronted with both the ISF pressure on the outside and the intraluminal pressure on the inside of the vessel (Figure 4). Between those compartments, there is a constant pressure gradient towards the lumen of lymphatic capillaries guiding the way for ISF influx (Benoit et al. 1989; Rahbar et al. 2014). The amount of ISF that is taken up by lymphatic capillaries can be adjusted via the intercellular spaces between LECs. Anchoring filaments and integrins connect LECs to the ECM and therefore transduce a swelling of the ECM caused by increased ISF volume to the LECs. The latter are consequently pulled apart from each other and thereby enlarge intercellular spaces to allow increased ISF influx into the lymphatic capillary (Gerli et al. 2000). The intraluminal pressure

can be further regulated via the opening and closing of lymphatic valves downstream of lymphatic capillaries (Davis et al. 2011; Scallan et al. 2012). LECs of lymphatic valves are morphologically adapted to the different flow patterns they are facing, induced by turbulences which occur due to the valve protruding into the lymphatic stream. LECs facing the regular lymph stream are morphologically elongated, whereas the LECs facing the turbulences beneath the valve appear to be more cuboidal in shape (Figure 4) (Sabine et al. 2012).

After the influx of ISF, the transport of lymph needs to be propelled by both the intrinsic pump, facilitated by contractions of lymphatic SMCs (von der Weid and Zawieja 2004) and the extrinsic pump, thus movements and pressure by the surrounding tissues and organs (Olszewski et al. 1977). Those forces from the outside of the lymphatic vessel are accompanied by intraluminal mechanical forces. The systolic and diastolic pressure by the lymph within collecting lymphatic vessels circumferentially stretch the surrounding LECs (Figure 4 (1)), while the lymph creates hydrostatic pressure (Figure 4 (2)). In addition, the LECs experience shear stress and longitudinal stretch (Figure 4 (3)) due to the lymph flow (Dixon 2010; Breslin 2014). In summary, LECs throughout the lymphatic system face several different mechanical forces which often cause a stretching of the respective LECs.

3.4 The lymphatic system is of clinical relevance

3.4.1 Lymphedema is caused by impaired lymphatic drainage

As every organ in the human body, the lymphatic system can be associated with pathological conditions. Those are mostly related to dysfunctions of the lymphatic system which can be identified by a swelling of tissues due to a pathological accumulation of lymph. This phenomenon is called lymphedema and can be caused by different circumstances. In addition to genetic defects causing primary lymphedema, some extrinsic factors can cause edema which are then classified as secondary lymphedema (reviewed in (Rockson 2001)). A disruption of lymphatic vessels, e.g. due to the removal of an organ such as the appendix or lymph nodes, stops the lymph flow at this point or from this point onwards (Figure 5).

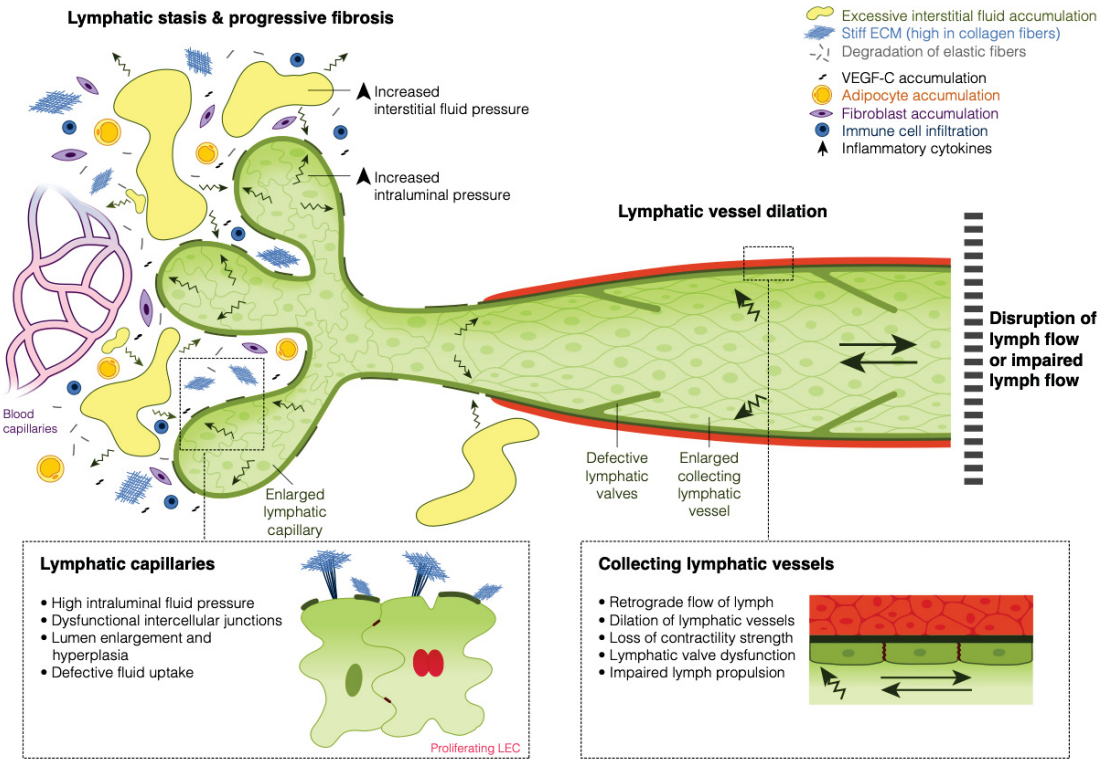

Figure 5: Secondary lymphedema and its effects on lymphatic vessels.
Secondary lymphedema can be caused by (surgical) disruption of the lymph flow, causing a retrograde flow within the lymphatic vasculature. Collecting lymphatic vessels consequently dilate, while lymphatic smooth muscle cells (SMCs) gradually lose their ability to contract. Lymphatic valves further become dysfunctional, resulting in impaired lymph propulsion. Due to lymph accumulation, lymphatic capillaries experience high intraluminal pressure which manifests in lumen enlargement and hyperplasia, as lymphatic endothelial cell (LEC) proliferation is initiated. Additionally, lymphatic capillaries lose their ability to take up interstitial fluid (ISF) fluid, because the intercellular junctions between LECs of the lymphatic capillaries become dysfunctional. This leads to lymphatic stasis characterized by excessive ISF accumulation, further resulting in high ISF pressure and progressive fibrosis. Moreover, the extracellular matrix (ECM) stiffens, because it becomes rich in collagen fibers, but low in elastic fibers. A strong accumulation of adipocytes and fibroblasts as well as high infiltration of immune cells can additionally be observed along with increased inflammatory cytokines. Reprinted from Urner et al. 2018b with permission from Elsevier provided by Rightslink® Copyright Clearance Center (License Number 4893661328147).

Therefore, lymph from afferent locations cannot be transported further towards the blood vasculature of the abdomen and either remains in the interstitium or in the lymphatic vessels which are now cut off from the remaining of the lymphatic network (reviewed in (Mortimer and Rockson 2014)). This is why the collecting lymphatic vessels on the site of impaired lymph flow dilate and lymphatic capillaries in edematous tissues appear to be hyperplastic due to increased LEC proliferation. Even though LECs proliferate excessively, the functionality of lymphatic capillaries remains impaired (Rutkowski et al. 2006; Gousopoulos et al. 2016).

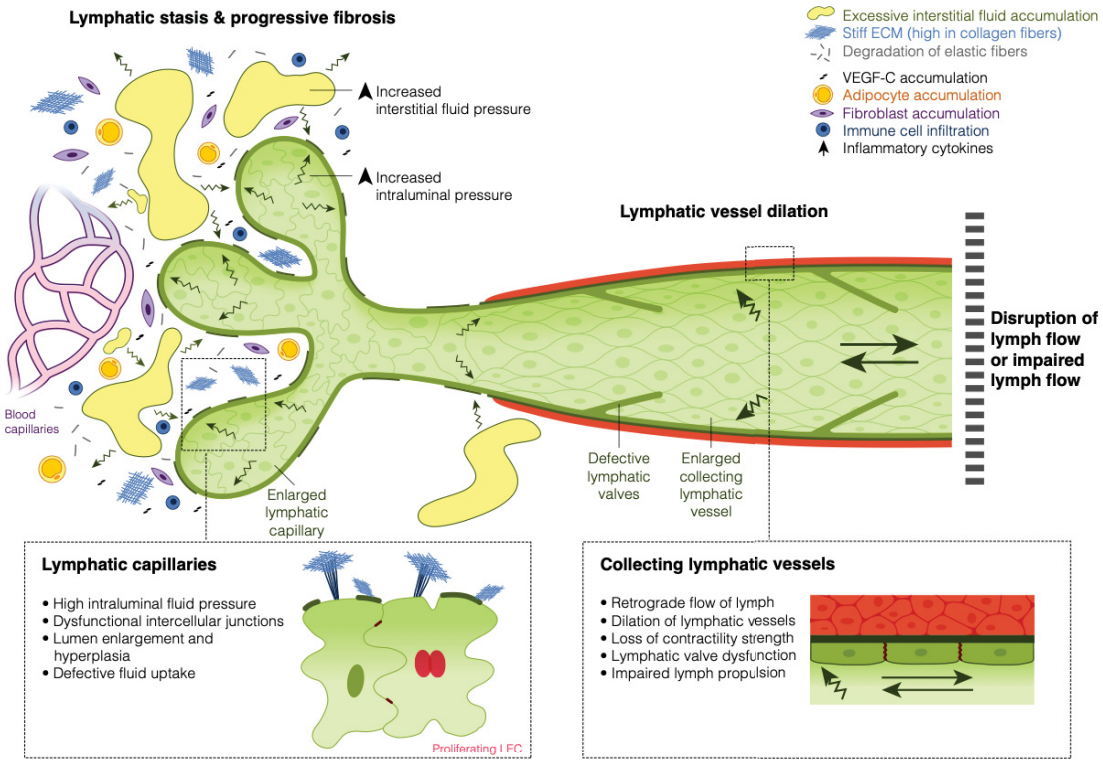

retrograde flow within the lymphatic vasculature. Collecting lymphatic vessels consequently dilate, while lymphatic smooth muscle cells (SMCs) gradually lose their ability to contract. Lymphatic valves further become dysfunctional, resulting in impaired lymph propulsion. Due to lymph accumulation, lymphatic capillaries experience high intraluminal pressure which manifests in lumen enlargement and hyperplasia, as lymphatic endothelial cell (LEC) proliferation is initiated. Additionally, lymphatic capillaries lose their ability to take up interstitial fluid (ISF) fluid, because the intercellular junctions between LECs of the lymphatic capillaries become dysfunctional. This leads to lymphatic stasis characterized by excessive ISF accumulation, further resulting in high ISF pressure and progressive fibrosis. Moreover, the extracellular matrix (ECM) stiffens, because it becomes rich in collagen fibers, but low in elastic fibers. A strong accumulation of adipocytes and fibroblasts as well as high infiltration of immune cells can additionally be observed along with increased inflammatory cytokines. Reprinted from Urner et al. 2018b with permission from Elsevier provided by Rightslink® Copyright Clearance Center (License Number 4893661328147).

Therefore, lymph from afferent locations cannot be transported further towards the blood vasculature of the abdomen and either remains in the interstitium or in the lymphatic vessels which are now cut off from the remaining of the lymphatic network (reviewed in (Mortimer and Rockson 2014)). This is why the collecting lymphatic vessels on the site of impaired lymph flow dilate and lymphatic capillaries in edematous tissues appear to be hyperplastic due to increased LEC proliferation. Even though LECs proliferate excessively, the functionality of lymphatic capillaries remains impaired (Rutkowski et al. 2006; Gousopoulos et al. 2016).

Furthermore, lymphedema itself can cause several other health issues. Due to its composition, an accumulation of lymph does not only cause swellings and a degradation of elastic fibers, but later on also leads to inflammation, fibrosis and even necrosis due to adipocyte and fibroblast accumulation, immune cell infiltration and the release of inflammatory cytokines (Figure 5) (Saito et al. 2013; Ghanta et al. 2015; Ly et al. 2017). To avoid the development of fibrosis or even necrosis, the drainage of the edematous region needs to be restored. This can either be done surgically with the reconnection of preexisting lymphatic vessels (Aschen et al. 2014; Maeda et al. 2018), further triggered by vascular endothelial growth factor-c (VEGF-C) treatment (Schindewolffs et al. 2014) or solved by bypassing ligated areas (Slavin et al. 1999). As the hypoxia inducible factor 2 α (HIF-2α) protein expression was found to be decreased upon mouse lymphedema and thereby caused lymphatic dysfunction, its restoration could possibly stabilize lymphatic function and drainage capacity, which might also be a future target for lymphedema treatment (Jiang et al. 2020). Another way of treating lymphedema and stimulating lymph flow is the manual lymph drainage therapy. During this therapy, the therapist massages the ISF manually from the most distant part of the lymphatic disruption towards the remaining functional lymphatic vessels. The therapy further increases the pumping activity of lymphatic collectors (Hutzschenreuter et al. 1989), implicating beneficial effects of external mechanical stimulation on lymphatic function.

Clinical relevance of the lymphatic vasculature is further underlined by its association with obesity (Harvey et al. 2005; Escobedo et al. 2016), tumor supply (He et al. 2004) and cancer progression (He et al. 2004; Saharinen et al. 2004; Karaman and Detmar 2014; Dieterich and Detmar 2016). Also ocular glaucoma (Thomson et al. 2014), myocardial infarction (reviewed in (Vuorio et al. 2017)) as well as myocardial edema, fibrosis (Brakenhielm et al. 2020) and inflammation due to myocardial infarction (Vieira et al. 2018) were shown to be associated with the lymphatic vasculature.

3.4.2 Lymphatic drainage capacity is associated with neurological diseases

The body's drainage systems might also be associated with neurological diseases, e.g. Alzheimer's disease. The latter is caused and its progression worsened by the accumulation of the neurotoxic substance β-amyloid to so called amyloid plaques (Revesz et al. 2009; Musiek and Holtzman 2015; Selkoe and Hardy 2016). This substance is produced in the CNS by cleavage of amyloid precursor protein (APP) by β-site of APP cleaving enzymes (BACE) which were found to be upregulated in Alzheimer's disease patients and the respective mouse model (Vassar et al. 1999; Yang et al. 2003; Devraj et al. 2016). To avoid

such neurotoxic effects, β-amyloid is usually eliminated via the BBB (Deane et al. 2004; Tarasoff-Conway et al. 2016) and – especially during sleep – by the glymphatic system (Iliff et al. 2012). Impaired sleep pattern thus might accelerate the progression or worsening of Alzheimer's disease due to the inevitable accumulation of β-amyloid, as it also happens during aging due to reduced paravascular CNS clearing (Kress et al. 2014). Interestingly, not only the glymphatic system but also the meningeal lymphatics might be associated with Alzheimer's disease (Sweeney and Zlokovic 2018). A mouse model lacking any meningeal lymphatic vessel admittedly did not reveal any changes in ISF pressure or water content of the CNS, but nevertheless, the macromolecule clearance from the brain was attenuated. Thus, meningeal lymphatics are important for removal of macromolecules (Aspelund et al. 2015) and therefore, the functionality of meningeal lymphatics is important to protect the body from neurological diseases caused by accumulation of neurotoxic substances such as β-amyloid (Louveau et al. 2016; Da Mesquita et al. 2018; Zinchenko et al. 2019). The brain-to-cervical lymph node pathway is further involved in systemic inflammation and brain injury after stroke (Esposito et al. 2019), aspects which highlight the importance of lymphatic drainage capacity in neurological diseases.

3.5 Vascular endothelial growth factor receptor 3 (VEGFR3)

3.5.1 The vascular endothelial growth factor (VEGFR) family

For the induction of lymphangiogenesis, the formation and growth of lymphatic vessels from preexisting ones, LECs need a trigger to increase their proliferation (reviewed in (Tammela and Alitalo 2010)). Multiple factors are able to activate the most important regulator of LEC proliferation, which is known as the vascular endothelial growth factor receptor 3 (VEGFR3) or fms-like tyrosine kinase 4 (Flt4) (Makinen et al. 2001; Karkkainen et al. 2004). In the adult, VEGFR3 expression is mainly restricted to LECs (Kaipainen et al. 1995) and only a few VECs such as fenestrated cells (Partanen et al. 2000) and tip cells (Tammela et al. 2008) express this receptor. Additionally, a number of non-endothelial cells including neuronal progenitors (Le Bras et al. 2006), osteoblasts (Orlandini et al. 2006) and macrophages (Schmeisser et al. 2006) were shown to express VEGFR3.

In humans, three different VEGFRs with different expression patterns are known. Amongst VEGFR3, there is also VEGFR1 or fms-like tyrosine kinase 1 (Flt1) to be named, which is expressed on vascular endothelial cells (VECs) (Fong et al. 1995). In addition, VEGFR2 or

fetal liver kinase 1 (Flk1) (Terman et al. 1991; Terman et al. 1992) is found on VECs and LECs (Feng et al. 2000; Nagy et al. 2002). Nevertheless, both VEGFR1 and VEGFR2 are also expressed on non-endothelial cells such as hematopoietic stem cells (Katoh et al. 1995; Hattori et al. 2002). VEGFR2 activity is important for both vasculogenesis and angiogenesis (Shalaby et al. 1995) and interestingly, the main function of VEGFR1 is to regulate VEGFR2 signaling (Hiratsuka et al. 1998). On the structural level, all VEGFRs share the features of an extracellular N-terminal part, a short transmembrane domain as well as an intracellular part. Within the intracellular part, the carboxyl-terminal (C-terminal) tail is accompanied by a short juxtamembrane domain and two tyrosine-kinase domains (reviewed in (Simons et al. 2016)). Despite of these shared features, the extracellular part of VEGFR3 differs from the other VEGFRs. In detail, the fifth immunoglobulin-like domain is replaced by a disulfide bridge as a consequence of proteolytic cleavage (Pajusola et al. 1992; Lee et al. 1996; Takahashi and Shibuya 2005).

3.5.2 Ligand induced VEGFR3 signaling

Signaling activity of receptor tyrosine kinases (RTKs) is usually initiated by ligand binding to the extracellular part of the receptor (reviewed in (Lemmon and Schlessinger 2010)). As a member of the RTK family, VEGFR3 shares this feature and is therefore activated by ligand binding of vascular endothelial growth factors c and d (VEGF-C and VEGF-D) to its extracellular part (Figure 6) (Joukov et al. 1996; Achen et al. 1998). The VEGFs build a family of five, including VEGF-A, -B, -C and -D but also the placental growth factor (PlGF) (reviewed in (Alvarez-Aznar et al. 2017)). Ligand binding of VEGF-C and VEGF-D to VEGFR3 induces the immediate dimerization of its extracellular domain, which either results in homodimers, or in heterodimers consisting of VEGFR3 and VEGFR2 (Ullrich and Schlessinger 1990; Heldin 1995; Dixelius et al. 2003; Schlessinger 2003; Leppanen et al. 2013). Dimerization of VEGFRs subsequently induces trans-phosphorylation between the partners in the dimer and thereby regulates their kinase activity (Dixelius et al. 2003). Multiple tyrosine residues in the C-terminal tail of VEGFR3 have been described to be phosphorylation sites until now, all inducing different intracellular signaling pathways upon their phosphorylation. VEGFR3 tyrosine phosphorylation creates docking sites for adapter proteins of downstream signaling pathways, inducing LEC survival, migration and proliferation (Salameh et al. 2005; Favier et al. 2006). Those signaling pathways likely include Akt and Erk1/2 being activated in a phosphoinositide 3-kinase (PI3K)- or in a protein kinase C (PKC)-dependent manner, respectively (Pajusola et al. 1994; Fournier et al. 1995; Makinen et al. 2001).

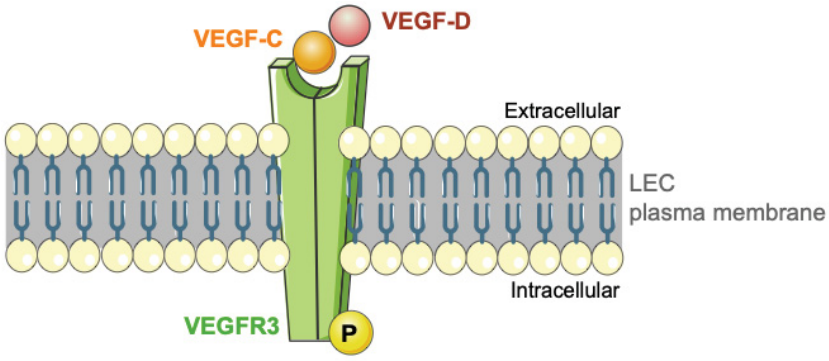

Figure 6: Ligand binding by VEGF-C or VEGF-D induces VEGFR3 phosphorylation in LECs. Binding of either the vascular endothelial growth factor c (VEGF-C) or vascular endothelial growth factor d (VEGF-D) to the extracellular domains of vascular endothelial growth factor receptor 3 (VEGFR3) of lymphatic endothelial cells (LECs) results in immediate receptor dimerization. VEGFR3 dimerization causes conformational changes of its intracellular part to induce autophosphorylation of tyrosine residues (P). This creates docking sides for adapter proteins, inducing downstream signaling for LEC survival, migration and proliferation. Modified Figure 4 of Sofia Urner's dissertation (Urner 2018a) using Servier Medical Art and used under the free-to-use Creative Commons Attribution 3.0 Unported License.

Interestingly, VEGFR3 signaling was further shown to be coupled with its internalization, a mechanism which is controlled by ephrinB2 (Olszewski et al. 1977; Wang et al. 2010; Nakayama et al. 2013). VEGFR3 internalization might lead to a prolonged signaling activity, as it has been shown for VEGFR2 (Lampugnani et al. 2006).

3.5.3 Interaction with β1 integrin induces VEGFR3 signaling activity

As already mentioned above, LECs experience different kinds of mechanical forces throughout the lymphatic system (3.3). All of those forces need to be monitored and processed by LECs in order to maintain vessel functionality. For this purpose, LECs are equipped with mechanosensitive adhesion proteins such as integrins. Integrins are a group of transmembrane proteins which form multiple heterodimers consisting of α- and β-subunits. In endothelial cells, integrins function as a scaffold between the outside and inside of cells, thereby facilitating 'outside-in' and 'inside-out' signaling (Fernandez et al. 1998; Giancotti and Ruoslahti 1999). Binding of integrin to parts of the ECM leads to a structural transformation of its extracellular domain towards its activated state, thereby increasing its affinity for ECM binding (Luo et al. 2007; Su et al. 2016). This leads to a clustering of integrins at the plasma membrane (X. Sun et al. 2016) and is followed by the recruitment of signaling molecules and F-actin towards integrin's intracellular domain (Z. Sun et al. 2016).

Intracellularly, integrins directly or indirectly bind to the F-actin cytoskeleton (Maniotis et al. 1997; Galbraith et al. 2007) and multiple other adapter proteins (Giancotti and Ruoslahti 1999) receptive for integrin signaling. This strong integration into complex protein structures allows integrins to sense all kinds of mechanical changes from the ECM, as well as from the F-actin cytoskeleton, and to modify their signaling as a response to them (Giancotti and Ruoslahti 1999).

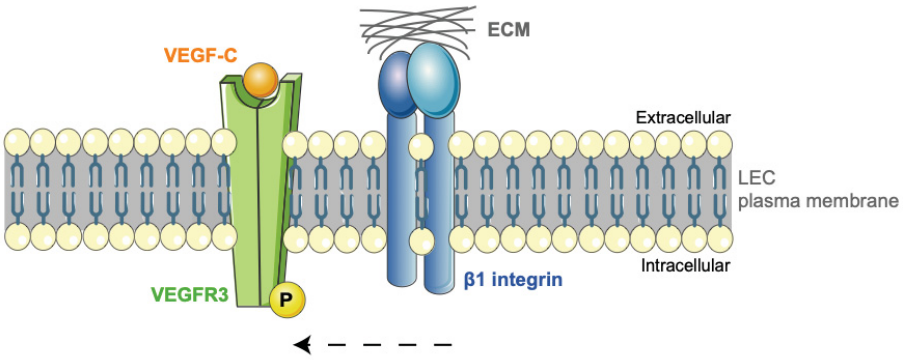

Figure 7: Interaction with β1 integrin induces VEGFR3 phosphorylation in LECs.
The mechanosensor β1 integrin is activated upon binding to the extracellular matrix (ECM) and is able to transduce signals from the ECM to the vascular endothelial growth factor receptor 3 (VEGFR3) by its interaction with the receptor. This interaction induces phosphorylation of tyrosine residues (P) in the intracellular part of VEGFR3, which triggers downstream signaling resulting in LEC survival, migration and proliferation, a mechanism which is independent from ligand binding to VEGFR3. Modified Figure 5 of Sofia Urner's dissertation (Urner 2018a) using Servier Medical Art and used under the free-to-use Creative Commons Attribution 3.0 Unported License.

Focusing on LEC functions, β1 integrins are particularly important. To induce lymphatic adaption processes, β1 integrin e.g. stimulates LEC proliferation upon binding to its ligand fibronectin, which is a part of the ECM (Zhang et al. 2005). The special importance of β1 integrins for the adaption of the lymphatic vasculature to fluid pressure could be demonstrated later. It could be shown that injection of fluids increased embryonic ISF fluid pressure, which resulted in stretched LECs, increased VEGFR3 signaling, as well as increased LEC proliferation and lymphatic vascular growth. Those adaptions to the changes in pressure environment were sufficient to finally normalize the ISF fluid pressure (Planas-Paz et al. 2012). Nonetheless, endothelial cell specific deletion of β1 integrin dramatically reduced VEGFR3 signaling and LEC numbers. *In vitro* stretch experiments with LECs revealed that stretching indeed increased VEGFR3 signaling but did not change VEGF-C expression and this is why it is likely that β1 integrin itself induces the monitored VEGFR3 signaling (Planas-Paz et al. 2012).

To induce an LEC reaction such as LEC proliferation to mechanical changes, β1 integrins are able to transactivate VEGFR3, both in absence and presence of VEGF-C (Figure 7) (Wang et al. 2001; Zhang et al. 2005). This transactivation process is probably facilitated indirectly by a recruitment of c-src family kinases, which consequently leads to VEGFR3 tyrosine phosphorylation and thus activates signaling cascades towards LEC survival, proliferation and migration (Zhang et al. 2005; Galvagni et al. 2010).

3.5.4 Regulation of VEGFR3 signaling

Taking into account that LECs constantly experience mechanical stimuli (3.3), regulation of the previously described mechanism of β1 integrin mediated VEGFR3 activation (3.5.3) is strictly required. Otherwise, the mechanical stimuli would probably cause excessive growth of lymphatic vessels due to uncontrolled LEC proliferation triggered by β1 integrin mediated VEGFR3 signaling. In addition, also VEGFR3 activity due to ligand binding needs to be regulated in order to maintain proper lymphatic function (Geng et al. 2020). Therefore, intensive investigation of potential regulators of VEGFR3 signaling has been done throughout the last years and by now, several ways to attenuate VEGFR3 activity have been described.

In the avascular cornea for example, it could be shown that soluble VEGFR3 and VEGFR2 trap or capture VEGF-C produced by the corneal tissue. This mechanism prevents the growth factor from binding to VEGFR3 of LECs in the highly vascularized limbus, a tissue that provides the corneal tissue. Induction of lymphangiogenesis in the limbus due to ligand binding of VEGF-C would otherwise cause lymphatic vessels to grow into the cornea and thereby to reduce the clarity of vision through the cornea (Albuquerque et al. 2009; Singh et al. 2013). Despite of this local regulation of VEGFR3 signaling, other and more globally working mechanisms have been described. As an example, suppression of vascular endothelial phosphotyrosine phosphatase but no other phosphotyrosine phosphatase could remarkably increase VEGF-C induced VEGFR3 activation. This indicates that the vascular endothelial phosphotyrosine phosphatase dephosphorylates VEGFR3's tyrosine residues and thereby regulates VEGFR3 activity under physiologic conditions (Deng et al. 2015). In addition, the protein tyrosine phosphatase PTPN14 is likely to contribute to the regulation of lymphangiogenesis, but its definite role in VEGFR3 activity remains undescribed until now (Au et al. 2010). Moreover, RTKs such as VEGFR3 can be internalized and degraded or recycled, processes which end VEGFR3 signaling (reviewed in (Bahram and Claesson-Welsh 2010)). Interestingly, specialized lipid rafts of endothelial cells, named caveolae, also seem to play an

intracellular role in VEGFR3 regulation. Caveolae are built by caveolin-1, a protein which is highly expressed in LECs (Podgrabinska et al. 2002; Sohn et al. 2016) and was further described to associate with VEGFR3 and to inhibit its activation by this (Galvagni et al. 2007). Especially during lymphatic valve development and collecting lymphatic vessel maturation (Liu et al. 2014), as well as for lymphangiogenesis under diabetic conditions (Wu et al. 2018), VEGFR3 regulation by epsins has been described. Epsins are multifunctional endocytic adapter proteins, involved in vascular development and functions (reviewed in (Bhattacharjee et al. 2020)). In LECs, epsins 1 and 2 potentially regulate VEGFR3 expression and signaling by binding to the RTK and inducing its internalization and degradation (Liu et al. 2014). Upon diabetic conditions, epsins 1 and 2 could be shown to induce VEGFR3's degradation in the Golgi compartment and thereby decrease its availability at the plasma membrane (Wu et al. 2018).

Despite from these mechanisms to attenuate VEGFR3 activity on protein levels, the RTK's activity can also be attenuated on transcript levels. In this context it has e.g. been reported that Notch signaling may regulate VEGFR3 expression in lymphatic endothelial cells and thereby the latter's reactivity to VEGF-C ligand binding, especially during tumor lymphangiogenesis (Shawber et al. 2007; Thomas et al. 2013). Another study on tumor lymphangiogenesis also indicated that CCAAT/enhancer-binding protein-δ (C/EBP-δ) might influence both VEGF-C and VEGFR3 expression in LECs and therefore contributes to the regulation of VEGFR3 signaling (Min et al. 2011). Another very interesting player in the regulation of VEGFR signaling in general is the tumor necrosis factor superfamily-15 (TNFSF15), which e.g. simultaneously downregulates plasma bound VEGFR1 levels and upregulates soluble VEGFR1 in vascular endothelial cells. Thereby, as it has been described for the mechanism of maintaining corneal clarity above, signals switch from pro-angiogenic to anti-angiogenic. Interestingly, TNFSF15 could be shown to stimulate VEGFR3 expression and signaling in LECs (reviewed in (Yang and Li 2018)). Furthermore, the matrix metalloproteinase (MMP)-9 might be involved in the regulation of VEGFR3 expression, as MMP-9 inhibition after induction of corneal inflammation, a process which usually triggers lymphangiogenesis, reduced VEGFR3 expression levels and corneal lymphangiogenesis (Du et al. 2017). Accordingly, lymphatic drainage capacity in mouse secondary lymphedema models was further reduced upon deletion of MMP-9 (Rutkowski et al. 2006).

3.6 The IPP complex and its association with β1 integrin

3.6.1 Integrin-linked kinase (ILK) is the center of the IPP complex

As β1 integrins are intracellularly bound to several proteins and protein complexes (Giancotti and Ruoslahti 1999), it is likely that one of those proteins or complexes might be involved in regulation of β1 integrin mediated VEGFR3 signaling. One of those candidates is the integrin-linked kinase (ILK) which functions as the central part of a protein complex called ILK/PINCH/parvin complex (IPP complex) (Tu et al. 2001; Legate et al. 2006). ILK is reported to be a pseudokinase with no catalytic capacity (Hanks et al. 1988; Fukuda et al. 2009; Wickstrom et al. 2010) and scaffolds the (in)direct integrin-actin connection. Therefore, ILK binds to β1 integrin with its C-terminal kinase-like domain (Hannigan et al. 1996) while on the other hand, ILK binds adapter proteins with connection to the F-actin cytoskeleton (Figure 8) (Boudeau et al. 2006; Dobreva et al. 2008; Wickstrom et al. 2010). This is why ILK is supposed to play an essential role in microtubule organization, cell-matrix and focal adhesions, cell spreading as well as cell migration and cell survival (reviewed in (Legate et al. 2006; Qin and Wu 2012) and (Widmaier et al. 2012)).

In vivo analyses of ILK in mice revealed that global genetical deletion of *Ilk* is embryonic lethal between embryonic day (E) E5.5 and E6.5 (Sakai et al. 2003), by which it is comparable to the deathly consequences of global embryonic *Itgb1* deletion (Fassler and Meyer 1995; Stephens et al. 1995). Furthermore, deletion of *ILK* was shown to cause caveolin-1 mislocation and thus impact RTK signaling (Malan et al. 2013). For the study of ILK's role in VEGFR3 signaling, endothelial cell specific *Ilk* deletion in mouse embryos, as well as inducible endothelial cell-specific *Ilk* deletion in the adult mouse system were performed (both referred to as 'ILK K.O.') (Urner et al. 2019). As the endothelial cell-specific deletion of *Itgb1* caused a dramatic reduction in VEGFR3 signaling and lymphatic vascular growth (Planas-Paz et al. 2012) a comparable phenotype upon deletion of the β1 integrin adaptor protein *Ilk* has been hypothesized. Surprisingly, experiments revealed ILK as a critical regulator of VEGFR3 signaling (Urner et al. 2019). This conclusion was supported by the results that VEGFR3 phosphorylation, as well as LEC proliferation and lymphatic vascular growth were significantly increased in the ILK K.O., both in the adult and the embryonic model. Even the usually avascular corneas of adult *Ilk* deficient mice revealed lymphatic vessels growing in from the highly vascularized limbus. Induction of myocardial infarction (MI) in these mice caused increased lymphatic vascular expansion when compared to wild-type mice upon MI (Urner et

al. 2019). Further, endothelial cell-specific *Itgb1* deletion on top of endothelial cell-specific *Ilk* deletion in mouse embryos genetically 'rescued' the ILK phenotype. Therefore, we concluded that ILK regulates VEGFR3 signaling in mice, in a β1 integrin dependent manner (Urner et al. 2019).

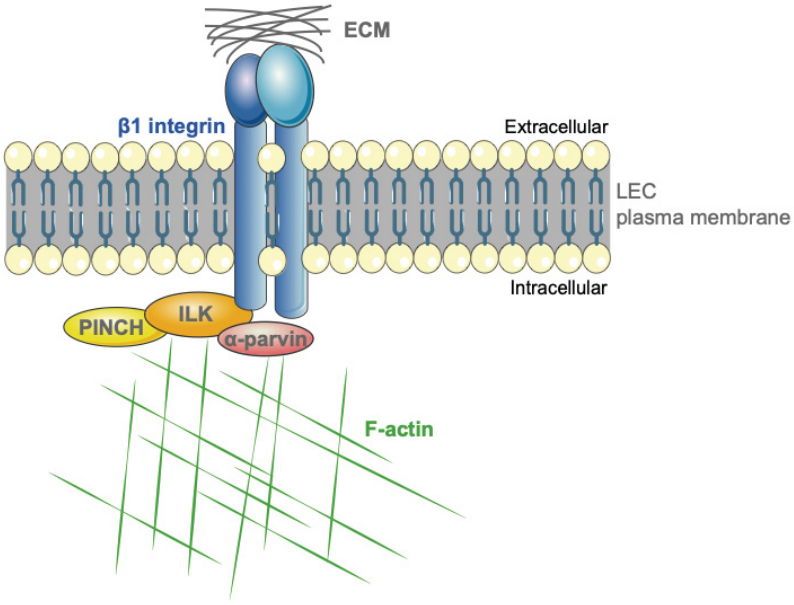

Figure 8: The ILK/PINCH/parvin (IPP) complex connects β1 integrin to the F-actin cytoskeleton of LECs.
The mechanosensor β1 integrin is able to transduce signals from the extracellular matrix (ECM) towards the F-actin cytoskeleton of lymphatic endothelial cells (LECs), as well as it transduces signals from the F-actin cytoskeleton towards the ECM . Therefore, β1 integrin binds to components of the ECM with its extracellular part, while the intracellular tail of β1 integrin is (in)directly connected to the F-actin cytoskeleton. This connection can be facilitated by the IPP complex, with ILK being the central part which interacts with β1 integrin and α-parvin binding to the F-actin cytoskeleton. Modified Figure 6 of Sofia Urner's dissertation (Urner 2018a) using Servier Medical Art and used under the free-to-use Creative Commons Attribution 3.0 Unported License.

Most functions of ILK nevertheless critically depend on the successful IPP complex formation, thus on ILK's binding to particularly interesting new cysteine-histidine-rich proteins (PINCH) and parvin. Successful complex formation ensures the stability of each complex member (Zhang et al. 2002b; Fukuda et al. 2003a). With both of ILK's complex partners having additional adapter proteins, the complex is consequently involved in many cellular functions and of high interest (Figure 8) (Legate et al. 2006).

3.6.2 PINCH and parvin complete the IPP complex

Two isoforms of PINCH exist that are able to interact with the C-terminal domain of ILK, but only one isoform can form this connection at a time (Legate et al. 2006). Both PINCH-1 and PINCH-2 are expressed throughout several tissues and are required for ILK to localize properly at focal adhesion sites (Li et al. 1999; Velyvis et al. 2001; Zhang et al. 2002b; Zhang et al. 2002c; Zhang et al. 2002a; Braun et al. 2003). Loss of *Pinch-1*, but not of *Pinch-2* causes embryonic lethality between E6.5 and E7.5 (Li et al. 2005; Liang et al. 2005; Stanchi et al. 2005), an effect which seem similar to the embryonic lethality upon loss of *Ilk* (Sakai et al. 2003). Interestingly, *Pinch-1* expression was found to be upregulated upon loss of *Pinch2*, thus suggesting overlapping functions or a compensatory mechanism between the isoforms (Stanchi et al. 2005).

The third IPP complex member is parvin, a protein with three mammalian isoforms of different distribution throughout the human tissues. The parvin family is divided into α-, β- and γ-parvin, of which α-parvin (Parva), also known as actopaxin or CH-ILKBP (Nikolopoulos and Turner 2000; Tu et al. 2001), seems to be the most important. While the highest β-parvin expression is to be found in the heart and skeletal muscles, γ-parvin expression is restricted to hematopoietic cells (Korenbaum et al. 2001; Yamaji et al. 2001). ILK is able to bind all three isoforms of the parvin family, by which it indirectly connects to the F-actin cytoskeleton (Nikolopoulos and Turner 2000; Olski et al. 2001; Yamaji et al. 2004). Out of all the ILK binding proteins, α-parvin reveals the most specific interaction with ILK (Dobreva et al. 2008). It is further expressed in almost all tissues (Korenbaum et al. 2001; Olski et al. 2001) and does not only bind F-actin filaments directly but also indirectly via F-actin binding protein paxillin (Nikolopoulos and Turner 2000). Global genetic deletion of *Parva* results in embryonic lethality between E10.5 and E14.5 due to severe cardiovascular issues. *Parva*-deficient embryos e.g. reveal dilated blood vessels, hemorrhages and severe edema (Montanez et al. 2009). Endothelial cell-specific deletion of *Parva* shifts the embryonic lethality to E14.5 onwards, but *Parva*-deficient embryos also reveal cardiovascular abnormalities and hemorrhages (Fraccaroli et al. 2015). These findings indicate that α-parvin is important for endothelial functions. Detailed analyses of the first lymphatic tissues in *Parva*-deficient embryos further supported this hypothesis. The first lymphatic structures in mouse embryos are the jugular lymph sacs (jls) or primordial thoracic ducts (pTD) (referred to as ‘jls/pTD’). In *Parva*-deficient embryos the jls/pTD showed an increased LEC proliferation and LEC number, as well as increased VEGFR3 signaling, all pointing towards a role of α-parvin in LECs and lymphangiogenesis (Urner et al. 2019).

Summarizing it is to say that IPP complex members – especially ILK and α-parvin – link the ECM via β1 integrin to the F-actin skeleton and thereby provide crucial cellular functions for β1 integrin signaling in LECs (Figure 8). As *in vivo* findings of IPP complex functions in endothelial cells of mice are very promising, it is likely that they also play a role in human endothelial cells.

3.7 β-site of amyloid precursor protein cleaving enzymes (BACE)

3.7.1 The amyloidogenic pathway in the brain requires β-site of amyloid precursor protein cleaving enzyme 1 (BACE1) and γ-secretase

Alzheimer's disease (AD) is a neurodegenerative disease leading to dementia (Kang et al. 2017) and there are several hypotheses explaining its development (Du et al. 2018). In one of these hypotheses, the β-site of amyloid precursor protein cleaving enzyme (BACE) family members are of special interest, because they are described to play a crucial role in AD development and worsening (Selkoe and Hardy 2016). In detail, this hypothesis describes AD to be caused by the formation of amyloid plaques (Wisniewski and Silverman 1997) due to the accumulation of β-amyloid (Selkoe and Hardy 2016; Zhang and Song 2017). During this so called amyloidogenic pathway, the amyloid precursor protein (APP) is first cleaved by β-site APP cleaving enzyme 1 (BACE1) to release either C-terminal fragment C89 or C99, depending on the β-cleavage site (Deng et al. 2013; Zhang et al. 2017). C99 is further cleaved by γ-secretase to shed the N-terminal fragment called β-amyloid (Figure 9) (Schenk et al. 1995; Selkoe et al. 1996; Zhang et al. 2017). With this, γ-secretase is of main responsibility for the generation of β-amyloid (Selkoe 1994; Szaruga et al. 2017; Voytyuk et al. 2018a) from APP and has therefore previously been targeted in order to lower β-amyloid production in the brain (De Strooper and Chavez Gutierrez 2015). Unluckily, the targeting of γ-secretase in clinical trials caused severe side effects and therefore the studies had to be dropped (Doody et al. 2013; De Strooper 2014).

Together with its family member γ-secretase, BACE1 facilitates the generation of β-amyloid from APP (De Strooper et al. 1998; Vassar et al. 1999; Hardy and Selkoe 2002). BACE1 is an integral membrane protein and a member of the pepsin family (Haniu et al. 2000), which mainly expressed in the brain (Bennett et al. 2000), as well as in the BBB endothelium and is further upregulated during AD (Devraj et al. 2016).

Therefore, BACE1 is considered to be the most promising target for AD treatment (Cole and Vassar 2007; Yan and Vassar 2014; Vassar et al. 2014; Barao et al. 2016). A *Bace1* deficient mouse model for AD did not reveal any β-amyloid in the brain (Luo et al. 2001; Cai et al. 2001) and pharmacological inhibition of BACE1 further highlighted BACE1 as a potential target for AD treatment (Chen et al. 2012; Ly et al. 2013). BACE inhibition by use of the inhibitor NB-360 e.g. was sufficient to reduce β-amyloid amounts, as well as neuroinflammation and other pathogenic conditions related to AD in an AD mouse model (Neumann et al. 2015; Keskin et al. 2017).

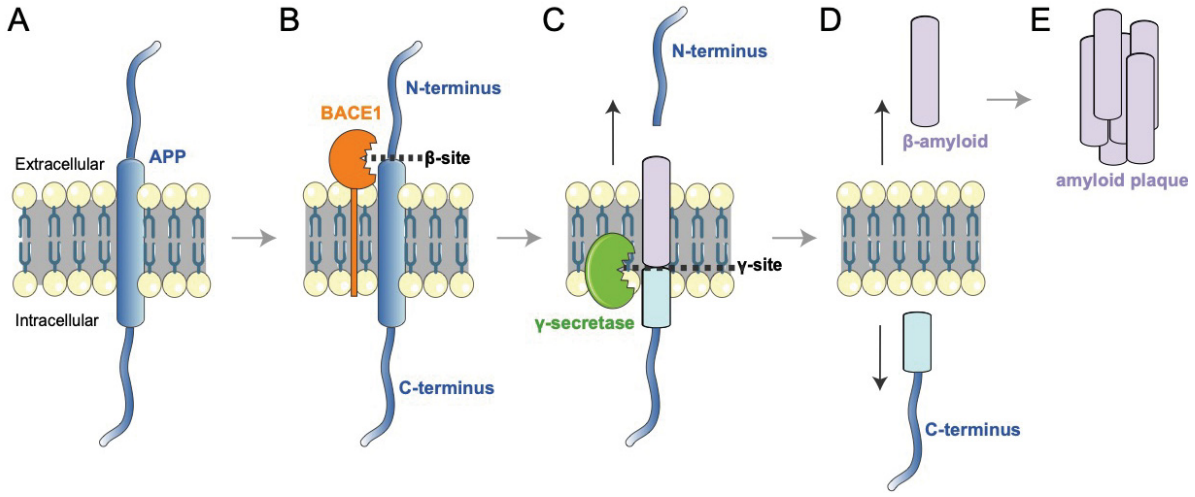

Figure 9: Simplified schematic overview of the amyloidogenic pathway.
(**A,B**) During the amyloidogenic pathway, the amyloid precursor protein (APP) is cleaved by β-site APP cleaving enzyme (BACE1) at its β-site. (**C**) This process separates the N-terminal from the C-terminal domain and the latter can be shed by γ-secretases at the respective γ-site. (**D**) The remaining C-terminus is released into the cytosol, while the shedded part of the transmembrane domain facing the extracellular site is released as β-amyloid. (**E**) Accumulated β-amyloid builds amyloid plaques, causing dementia. Modified from Servier Medical Art and used under the free-to-use Creative Commons Attribution 3.0 Unported License.

Nevertheless, BACE1 has different other substrates amongst APP (Kuhn et al. 2012; Zhou et al. 2012; Dislich et al. 2015), which makes it risky to cause side effects upon targeting BACE1 as an AD treatment. Due to its close homology to BACE2, many recently developed BACE1 inhibitors also target BACE2 (Bennett et al. 2000; Farzan et al. 2000; Alexander et al. 2014; Neumann et al. 2015; Kennedy et al. 2016; Scott et al. 2016; Cebers et al. 2017) and therefore probably cause BACE2 inhibition related side effects. One of the BACE1 inhibitors tested in phase III clinical trials is Merck's verubecestat or MK-8931, shown to decrease β-amyloid amounts both in treated mice brains and human AD patients. Nonetheless, it also targets BACE2 and treatment of AD patients with verubecestat caused severe side effects (Kennedy et al. 2016; Scott et al. 2016). Reported side effects of verubecestat treatment were increased

risk for falls or injuries, as well as rash, hair color change, weight loss, sleep disturbances and suicidal ideation. The treatment further did not improve clinical ratings of dementia in patients and the outcome worsened upon increased verubecestat dosage, so that cognition and daily function of AD patients upon verubecestat treatment was worse when compared to the placebo treated control group (Egan et al. 2019b; Egan et al. 2019a; Egan et al. 2018). Consequently, these clinical trials were stopped (Hawkes 2017).

3.7.2 BACE2 has several functions in different tissues

BACE2 shares 45% of BACE1's amino acid residues, as well as the feature of being a type I transmembrane protein in the pepsin family of aspartyl proteases (Bennett et al. 2000). Despite of this homology, the expression patterns of BACE1 and BACE2 differ from each other. BACE2 expression is to be found in several peripheral tissues such as the colon, kidney and also in the pancreas (Bennett et al. 2000). BACE2 is involved in melanosome formation in pigment cells (Rochin et al. 2013) and this is why BACE2 deficient mice appear to have a depigmented fur color (Dominguez et al. 2005). Direct pharmacological inhibition of BACE2, as well as indirect BACE2 inhibition via unspecific inhibition of BACE1 also caused this phenotype in preclinical trials (Cebers et al. 2016; Shimshek et al. 2016; Voytyuk et al. 2018a). Further examination of BACE2 distribution later revealed that BACE2 is also expressed in parts of the CNS, including subsets of neurons, oligodendrocytes and astrocytes (Voytyuk et al. 2018b).

Nevertheless, due to the structural homology between BACE1 and BACE2, BACE2 was suggested to be a second β-site APP cleaving enzyme (Yan et al. 1999; Farzan et al. 2000; Lin et al. 2000). Later studies however demonstrated that BACE2 cleaves APP within the β-amyloid domain and thereby prevents β-amyloid generation (Sun et al. 2006), speaking against the hypothesis of BACE2 being a β-secretase (Yan et al. 2001; Fluhrer et al. 2002; Basi et al. 2003). Only a damage of APP's juxtamembrane helix (JH) can trigger a β-secretase activity of BACE2, hence labeling it a conditional β-secretase (Wang et al. 2019). JH damage can e.g. happen due to binding of clusterin, a neuronal chaperone (McGeer et al. 1992), to the JH of APP (Wang et al. 2019). Clusterin is considered a top 3 sporadic AD risk gene (Wang et al. 2019), because it is induced by multiple AD risk factors and is further upregulated during AD (May et al. 1990; Kida et al. 1995; Lidstrom et al. 1998; Beeg et al. 2016). Interestingly, the β-secretase activity and BACE2 expression, as well as clusterin expression are upregulated during aging, while BACE1 expression is not altered (Fukumoto et al. 2004). The combination of these findings point into the direction, that BACE2 is responsible for the

increase in β-secretase activity of aging brains, due to increased clusterin expression (Wang et al. 2019). This hypothesis is further supported by the increased BACE2 activity during preclinical AD, correlating with AD pathogenesis (Holler et al. 2012). In its function as a protease, BACE2 has several different substrates depending on the tissue type it is expressed in. In the CNS, BACE2 cleaves vascular cell adhesion molecule 1 (VCAM1), delta and notch-like epidermal growth factor-related receptor (DNER), fibroblast growth factor receptor 1 (FGFR1) and plexin domain containing 2 (PLXDC2) (Voytyuk et al. 2018b). Interestingly, the study on BACE2 distribution throughout the brain also highlighted a connection between BACE2 activity and Alzheimer's disease. Vyotyuk et al. found the cleavage of VCAM1 by BACE2 to be strongly upregulated both *in vitro* and *in vivo* upon inflammatory conditions (Voytyuk et al. 2018b), an environment which is also present in the periphery and brains of AD patients (Akiyama et al. 2000; Sastre et al. 2006; Wang et al. 2015; Lai et al. 2017).

In the periphery, BACE2 processes e.g. melanocyte protein in pigment cells (Rochin et al. 2013) and islet amyloid polypeptide (IAPP) in the pancreas (Rulifson et al. 2016; Alcarraz-Vizan et al. 2017). In the latter, BACE2 is involved in the regulation of β-cell mass and function (Esterhazy et al. 2011), but also in the regulation of glucose tolerance and β cell survival (Rulifson et al. 2016; Alcarraz-Vizan et al. 2017). Therefore, BACE2 might be a target for diabetes treatment (Esterhazy et al. 2011; Stutzer et al. 2013). Detailed analyses of the mechanisms, how BACE2 impacts diabetic conditions, revealed that it is involved in the pancreatic amyloidogenic pathway (Alcarraz-Vizan et al. 2017). Thereby, BACE2 mediated processing of IAPP and the latter's misfolding and accumulation causes the formation of amyloid plaques in type 2 diabetes (Mukherjee et al. 2015; Cooper et al. 1987; Clark et al. 1996). This formation of amyloid plaques in the pancreas causes an increase in the abundance of reactive oxygen species (ROS) (Zraika et al. 2009). In LECs of diabetic mice, ROS could be shown to both mediate VEGFR3 phosphorylation and degradation in the Golgi apparatus, reducing VEGFR3 availability at the plasma membrane in an epsin dependent manner (Wu et al. 2018). Epsins are known to be involved in several endocytic processes. In LECs, epsins 1 and 2 interact with VEGFR3 and thereby induce its internalization and degradation (Liu et al. 2014). According to this, the increased ROS production due to BACE2 mediated amyloid accumulation causes a reduced VEGFR3 abundance at the LEC surface and hence the reactivity of VEGFR3 to possible ligand binding by VEGF-C or -D is decreased. As a result, lymphangiogenesis is impaired under diabetic conditions, a phenotype which could be rescued by genetical deletion of epsin 1 and 2 in diabetic mice (Wu et al. 2018).

In summary, the BACE proteases are critically involved in amyloid plaque formation and therefore in AD and type 2 diabetes development and worsening. While γ-secretase and BACE1 are mainly responsible for APP processing to neurotoxic β-amyloid in the brain, BACE2 has several peripheral substrates and only functions as a conditional β-secretase upon AD conditions. In the periphery, BACE2 is involved in a pancreatic amyloidogenic pathway and thereby indirectly in the regulation of lymphangiogenesis under diabetic conditions. Therefore, unintentional BACE2 inhibition by unspecific BACE1 inhibitors is likely to cause peripheral side effects.

3.8 Aims of this study

Regulation of VEGFR3 signaling in LECs is required to prevent the lymphatic vasculature from uncontrolled overgrowth and to maintain its physiological functions. One way to activate VEGFR3 signaling is its interaction with the mechanoreceptor β1 integrin, triggered by mechanical stimuli. This is why injection of additional fluid into mouse embryos morphologically stretched the LECs and thereby induced both VEGFR3 phosphorylation and LEC proliferation, resulting in enlarged jls/pTDs as a sign for increased lymphatic vascular growth. Further, genetical deletion of *Itgb1* in endothelial cells of mice dramatically reduced VEGFR3 signaling and lymphatic vascular growth (Planas-Paz et al. 2012). ILK is an intracellular adapter protein of β1 integrin which forms the IPP complex together with PINCH and parvin and thereby connects β1 integrin to the F-actin cytoskeleton. Previous investigations questioned whether genetical deletion of *Ilk* would result in similar issues with regards to VEGFR3 signaling and vascular growth as it could be shown for *Itgb1* deficient mice. Surprisingly, endothelial cell specific deletion of *Ilk* resulted in the opposite phenotype; VEGFR3 signaling was strongly increased, as it was LEC proliferation and lymphatic vascular growth. Therefore, we concluded that ILK functions as a critical regulator of VEGFR3 signaling in mice (Urner et al. 2019). The endothelial cell specific deletion of *Parva* in mouse embryos further revealed that α-parvin contributes to the regulation of VEGFR3 signaling. We found increased VEGFR3 phosphorylation, LEC proliferation and enlarged jls/pTD, even though this phenotype was milder than the ILK phenotype (Urner et al. 2019). Nevertheless, little was known about the role of the IPP complex in adult human LECs and human VEGFR3 signaling and therefore one main aim of this thesis was to determine whether the IPP complex would be an intracellular mechanism to attenuate VEGFR3 activity in the human system.

On the other hand, BACE1 is meant to play an impelling role in the development and worsening of Alzheimer's disease (AD) (Cole and Vassar 2007). This is why several companies are currently developing inhibitors against this β-secretase, but BACE1 inhibition with inhibitors such as verubecestat caused severe side effects in human patients. One reason for these side effects might be the unintended inhibition of BACE1's close homologue BACE2 (Egan et al. 2018; Egan et al. 2019a). The latter works as a conditional β-secretase in the brain (Wang et al. 2019) and therefore plays no major role in AD, but still has several peripheral substrates which might be impaired by BACE2 inhibition. For this reason, institutions are aiming to both discover more specific inhibitors against BACE1, but also to uncover additional substrates of BACE2. Those substrates could function as a potential read-out to shed light on the specificity of the newly developed inhibitors and therefore to prevent adverse effects caused by unintentional BACE2 inhibition. On the search for potential substrates of BACE2, the group of Prof. Dr. Lichtenthaler at the DZNE e.V. in Munich found VEGFR3 to be altered upon BACE inhibition and in *Bace2* deficient mice, but not in *Bace1* deficient mice (unpublished data). Since VEGFR3 is known to be primarily expressed on LECs, the question arose, whether side effects of verubecestat treatment would be caused due to unintended BACE2 inhibition causing VEGFR3 alterations and impairment of lymphatic drainage capacity. By now, little is known about VEGFR3 as a possible BACE2 substrate and more importantly, whether BACE2 might attenuate VEGFR3 signaling in human LECs. As we provide an established *in vitro* cell culture of adult human LECs, we aimed to support the Lichtenthaler group with answering these questions. Consequently, the major aim of this thesis was to analyze the attenuation of VEGFR3 activity in adult human LECs, both via intracellular and extracellular mechanisms.

4. Experimental procedures

4.1 *In vitro* methods

4.1.1 Adult human LEC culture and transfections

All *in vitro* studies were performed with primary adult human dermal microvascular LECs (either HMVEC-dLyAd by Lonza, CC-2810 or HDLEC-c adult by PromoCell, C-12217). For this purpose, LECs were cultured in endothelial cell growth medium (EGM-2, PromoCell or Lonza) at 37°C, 5% CO_2 atmosphere in a humidified incubator. LECs were used at passages ≤ P7 with a confluence of 80-90% and for all transfections, the 4D Nucleofector System™ (Lonza) was used. To achieve knockdowns of either *ILK*, *PARVA, BACE1* or *BACE2,* LECs were transfected with three different stealth siRNAs (Invitrogen), respectively as listed below. As control, non-targeting siRNAs with similar GC contents as the used stealth siRNAs were used (Invitrogen). Stealth siRNAs and control siRNAs were transfected to 500.000 LECs per transfection in the listed concentrations:

Target	siRNA	siRNA sequence (5'→3')	Concentration
ILK	ILK 1	GCCUGUGGCUGGACAACACGGAGAA	500 nM
	ILK 2	CAGCCAGUCAUGGACACCGUGAUAU	
	ILK 3	GCAUUGACUUCAAACAGCUUAACUU	
PARVA	PARVA 1	CAAGCUGAAUGUGGUGAAA	100 nM
	PARVA 2	CCUGAAAUCUACACUACGA	
	PARVA 3	GAACUGAUGAAGGUAUUAA	
BACE1	BACE1 1	GGGUGGAGAUCAAUGGACAGGAUCU	100 nM
	BACE1 2	UCCCAGUCAUCUCACUCUACCUAAU	
	BACE1 3	GCAGCUUUGUGGAGAUGGUGGACAA	
BACE2	BACE2 1	GGACCAACGGAGGUAGUCUUGUCUU	100 nM
	BACE2 2	GCCUUAAUCUGGACUGCAGAGAGUA	
	BACE2 3	GCUCAGUCUUUGAGCGAGCCCAUUU	

Transfected LECs were subsequently resuspended in fresh EGM-2 MV and distributed into previously coated cell culture dishes. Coating was performed with fibronectin in a concentration of 2.5 µg/cm^2 (Human Plasma Fibronectin Purified Protein, Millipore).

For stainings and proliferation assays, LECs were plated on fibronectin coated coverslips (VWR), while for quantitative real-time PCR or Western Blotting LECs were cultured on fibronectin coated tissue culture plates (SARSTEDT or VWR). After an incubation of 48-72 hours LECs were used for further analyses (see 4.1.5 – 4.4.1).

For co-immunoprecipitation (Co-IP) (see 4.3.1) after mechanical stretch experiments, human LECs were transfected with a plasmid encoding the expression of C-terminally Human influenza hemagglutinin (HA)-tagged β1 integrin (Sino Biological, HG10587-CY). The plasmid was previously transformed into DH5α competent cells (Invitrogen), and amplified using a QIAGEN Plasmid Midi Kit according to the manufacturer's protocol. Afterwards, 1 µg plasmid was used for transfection of 500.000 human LECs. Cells were subsequently distributed into fibronectin-coated STREX stretch chambers (BioCat, ST-CH-04-BR), and used for mechanical stretch experiments 48 hours after transfection (see 4.1.2).

4.1.2 *In vitro* mechanical stretch experiments

For mechanical stretch experiments, STREX stretch chambers (BioCat, ST-CH-04-BR) were coated with fibronectin in a concentration of 2.5 µg/cm^2 (Human Plasma Fibronectin Purified Protein, Millipore). Cultured LECs and LECs transfected with the (HA)-tagged β1 integrin plasmid (see 4.2.1) were distributed into stretch chambers and left to attach o/n before mechanical stretch was carefully induced the next day. Upon the maximum level of stretching, LECs were kept in culture for 30 – 120 minutes. Afterwards, the chambers were left in stretched conditions and immediately put on ice for subsequent RNA isolation, cell lysis or stainings (see 4.2.1, 4.3.1, 4.3.3 and 4.4.1).

4.1.3 *In vitro* inhibitor treatments

For inhibitor treatments, LECs were cultured as described in 4.2.1 and distributed to fibronectin coated (Human Plasma Fibronectin Purified Protein, Millipore, 2.5 µg/cm^2) cell culture plates or coverslips as required for the respective analyses (4.1.5, 4.2.1, 4.3.3, 4.4.1). Adherent LECs were treated for 6 – 24h with the respective inhibitor diluted in endothelial growth medium (EGM-2, PromoCell or Lonza). Following inhibitors were used:

Inhibitor	Concentration
β-Secretase Inhibitor IV – CAS 797035-11-1 (Calbiochem, 565788)	500 nM
Verubecestat – CAS 1286770-55-5 (provided by the Institute of Neuroproteomics, DZNE Munich)	100 nM

As control, DMSO was diluted in EGM-2 in the same concentration as in the treatment medium. After the treatment, cells were briefly washed with PBS (Gibco® by Life Technologies™) and placed on ice for subsequent RNA isolation, cell lysis or staining (see 4.1.5, 4.2.1, 4.3.3, 4.4.1).

4.1.4 *In vitro* treatments with recombinant proteins

For treatment with BACE recombinant proteins, LECs were cultured as described in 4.2.1 and distributed to fibronectin coated (Human Plasma Fibronectin Purified Protein, Millipore, 2.5 µg/cm^2) cell culture plates. Once LECs were attached, they were treated for 6 hours with 250 ng/ml Recombinant Human BACE-2 Protein, CF (R&D Systems, 4097-ASB-020) diluted in endothelial growth medium (EGM-2, PromoCell or Lonza), which was renewed after 6 hours of incubation, if treatment was necessary for a longer period of time. As a control, EGM-2 only was used, because the recombinant proteins were solved in dH2O. After the treatment, cell culture plates were put on ice and LECs could be lysed for Western Blotting (see 4.3.3).

4.1.5 *In vitro* proliferation assays

Proliferation of *in vitro* cultured adult human LECs was determined by performing 5-bromo-2'-deoxyuridine (BrdU) incorporation assays. After transfections and the incubation time of 48 hours, medium was removed and LECs were incubated with 10 µM BrdU (Sigma) and 100 ng/ml VEGF C156S (R&D Systems, 752-VC-025) diluted in endothelial basal medium (EBM-2, PromoCell or Lonza) for 1-3 hours. For the case of inhibitor treatments, the BrdU incorporation was performed during the inhibitor treatment. First, a pre-incubation of 3 hours with the respective inhibitor or DMSO control diluted in endothelial growth medium (EGM-2, PromoCell or Lonza) was performed. Afterwards, 10 µM BrdU (Sigma) were added to the EGM-2 containing the respective inhibitor or DMSO control. After a brief shaking, LECs were incubated for additional 3 hours.

After the respective incubation time, LECs were fixed with ethanol fixative, consisting of 70% absolute ethanol (Honeywell Riedel-de Haen) and 30% glycine (50 nM, AppliChem), for 20 minutes on ice. For cell denaturation, LECs were incubated with 2M HCl (Sigma- Aldrich) for 20 minutes at room temperature (RT), followed by a neutralization step with 0.1M sodium tetraborate (pH 8.5, Aldrich Chemistry) for 2 minutes at RT. In between, cells were washed with buffer containing 0.5% bovine serum albumin (BSA, AppliChem) in PBS (Gibco® by Life Technologies™), which was further used for antibody dilutions. Following primary and secondary antibodies were used:

Primary antibody	Dilution	Secondary antibodies	Dilution
Mouse anti-BrdU (BD Bioscience, 555627)	1/500	Donkey anti-mouse AF488-conjugated (Molecular probes)	1/500
		DAPI (Sigma)	1/1000

Cells were incubated under agitation with primary antibody for 1 hour (at RT), while the secondary antibody was incubated for 30 minutes at RT, also under agitation. In addition, DAPI was used to counterstain cell nuclei. Coverslips were mounted with Fluoroshield™ (Sigma), and subsequently analyzed by use of Fluorescence microscopy (Zeiss LSM 710) and the ImageJ/Fiji software. Proliferation rates of each condition were determined by the number of BrdU-positive LECs divided by the total number of LECs.

4.2 Molecular biological methods

4.2.1 Quantitative real-time PCR

For analysis of knockdown efficiencies and treatment effects *in vitro*, human LECs were briefly washed with PBS (Gibco® by Life Technologies™) and RNA was isolated by use of High Pure RNA Isolation Kit (Roche) according to manufacturer's protocol. The subsequent cDNA synthesis was performed using SuperScript™ II Reverse Transcriptase (Invitrogen by Thermo Fisher Scientific) according to manufacturer's protocol.

Following master-mix was used for quantitative real-time PCR per sample:

5 µl Mix1 (FastStart Essential DNA Green Master, Roche)
2 µl Primer-Mix (fwd and rev, pre-diluted to 3µM, see below)
2 µl dH_2O (Mix2, FastStart Essential DNA Green Master, Roche)
1 µl cDNA

Primers with following sequences were used:

Primer	Primer sequences
Human *ILK* (Eurofins)	fwd: 5'- AAG GTG CTG AAG GTT CGA GA -3'
	rev: 5'- ATA CGG CAT CCA GTG TGT GA -3'
Human *PARVA* (Eurofins)	fwd: 5'- TTC TTG GGG AAA CTC GGA GG -3'
	rev: 5'- TCT TGA AGC TTG GGG TCA CT -3'
Human *BACE1* (Eurofins)	fwd: 5'- GGT GGA GAT CAA TGG ACA GG -3'
	rev: 5'- CGT GGA TGA CTG TGA GAT GG -3'
Human *BACE2* (Eurofins)	fwd: 5'- TGG AGA CCT TCT TCG ACT CCC TGG -3'
	rev: 5'- TCC ACC CAA GAC AAG ACT ACC TCC G -3'
Human VEGFR3 (Eurofins)	fwd: 5'- CAA CAG ACC CAC ACA GAA CT -3'
	rev: 5'- TTT CCA TCC TTG TAC CAC TG -3'
Human *B2M* (Eurofins)	fwd: 5'- TTT CAT CCA TCC GAC ATT GA -3'
	rev: 5'- CCT CCA TGA TGC TGC TTA CA -3'
Human *HPRT1* (Eurofins)	fwd: 5'- AAA-TTC-TTT-GCT-GAC-CTG-CTG -3'
	rev: 5'- TGA-CCA-AGG-AAA-GCA-AAG-TCT-G -3'
Human *RPLP0* (Eurofins)	fwd: 5'- GAA-GAC-AGG-GCG-ACC-TGG-AA -3'
	rev: 5'- CCA-CAT-TGT-CTG-CTC-CCA-CA -3'

Quantitative real-time PCR was run on the LightCycler Nano Device (Roche) with following protocol:

Step	Repetition	Temperature	Duration
Pre-Incubation	1x	95 °C	10 min
Amplification	45x	95 °C	20 sec
		60 °C	20 sec
		72 °C	20 sec
Melting (initial stage)	1x	65 °C	60 sec
Melting (final stage)	1x	95 °C	1 sec

All experiments were performed in duplicates or triplicates. For analysis of knockdown efficiencies and general effects of treatments on mRNA levels, acquired mRNA levels were always at least normalized to the housekeeping gene *beta-2-microglobulin* (*B2M*). Quantitative real-time PCRs in experiments dealing with BACE inhibition were even performed with two additional housekeeping genes *ribosomal phosphoprotein P0* (*RPLP0*) and *hypoxanthine phosphoribosyltransferase* (*HPRT1*).
For all analyses, the comparative CT method was used, in which 2-ΔCT is presented (with ΔCT defined as CT gene of interest – CT housekeeping gene), as previously described (Livak and Schmittgen 2001; Schmittgen and Livak 2008).

4.3 Biochemical methods

4.3.1 Co-immunoprecipitation (Co-IP)

Co-immunoprecipitation (Co-IP) experiments were performed with LECs that were previously transfected with HA-tagged β1 integrin plasmids. Transfected LECs were placed on stretch chambers and allowed to attach o/n at 37°C, 5% CO_2, as described in 4.1.2. The next day, transfected LECs were stretched for 30 minutes and afterwards kept on ice for a brief washing with PBS (Gibco® by Life Technologies™). LECs were immediately lysed in following lysis buffer (300 µl / chamber) for 20 minutes on ice:

50 mM HEPES pH 7.0 (Fisher Scientific)
150 mM NaCl (Fisher Chemical)
10% glycerol (Roth)
1% Triton X-100 (AppliChem)
1 mM Na3VO4 (Aldrich)
1x cocktail of protease inhibitors (25x, Roche)
1x cocktail of phosphatase inhibitors (10x, Roche or 100x, Sigma)
in dH2O

LECs were scraped off the chambers using cell scraper (SARSTEDT), and lysates were centrifuged for 10 minutes at 13.000rpm at 4°C. The supernatants were collected and protein concentrations were determined using the Pierce™ BCA Protein Assay (Thermo Fisher Scientific). 300 µg protein of each sample were taken for a pre-clearing step with 30 µl Protein G Plus/Protein A Agarose Suspension (Millipore, IP05-1.5ml) for 1 hour at 4°C under rotation.

After centrifugation for 10 minutes at 5.000g and 4°C, supernatants were incubated with 3 µl rabbit anti-HA tag antibody (Cell Signaling, 3724) at 4°C o/n under rotation. On the next day, 15 µl Protein G Plus/Protein A Agarose Suspension were added to the lysates, and incubated for 3 hours at 4°C under rotation. Afterwards, supernatants were removed. The remaining beads were washed three times using the lysis buffer and short centrifugation steps (1 minute at 5.000g, 4°C) in between, in which the supernatants were discarded. For Western Blotting, beads were finally collected in 2x Laemmli buffer following the protocol described in 4.3.3.

4.3.2 ELISA

To determine VEGFR3 tyrosine phosphorylation levels in adult human LEC lysates, transfected LECs were starved after their required incubation time o/n in EBM-2 (0.5% Fetal Bovine Serum, FBS, Gibco® by Life Technologies™), washed with PBS (Gibco® by Life Technologies™), and stimulated with 100 ng/ml VEGF-C156S (R&D Systems, 752-VC-025) diluted in EBM-2 only (PromoCell or Lonza). After 5 minutes of incubation, cells were put on ice, immediately washed with ice-cold PBS (Gibco® by Life Technologies™), and incubated with lysis buffer on ice:

50 mM HEPES pH 7.0 (Fisher Scientific)
150 mM NaCl (Fisher Chemical)
10% glycerol (Roth)
1% Triton X-100 (AppliChem)
1 mM Na3VO4 (Aldrich)
1x cocktail of protease inhibitors (25x, Roche)
1x cocktail of phosphatase inhibitors (10x, Roche or 100x, Sigma)
in dH2O

After 30 minutes of incubation, lysates were scratched off the plates and centrifuged for 10 minutes at 13.000rpm at 4°C, supernatants were collected. Protein content was subsequently determined using the Pierce™ BCA Protein Assay (Thermo Fisher Scientific) to load equal amounts of protein on ELISA plates within each experiment. The human phosphotyrosine VEGFR3 ELISA (RayBiotech) was used for all experiments and ELISA results were determined by using a NanoQuant Infinite M200 Reader (TECAN). Since the same protein amounts were used for all conditions of the experiments, no further normalization needed to be done.

4.3.3 Western Blotting

Western Blotting was performed to determine knockdown efficiencies, effects of inhibitor treatments, recombinant protein treatments and for Co-IP experiments. After siRNA transfections, as well as after inhibitor treatments and recombinant protein treatments, LECs were briefly washed with PBS (Gibco® by Life Technologies™), and either directly collected with 1x Laemmli buffer or with ice-cold Laemmli-free lysis buffer (for subsequent BCA assay) of following composition:

1x Laemmli buffer	Laemmli-free buffer
10 mM NaF (Sigma-Aldrich)	50 mM HEPES pH 7.0 (Fisher Scientific)
1 mM Na_3VO_4 (Aldrich)	150 mM NaCl (Fisher Chemical)
1x cocktail of protease inhibitors (25x, Roche)	10% glycerol (Roth)
1x cocktail of phosphatase inhibitors (10x, Roche or 100x, Sigma)	1x cocktail of phosphatase inhibitors (10x, Roche or 100x, Sigma)
1x Laemmli Sample Buffer (4x, Bio-Rad)	1x cocktail of protease inhibitors (25x, Roche)
1% 2-Mercaptoethanol (Roth)	1% Triton X-100 (AppliChem)
in dH2O	in dH2O

Lysates collected in 1x Laemmli buffer were immediately heated at 95°C for 5 minutes, and Western Blotting was either started directly, or lysates were stored at -80°C, and heated up again before starting the Western Blot. Lysates collected in Laemmli-free lysis buffer were either directly used for protein content determination via Pierce™ BCA Protein Assay (Thermo Fisher Scientific) or stored at -80°C before they were used for Western blotting. Therefore, they were additionally supplemented with Laemmli to a final concentration of 1x Laemmli and then heated at 95°C for 5 minutes before starting the process of protein separation. For protein separation of experiments that were used for analysis of potential intracellular regulators of VEGFR3 signaling (see 5.1) Invitrogen Novex Mini-Cell Device (Thermo Fisher Scientific) was used with 1x MOPS buffer (Novex by Life Technologies). Gels (NuPAGE™ 4-12% Bis-Tris Gel, Invitrogen by Thermo Fisher Scientific) were loaded with 20-25 µl lysate, and protein separation was run for around 90 minutes at 180 V. Afterwards, gels were briefly incubated in 2x Transfer buffer (Novex by Life Technologies) containing 10% methanol.

For experiments that were used for the analysis of potential extracellular regulators of VEGFR3 signaling (see 5.2), protein separation of 20µg sample was performed by use of the Mini-PROTEAN® Tetra Vertical Cell device (Bio-Rad) and the respective combination of Mini-PROTEAN® TGX Stain-Free™ Precast Gels (4-15%, Bio-Rad) and 1x Tris/Glycine/SDS Buffer (Bio-Rad). In both cases, gels were subsequently used for Western Blotting with Trans-Blot® Turbo™ Mini PVDF Transfer Packs (Bio-Rad) and the Trans-Blot Turbo Transfer System (Bio-Rad). The high molecular weight program was run twice for 13 minutes each. Membranes were blocked with PBS (Ca^{2+}, Mg^{2+}) containing 5% BSA (AppliChem) and 0.5% Tween-20 (AppliChem) for 1 hour at RT under agitation, and blocking buffer was used for the dilution of following primary and secondary antibodies:

Primary antibodies	Dilution	Secondary antibodies	Dilution
rabbit anti-ILK (Cell Signaling, 3862)	1/1000	donkey anti-rabbit HRP-conjugated (Dianova, Jackson ImmunoResearch)	1/2000
rabbit anti α-Parvin (Cell Signaling, 4026)	1/1000		
rabbit anti BACE1 (Invitrogen by ThermoFisher, PA1-757)	1/1000		
rabbit anti-BACE2 (Abcam, ab5670)	1/500		
rabbit anti VEGF Receptor 3 (Abcam, ab154079)	1/1000	goat anti-rabbit HRP-conjugated (Cell Signaling, 70745)	1/5000
rabbit anti phospho-VEGFR3 (Cell Applications, CY1115)	1/1000		
rabbit anti GAPDH (Abcam, ab9485)	1/5000		

Primary antibodies were diluted in blocking solution and incubated o/n at 4°C under agitation. After washing with 0.5% Tween-20 (AppliChem) in PBS (Ca^{2+}, Mg^{2+}), Horse Radish Peroxidase (HRP)-conjugated secondary antibodies were incubated for 1 hour at RT under agitation on the next day, diluted in blocking solution. For detection, Clarity™ Western ECL Substrate solution (Bio-Rad) and the Chemidoc™ MP Imaging System (Bio-Rad) were used. The amounts of detected protein levels were normalized to the amount of detected GAPDH levels within the respective sample. Analysis of protein bands was performed with ImageJ/Fiji software using the gel analysis tool.

4.4 Immunohistochemistry

4.4.1 Proximity ligation assays (PLA)

Proximity ligation assays (PLA) were used to detect VEGFR3 tyrosine phosphorylation as well as interactions between VEGFR3 and β1 integrin. PLAs were performed using the Duolink In situ reagents (Sigma-Aldrich) according to the manufacturer's protocol. PBS (Ca^{2+}, Mg^{2+}) was used for washing steps. Stretch chambers or glass coverslips in cell culture dishes with human LECs were blocked in PBS (Ca^{2+}, Mg^{2+}) containing 5% NDS (Jackson ImmunoResearch), 1% BSA (AppliChem) and 0.2% Triton X-100 (AppliChem) for 1 hour at RT, cell culture dishes under agitation and stretch chambers by use of humidified chambers. Blocking buffer was used for the dilution of following primary and secondary antibodies:

Primary antibodies	Dilution	Secondary antibodies	Dilution
goat anti-human VEGFR3 (R&D Systems, AF349)	1/100	AF488-conjugated Phalloidin (Invitrogen by Thermo Fisher Scientific, A12379)	1/200
mouse anti-human β1 integrin (Millipore, MAB19887)	1/100		
mouse anti-phospho-Tyrosine 4G10 Platinum (Millipore, 05-1050)	1/100	DAPI (Sigma)	1/1000

An antibody against Phalloidin was used for co-staining of the F-actin cytoskeleton. Primary antibodies were incubated o/n at 4°C. In addition, DAPI was used to counterstain cell nuclei. After stainings, the stretch chambers were cut, and only the thin part containing the cell layer was mounted on slides using Fluoroshield™ (Sigma). Glass coverslips were removed from cell culture dishes and mounted with Fluoroshield™ (Sigma) on slides in a way that the cell monolayer faces the slide. All slides were stored at -20°C until imaging and analysis (Urner 2018a, see 4.4.2).

4.4.2 Imaging and image analysis

Images were acquired using Laser Scan Microscopy (LSM 710, Zeiss), and analyzed using the ImageJ/Fiji Software. PLAs were imaged as z-stacks. Maximum intensity projections were performed for all z-stacks before analysis. Standardized macros were established and used in ImageJ/Fiji to determine cell numbers and BrdU positive cells in *in vitro* studies.

If macros did not fit, cell numbers and/or BrdU positive cells were quantified manually. PLA sites were analyzed by using standardized macros for all images within one experiment, or quantified manually if the macros did not fit. The number of PLA dots was normalized to the number of cells in the analyzed image.

4.5 Statistics

Statistical significance was determined by using Prism software (GraphPad Inc.). For comparisons of two groups, unpaired two-tailed Student's t-test was performed. For multiple comparisons, one-way ANOVA followed by Dunnett's post hoc-test was used. Statistical differences were considered significant with a *P* value less than or equal 0.05 and the exact *P* values are shown in the figures. All quantified data are presented as mean ± standard error of the mean (SEM). Significant outliers were detected by the extreme studentized deviate method (Grubbs' test) and excluded from the statistical analysis.

4.6 Personal contributions

Laura Sophie Hilger performed most of the presented experiments and was supervised by Prof. Dr. Eckhard Lammert; funded by the DFG, IRTG1902.

Dr. Lara Planas-Paz started the ILK project and performed first *in vitro* studies which are presented in this thesis; funded by the DFG, LA-1216/5-1. Dr. Sofia Urner continued the ILK project and performed some of the *in vitro* experiments presented in this thesis; funded by the DFG, IRTG1902.

Ida Marie Stöppelkamp was co-supervised by Laura Sophie Hilger during an internship of three months in 2019, and contributed to some *in vitro* results.

Laura Isabelle Hofmann and Andree Schmidt are part of the Institute for Neuroproteomics (DZNE e.V., Munich) and contributed to one of the presented *in vitro* experiments in this thesis, which has been performed during their research stay at the Institute of Metabolic Physiology in Düsseldorf under supervision of Laura Sophie Hilger.

5. Results

5.1 Intracellular mechanism for attenuation of VEGFR3 activity

VEGFR3 is known to be a key regulator of LEC behavior such as LEC survival, migration and proliferation. Especially LEC proliferation is crucial for the development and growth of lymphatic vessels, also known as lymphangiogenesis, both in health and disease. Regulation of VEGFR3 signaling is required to prevent lymphatic overgrowth and maintain physiologic lymphatic function. In this context our lab could point to the importance of the mechanoreceptor β1 integrin for VEGFR3 signaling in LECs and lymphatic development, since its endothelial cell-specific deletion in *in vivo* mouse models (referred to as 'β1 integrin K.O.') caused severe developmental issues and decreased VEGFR3 signaling (Planas-Paz et al. 2012). In further studies we suggested that ILK might have similar functions as β1 integrin, because it is known to be one of the latter's intracellular adapter proteins. Nevertheless, the endothelial cell-specific deletion of *Ilk* (referred to as 'ILK K.O.') in mouse embryos surprisingly resulted in increased VEGFR3 phosphorylation, LEC proliferation and enlarged jugular lymph sacs (jls) or primordial thoracic ducts (pTD) (jls/pTD). The inducible ILK K.O. in lymphatic endothelial cells of adult mice furthermore resulted in increased VEGFR3 phosphorylation, LEC proliferation and lymphatic vascular growth as it was detected in adult mouse ear skins. The combination of the ILK K.O. and the β1 integrin K.O. caused a 'genetic rescue' of the ILK phenotype. We concluded that ILK regulates mouse VEGFR3 signaling and lymphatic vascular growth in a β1 integrin dependent manner (Urner et al. 2019).

5.1.1 ILK regulates VEGFR3 signaling and adult human LEC proliferation

To transfer the obtained results on ILK from the *in vivo* mouse system to the adult human system, we chose the *in vitro* culture of primary adult human LECs. As the first step, we silenced human *ILK* via transfection with siRNAs in these LECs. Aiming for an increased precision of the results, we used three different ILK siRNAs (ILK siRNA 1, 2, 3) and a non-targeting control siRNA with comparable GC content (control). As determined by Western Blotting (Figure 10A), we observed a significant reduction of ILK protein levels by around 46-83% upon use of all three ILK siRNAs (Figure 10B).

This *ILK* silencing system was further used to investigate the influence of ILK on VEGFR3 signaling in adult human LECs. As an indicator for VEGFR3 signaling activity, we analyzed VEGFR3 phosphorylation in lysates of *ILK* silenced adult human LECs upon stimulation with VEGF-C C156S for 5 minutes by use of ELISA. We detected a significant increase of VEGFR3 phosphorylation by around 73-121% after transfection with ILK siRNAs (Figure 10C).

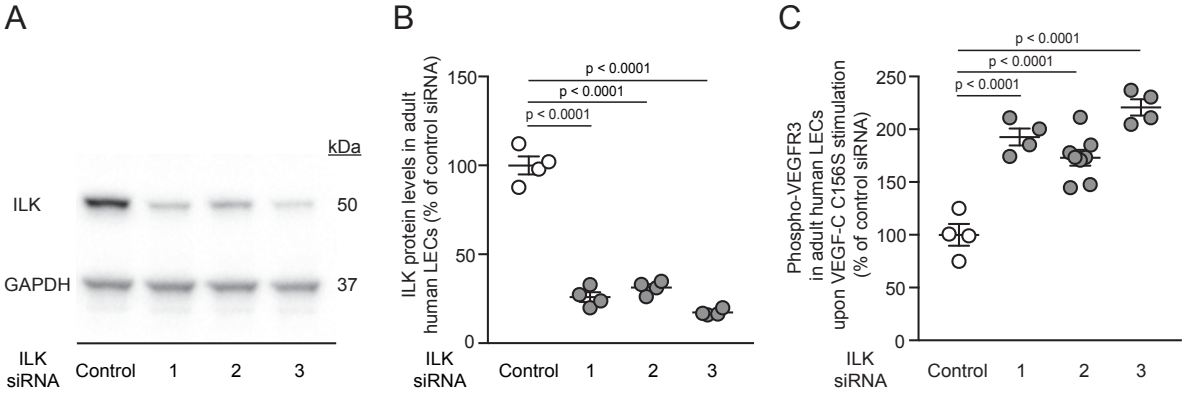

Figure 10: Silencing of *ILK* increases VEGFR3 phosphorylation in adult human LECs.
(**A**) Representative Western Blot image of adult human LEC lysates 72 hours after transfection with control siRNA (Control) or one of three different ILK siRNAs (ILK siRNA 1, 2, 3) showing protein bands of ILK and GAPDH serving as loading control. (**B**) Quantifications of ILK protein levels in adult human LECs 72 hours after transfection with control and ILK siRNAs, shown as percentage of control siRNA. (**C**) Quantifications of phosphorylated VEGFR3 upon VEGF-C C156S stimulation as determined by ELISA in adult human LECs 72 hours after transfection with control and ILK siRNAs, shown as percentage of control siRNA. (**B, C**) All values are shown as means ± SEM with n ≧ 3 independent transfections per siRNA; statistical significance was determined by one-way ANOVA and Dunnett's multiple comparisons test. Dr. Sofia Urner performed presented experiments and Laura Sophie Hilger reproduced them with comparable results.

These results indicate that ILK might be relevant for the regulation of VEGFR3 signaling in adult human LECs. To further determine whether the increased VEGFR3 phosphorylation in *ILK* silenced adult human LECs (Figure 10) also affects LEC proliferation, we next performed BrdU incorporation assays. BrdU is a thymidine analogue and is therefore incorporated into the newly synthesized DNA of proliferating cells. BrdU-positive and the total number of nuclei were detected by use of immunohistochemistry (Figure 11A,B). Via normalization of BrdU-positive cells to the total number of nuclei, we quantified a significant increase of LEC proliferation by around 59-130 % upon silencing of *ILK* (Figure 11C). The significantly increased VEGFR3 phosphorylation (Figure 10) and adult human LEC proliferation upon silencing of *ILK* (Figure 11) indicate that ILK plays an important role in the regulation of VEGFR3 signaling in adult human LECs. We therefore next aimed to uncover the underlying mechanism.

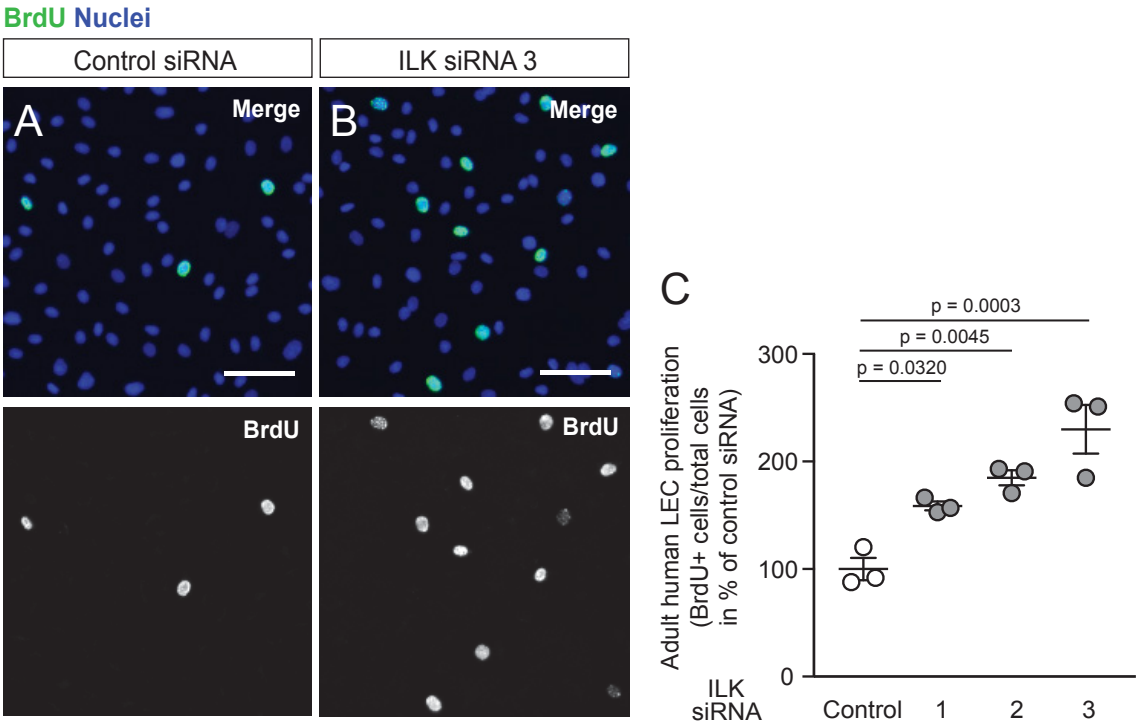

Figure 11: Silencing of *ILK* results in increased adult human LEC proliferation.
(**A, B**) Representative images of human LECs 72 hours after transfection with control siRNA (A) or ILK siRNA (ILK siRNA 3) (B) and incubation with VEGF-C156S and the proliferation marker BrdU for 1 hour. Staining of nuclei is shown in blue and staining of BrdU is shown in green. Scale bars 50 µm. (**C**) Quantifications of BrdU positive LECs normalized to total LECs that were transfected with either control or one of three different ILK siRNAs (ILK siRNA 1, 2, 3), shown as percentage of control siRNA. All values are shown as means ± SEM with n ≧ 3 independent transfections per siRNA; statistical significance was determined by one-way ANOVA and Dunnett's multiple comparisons test. Dr. Sofia Urner performed the presented experiments and Laura Sophie Hilger reproduced them with comparable results.

5.1.2 ILK controls the number of interactions between VEGFR3 and β1 integrin in adult human LECs

As Planas-Paz et al. could already show with the respective *in vivo* mouse models, VEGFR3 signaling depends on its interactions with β1 integrin (Planas-Paz et al. 2012). We therefore questioned whether ILK – as an integrin adapter protein – might control those interactions between VEGFR3 and β1 integrin and thereby regulate VEGFR3 signaling. To answer this question, we silenced *ILK* in adult human LECs with ILK siRNAs and analyzed the interactions between VEGFR3 and β1 integrin by use of proximity ligation assay (PLA) (Figure 12A,B). A PLA is capable to combine signals of two different antibodies bound to their respective antigens to one signal, labeling the site where both antibodies are located in close proximity

to each other (referred to as 'PLA site'). With this method, we could show that silencing of *ILK* leads to increased interactions between VEGFR3 and β1 integrin in adult human LECs, as indicated by the increase in the number of PLA sites per LEC by around 30-82% (Figure 12C). The increased interactions between VEGFR3 and β1 integrin upon silencing of *ILK* (Figure 12) indicate that ILK regulates the β1 integrin mediated VEGFR3 signaling in adult human LECs.

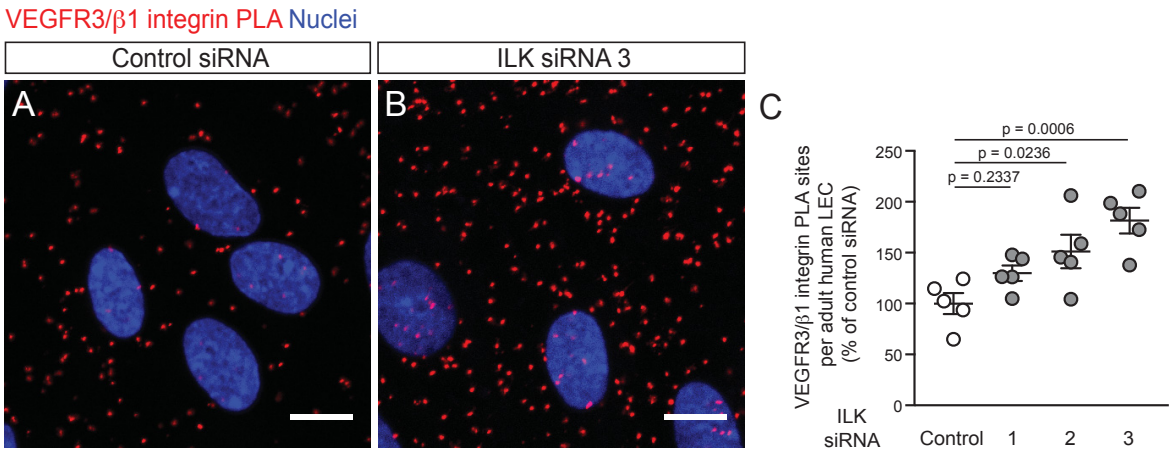

Figure 12: Silencing of *ILK* leads to increased interactions between β1 integrin and VEGFR3 in adult human LECs.
(**A, B**) Representative LSM images of human LECs 72 hours after transfection with control siRNA (A) or ILK siRNA 3 (B), showing VEGFR3/β1 integrin proximity ligation assay (PLA) sites (red) and nuclei (blue). Scale bars 10 µm. (**C**) Quantifications of VEGFR3/β1 integrin proximity ligation assay (PLA) sites per LEC. LECs were transfected with either control (Control) or one of three different ILK siRNAs (ILK siRNA 1, 2, 3), shown as percentage of control siRNA. All values are shown as means ± SEM with n = 5 independent transfections per siRNA; statistical significance was determined by one-way ANOVA and Dunnett's multiple comparisons test. Dr. Sofia Urner performed the presented experiments and Laura Sophie Hilger reproduced them with comparable results.

5.1.3 Mechanical stretching of adult human LECs affects β1 integrin's interactions with VEGFR3 and ILK

In the *in vivo* mouse model, β1 integrin functions as a mechanoreceptor on LECs. This enables mechano-induced VEGFR3 signaling and lymphatic vascular growth upon the application of e.g. increased fluid pressure in the system, leading to visibly stretched LECs (Planas-Paz et al. 2012). To mimic these mechanical forces and to further test this mechanism *in vitro*, we next cultured adult human LECs on silicone membranes of stretching chambers. After the subsequent mechanical stimulation by stretch for 30 minutes, LECs were fixed on

the membranes and a PLA assay for VEGFR3/β1 integrin interactions was performed (Figure 13A-D). The mechanical stretch of adult human LECs resulted in significantly increased interactions between VEGFR3 and β1 integrin by around 126% when compared to unstretched controls (Figure 13E). According to our results, mechanical stimulation by stretch of adult human LECs seems to have similar effects on the interactions between VEGFR3 and β1 integrin as the silencing of *ILK* (Figure 12 and Figure 13).

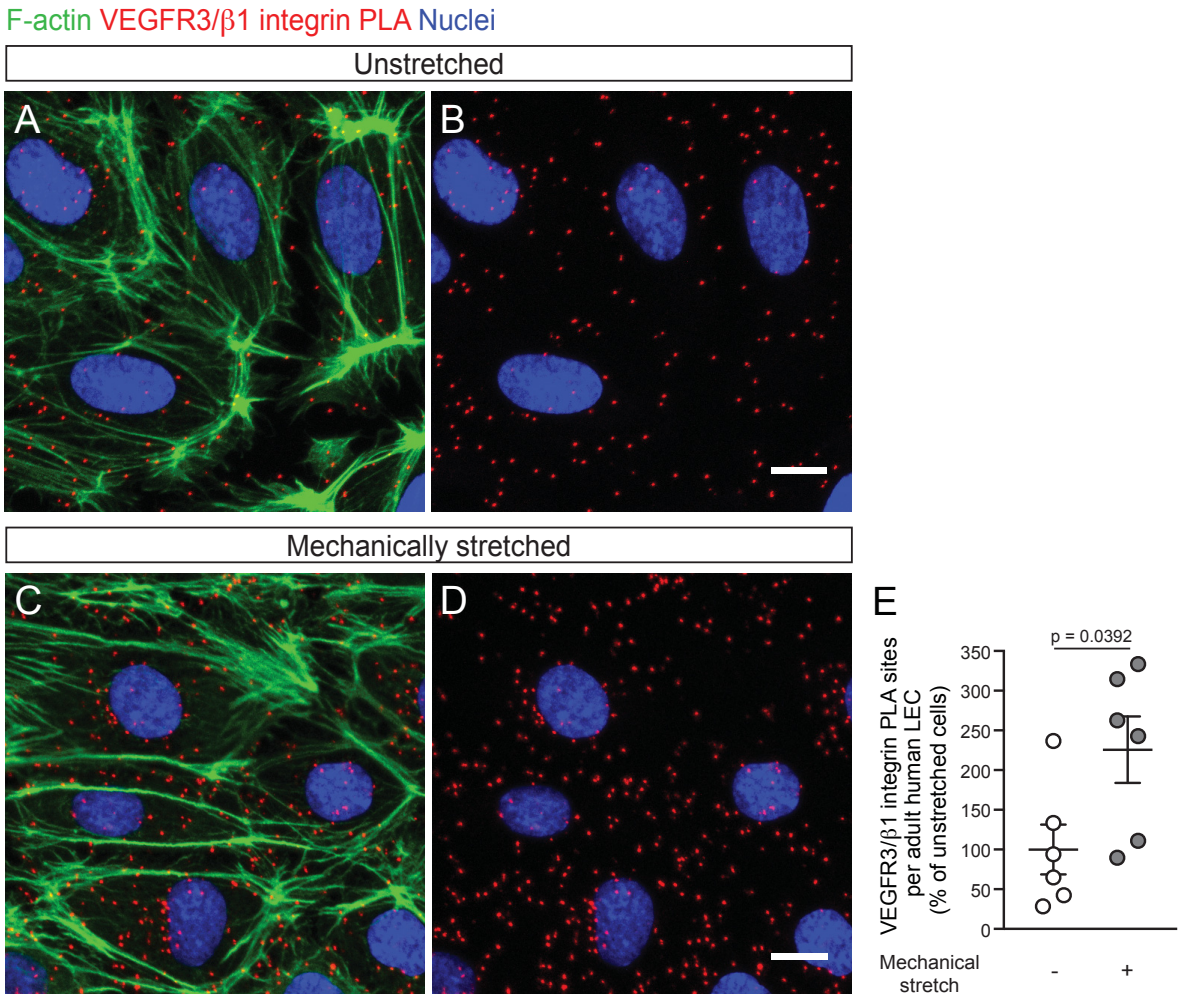

Figure 13: Mechanical stretching of adult human LECs leads to increased interactions between β1 integrin and VEGFR3.
(**A-D**) Representative LSM images of adult human LECs that were either kept unstretched (**A, B**) or were mechanically stretched for 30 minutes (**C, D**), showing VEGFR3/β1 integrin proximity ligation assay (PLA) sites (red). Co-stainings for F-actin (green) and nuclei (blue) are also shown. Scale bars, 10 µm. (**E**) Quantification of VEGFR3/β1 integrin PLA sites per adult human LEC; cells were either unstretched (-) or mechanically stretched (+); shown as percentage of unstretched cells. All values are shown as means ± SEM with n = 6 independent stretch experiments; statistical significance was determined by an unpaired two-tailed Student's t-test. Laura Sophie Hilger and Dr. Sofia Urner performed the presented experiments.

For the support of our hypothesis that ILK regulates the interactions between VEGFR3 and β1 integrin and thereby most importantly regulates VEGFR3 signaling, we next aimed to show that mechanical stretching of adult human LECs affects the interactions between β1 integrin and ILK. Since a reliable immunostaining of ILK was technically impossible, we used the method of co-immunoprecipitation (referred to as 'co-IP') instead of PLA to show that β1 integrin's adapter protein ILK loses its contact to β1 integrin upon mechanical stretching for 30 minutes (Figure 14). We expressed HA-tagged β1 integrin via transfection with plasmids in adult human LECs and immunoprecipitated it from unstretched versus stretched LECs by use of antibodies against the HA-tag. In the subsequently performed Western Blot with the precipitated lysates we detected both the HA-tagged β1 integrin and ILK (Figure 14A) and normalized the protein expression of ILK to the immunoprecipitated amounts of HA-tagged β1 integrin. The quantification revealed a significant decrease of ILK co-immunoprecipitated with HA-tagged β1 integrin by 48% in lysates of adult human LECs after 30 minutes of mechanical stretch (Figure 14B).

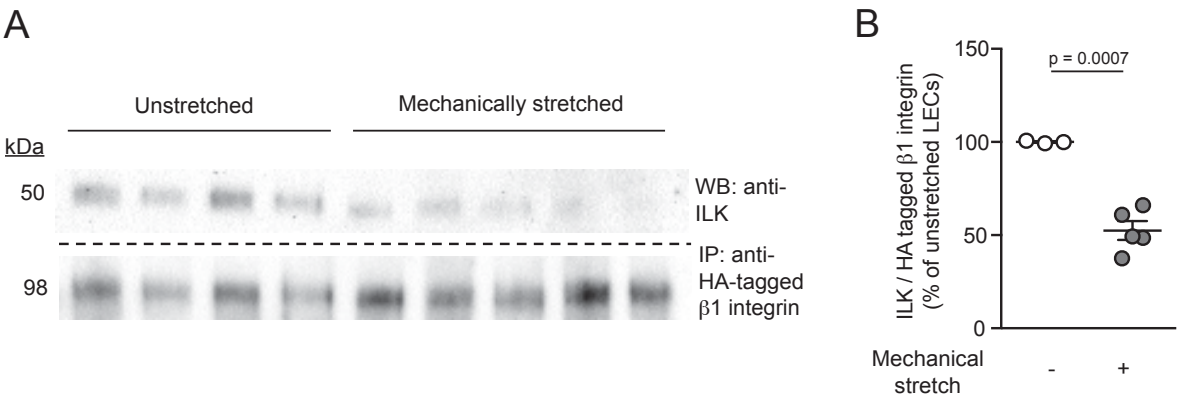

Figure 14: Mechanical stretching of adult human LECs results in decreased interactions between ILK and β1 integrin.
(**A**) Representative Western Blot image of adult human LECs that were either kept unstretched or were mechanically stretched for 30 minutes, subsequently lysed and used for Immunoprecipitation (IP) of HA-tagged β1 integrin from whole cell lysates. Immunoprecipitation was performed with antibodies against HA-tag and HA-tagged β1 integrin was detected in Western blot (WB) by antibodies against β1 integrin. ILK protein interacting with immunoprecipitated HA-tagged β1 integrin was detected by antibodies against ILK. (**B**) Quantification of the amount of detected ILK protein in immunoprecipitated LEC lysates, normalized to the respective amount of HA-tagged β1 integrin in unstretched or mechanically stretched LECs; shown as percentage of unstretched LECs. All values are shown as means ± SEM with n ≥ 4 independent stretch experiments; statistical significance was determined by an unpaired two-tailed Student's t-test. Dr. Sofia Urner performed the presented experiments.

The reduction of ILK/β1 integrin interactions upon mechanical stretching of adult human LECs (Figure 14) suggests an inverse correlation between ILK/β1 integrin interactions and VEGFR/β1 integrin interactions. Accordingly, we detected increased VEGFR3/β1 integrin interactions and VEGFR3 signaling, when ILK lost contact to β1 integrin.

5.1.4 α-parvin protein levels are affected by mechanical stretch and depend on ILK protein levels

After we found these correlations, we next questioned whether protein levels of IPP complex members would be impacted by mechanical stretching of adult human LECs in general. This is why we tested lysates of adult human LECs, which were mechanically stretched for 30 minutes, for the total protein amounts of ILK – as the central IPP complex protein – and its complex member α-parvin (Figure 15A). Our Western Blot analyses showed that both ILK and α-parvin protein levels decreased upon mechanical stretching of LECs. We noticed the reduction of α-parvin protein levels by around 33-42% to be significant (Figure 15C), while the reduction of ILK protein levels by around 10-22% was only by trend (Figure 15B).

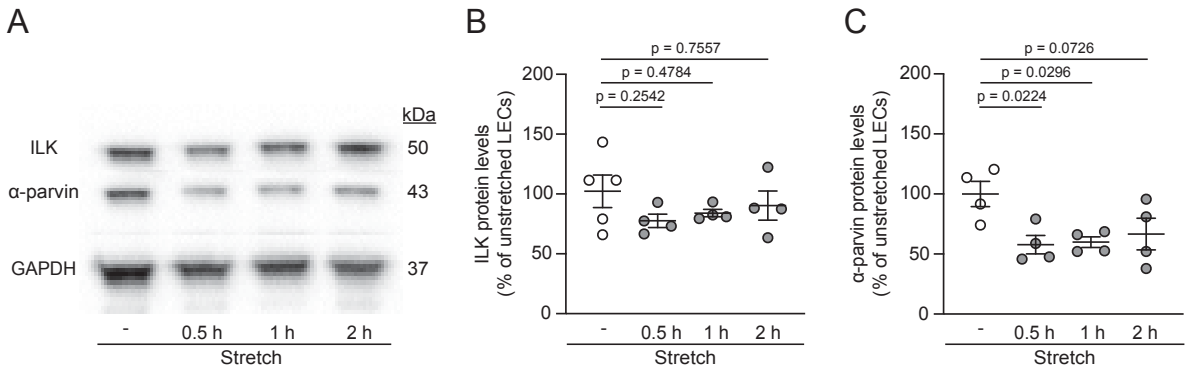

Figure 15: Mechanical stretching of adult human LECs has no major effect on ILK protein levels, but reduces protein levels of α-parvin.
(**A**) Representative Western Blot image of adult human LEC lysates that were either kept unstretched (-) or were mechanically stretched for 0.5 – 2 hours, showing protein bands of ILK and α-parvin with GAPDH serving as loading control. (**B**) Quantifications of ILK protein levels in adult human LEC lysates, normalized to the respective amount of GAPDH in unstretched or mechanically stretched LECs; shown as percentage of unstretched LECs. (**C**) Quantifications of α-parvin protein levels in adult human LEC lysates, normalized to the respective amount of GAPDH in unstretched or mechanically stretched LECs; shown as percentage of unstretched LECs. All values are shown as means ± SEM with n ≥ 4 independent stretch experiments; statistical significance was determined by one-way ANOVA and Dunnett's multiple comparisons test. Laura Sophie Hilger performed the presented experiments.

The significant reduction of α-parvin protein levels upon mechanical stretching of adult human LECs (Figure 15) indicates that not only ILK as the central part of the IPP complex and especially its interactions with β1 integrin gets affected by mechanical stretch (Figure 14). Thus, we next aimed to analyze the potential role of IPP complex member α-parvin in the regulation of VEGFR3 signaling.

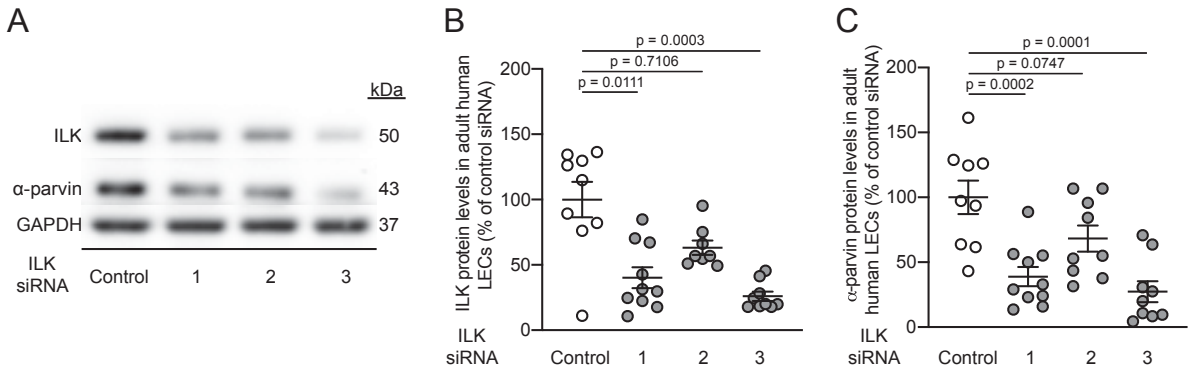

Figure 16: Silencing of *ILK* in adult human LECs leads to a parallel reduction of α-parvin protein levels.
(**A**) Representative Western Blot image of human LEC lysates 72 hours after transfection with control siRNA (Control) or one of three different ILK siRNAs (ILK siRNA 1, 2, 3) showing protein bands of ILK, α-parvin and GAPDH serving as loading control. (**B**) Quantifications of ILK protein levels in adult human LECs 72 hours after transfection with control and ILK siRNAs, shown as percentage of control siRNA. (**C**) Quantifications of α-parvin protein levels in adult human LECs 72 hours after transfection with control and ILK siRNAs, shown as percentage of control siRNA. All values are shown as means ± SEM with n ≧ 3 independent transfections per siRNA; statistical significance of (B) was determined by Kruskal-Wallis and Dunn's multiple comparisons test, while statistical significance of (C) was determined by one-way ANOVA and Dunnett's multiple comparisons test. Laura Sophie Hilger performed the presented experiments.

Based on the interesting result, that α-parvin protein levels were more strongly decreased upon mechanical stretching of adult human LECs than the protein levels of its complex partner ILK (Figure 15), we wondered whether α-parvin and ILK protein levels might depend on each other. Therefore, we analyzed *ILK* silenced LEC lysates for α-parvin protein levels via Western Blotting (Figure 16A). The siRNA mediated knockdown of *ILK* reduced ILK protein levels by around 37-74% (Figure 16B) and the simultaneous analysis of α-parvin protein levels revealed a significant reduction of α-parvin protein levels by around 32-73% (Figure 16C). The parallel reduction of α-parvin protein levels to ILK protein decrease (Figure 16) indicates that α-parvin protein levels depends on the ILK protein amount present in adult human LECs. This finding is in line with previously published studies on the interdependency of IPP complex members in other cell types (Xu et al. 2005; Fukuda et al. 2003a).

5.1.5 Efficient silencing of *PARVA* in adult human LECs has no major effect on ILK protein levels

As we found out that α-parvin protein levels decrease upon both mechanical stretching (Figure 15) and upon silencing of *ILK* (Figure 16) – two processes shown to affect VEGFR3 signaling – we suggested a coherence between α-parvin levels and VEGFR3 signaling. To further examine this hypothesis, we silenced human *PARVA* by use of transfection with PARVA siRNA in adult human LECs. Aiming for more precise results, we used three different PARVA siRNAs and a non-targeting control siRNA. The success of *PARVA* silencing was confirmed on mRNA levels, which revealed a downregulation of *PARVA* mRNA expression levels by around 78-92% depending on the siRNA (Figure 17A). Further Western Blotting of LEC lysates (Figure 17B) revealed a significant decrease of α-parvin protein levels upon transfection with PARVA siRNAs by around 61-97% (Figure 17C).

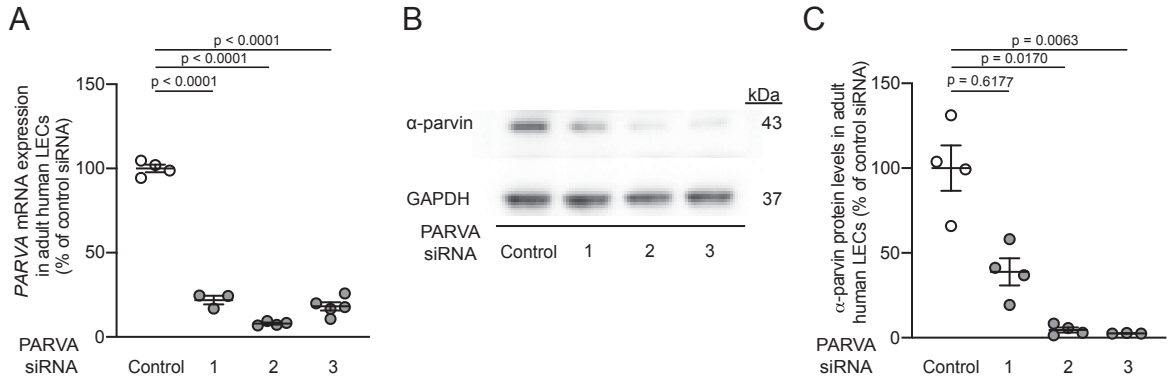

Figure 17: *PARVA* is efficiently silenced in adult human LECs by use of PARVA siRNAs. (**A**) Quantifications of *PARVA* mRNA expression levels in adult human LECs 48 hours after transfection with control siRNA (Control) or one of three different PARVA siRNAs (PARVA siRNA 1, 2, 3), shown as percentage of control siRNA. (**B**) Representative Western Blot image of adult human LEC lysates 48 hours after transfection with control and PARVA siRNAs showing protein bands of α-parvin and GAPDH serving as loading control. (**C**) Quantifications of α-parvin protein levels in adult human LECs 48 hours after ntransfection with control and PARVA siRNAs, shown as percentage of control siRNA. All values are shown as means ± SEM with n ≧ 3 independent transfections per siRNA; statistical significance of (A) was determined by one-way ANOVA and Dunnett's multiple comparisons test, while statistical significance of (C) was determined by Kruskal-Wallis and Dunn's multiple comparisons test. Laura Sophie Hilger performed the presented experiments.

After the successful silencing of *PARVA* in adult human LECs (Figure 17), we next analyzed ILK protein levels in the respective lysates (Figure 18A). With this, we tested whether the dependency of α-parvin protein levels on ILK protein levels was also true for the opposite case. When compared to controls, α-parvin protein levels were significantly decreased by around 61-97% upon transfection with PARVA siRNAs (Figure 18B), whilst ILK protein levels in the same samples were only non-significantly reduced by around 37-52% (Figure 18C).

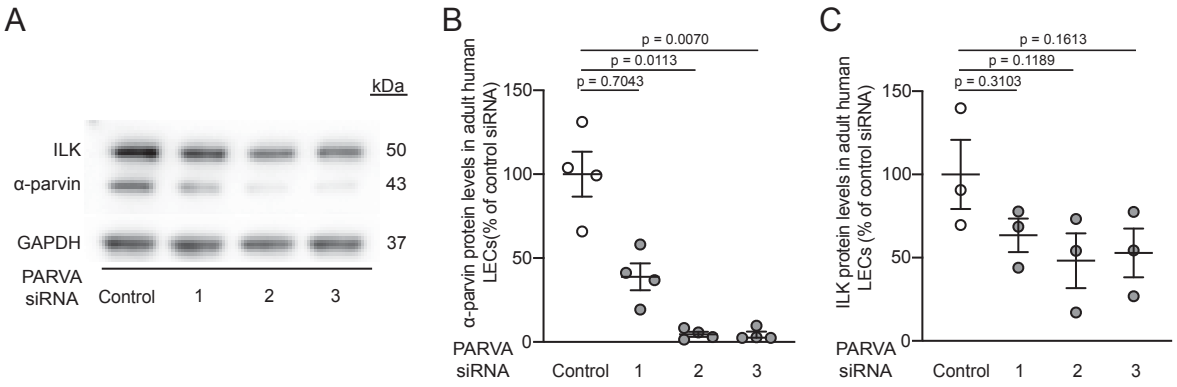

Figure 18: Silencing of *PARVA* has no major effect on ILK protein levels in adult human LECs. (**A**) Representative Western Blot image of adult human LEC lysates 48 hours after transfection with control (Control) and one of three different PARVA siRNAs (PARVA siRNA 1, 2, 3) showing protein bands of α-parvin, ILK and GAPDH serving as loading control. (**B**) Quantifications of α-parvin protein levels normalized to respective GAPDH levels in adult human LECs 48 hours after transfection with control and PARVA siRNAs, shown as percentage of control siRNA. (**C**) Quantifications of ILK protein levels normalized to respective GAPDH levels in adult human LECs 48 hours after transfection with control and PARVA siRNAs, shown as percentage of control siRNA. All values are shown as means ± SEM with n ≧ 3 independent transfections per siRNA; statistical significance of (B) was determined by Kruskal-Wallis and Dunn's multiple comparisons test, while statistical significance of (C) was determined by one-way ANOVA and Dunnett's multiple comparisons test. Laura Sophie Hilger performed the presented experiments.

The reduction of ILK protein levels by trend upon silencing of *PARVA* in adult human LECs (Figure 18) reveals an uneven interdependency between protein levels of ILK and α-parvin. In this interdependency, α-parvin protein levels seem to depend more strongly on ILK protein levels (Figure 16) than ILK protein levels depend on α-parvin protein levels, which indicates that ILK might be upstream of α-parvin.

5.1.6 α-parvin contributes to the regulation of VEGFR3 signaling and adult human LEC proliferation

Nevertheless, the dependency of α-parvin protein levels on ILK protein levels (Figure 16) and the further dramatical reduction of α-parvin protein levels upon mechanical stretching (Figure 15) indicated a potential role of α-parvin in the β1 integrin dependent regulation of VEGFR3 signaling in adult human LECs by ILK. To increase our knowledge about the indicated coherences, we next analyzed *PARVA* silenced LEC lysates in phospho-VEGFR3 ELISAs (Figure 19A) and by use of Western Blotting (Figure 19B). Both methods revealed an increase in VEGFR3 phosphorylation upon silencing of *PARVA* with siRNA 3 when compared to controls. Upon transfection with PARVA siRNA 3, we detected a significant increase in VEGFR3 phosphorylation by about 102% as detected by ELISA while the effect of the two other siRNAs was milder and not statistically significant (Figure 19A). *PARVA* silencing with siRNA 3 also lead to the strongest increase in VEGFR3 phosphorylation by around 63% by trend as detected by Western Blotting (Figure 19B,C).

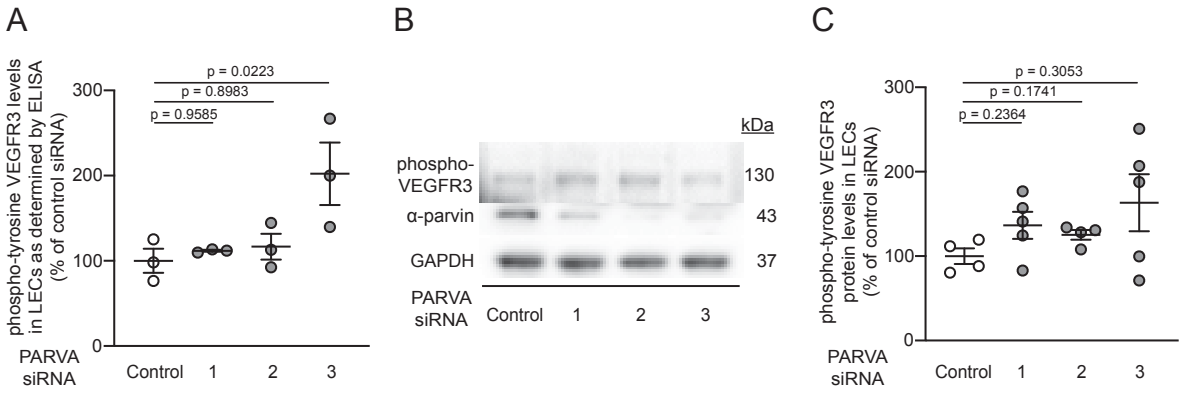

Figure 19: *PARVA* silencing increases VEGFR3 phosphorylation in adult human LECs by trend.
(**A**) Quantifications of phosphorylated VEGFR3 in *PARVA* silenced adult human LEC lysates as determined by ELISA. Adult human LECs were either transfected with control siRNA (Control) or with one of three different PARVA siRNAs (PARVA siRNA 1, 2, 3) and incubated for 48h before lysis and subsequent determination of protein content. Values are shown as percentage of control siRNA. (**B**) Representative Western Blot image of adult human LEC lysates 48 hours after transfection with control and PARVA siRNAs showing protein bands of phosphorylated VEGFR3 (phospho-VEGFR3), α-parvin and GAPDH serving as loading control. (**C**) Quantifications of phosphorylated VEGFR3 protein levels normalized to respective GAPDH levels in adult human LECs 48 hours after transfection with control and PARVA siRNAs, shown as percentage of control siRNA. All values are shown as means ± SEM with n ≧ 3 independent transfections per siRNA; statistical significance of (A) was determined by one-way ANOVA and Dunnett's multiple comparisons test, while statistical significance of (C) was determined by Brown-Forsythe and Welch ANOVA tests. Laura Sophie Hilger performed the presented experiments.

As increased VEGFR3 phosphorylation usually leads to increased LEC proliferation, we wondered whether the mild increase in VEGFR3 phosphorylation upon silencing of *PARVA* (Figure 19) would be sufficient to induce adult human LEC proliferation. Therefore, we used the BrdU incorporation assay to monitor LEC proliferation and further compared proliferation rates of *PARVA* silenced LECs to those which were transfected with control siRNAs (Figure 20A,B). Normalization of BrdU-positive LECs to the total nuclei count revealed that silencing of *PARVA* with PARVA siRNA 2 increased the LEC proliferation by about 71%, an increase which was close to significance. Transfections with PARVA siRNAs 1 and 3 also lead to increased LEC proliferation rates by around 44-61% by trend (Figure 20C).

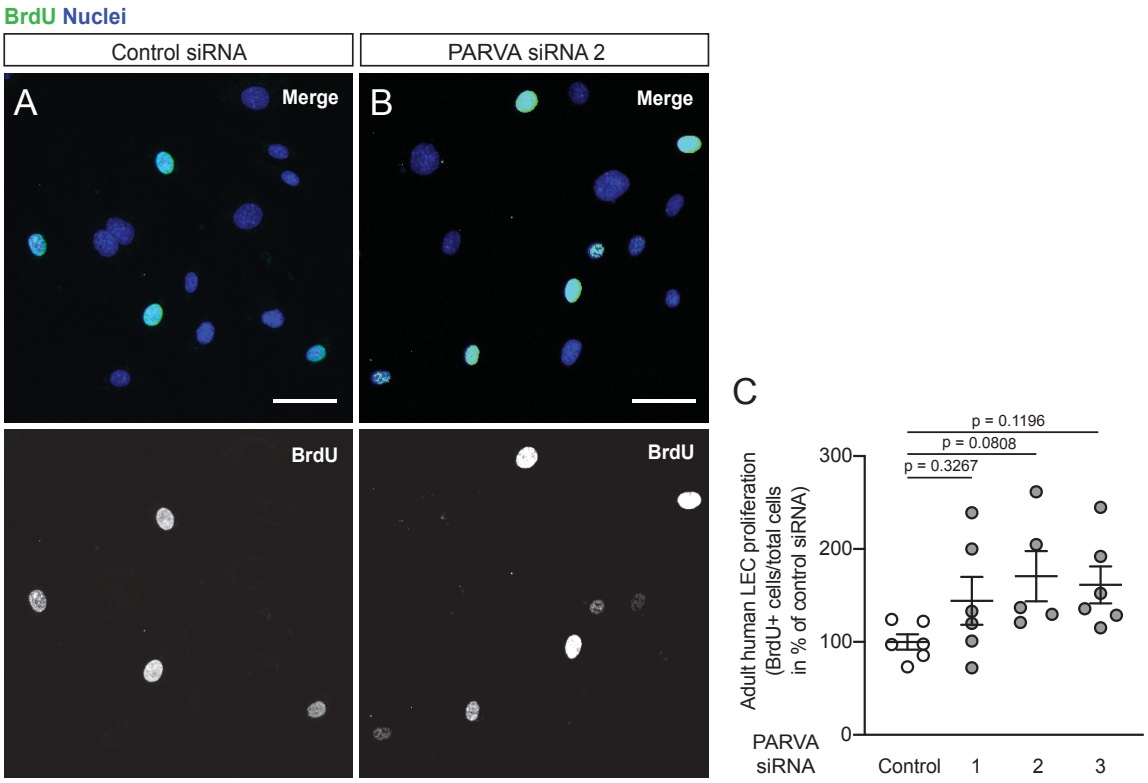

Figure 20: Silencing of *PARVA* results in slightly increased adult human LEC proliferation. (**A, B**) Representative images of adult human LECs after transfection with control siRNA (A) or PARVA siRNA 2 (B) and incubated with VEGF-C156S and the proliferation marker BrdU for 3 hours. Staining of nuclei is shown in blue and staining of BrdU is shown in green. Scale bars 50 µm. (**C**) Quantifications of BrdU positive LECs normalized to total LECs that were transfected with either control (Control) or one of three different PARVA siRNAs (PARVA siRNA 1, 2, 3), shown as percentage of control siRNA. All values are shown as means ± SEM with n ≧ 5 independent transfections per siRNA; statistical significance was determined by one-way ANOVA and Dunnett's multiple comparisons test. Laura Sophie Hilger performed the presented experiments.

Our findings suggest that even the increase of VEGFR3 phosphorylation by trend upon silencing of *PARVA* (Figure 19) could be sufficient to induce increased adult human LEC proliferation (Figure 20). Our experiments thus support the hypothesis that α-parvin might be involved in the regulation of VEGFR3 signaling in adult human LECs as a downstream IPP complex partner of ILK.

5.2 Extracellular mechanism for attenuation of VEGFR3 activity

In addition to the previously described intracellular mechanism of VEGFR3 attenuation, there might also be extracellular proteins contributing to the attenuation of VEGFR3 signaling in adult human LECs. In studies on β-site of amyloid precursor protein cleaving enzymes (referred to as 'BACE'), which play a crucial role in the development and worsening of Alzheimer's disease (Selkoe and Hardy 2016), there was one BACE family member found which turned out to be potentially important for this study. In general, BACE1 is supposed to be responsible for the bad outcome and worsening of Alzheimer's disease and this is why several institutions are currently searching for effective inhibitors of this protease (Cole and Vassar 2007; Yan and Vassar 2014). Common BACE1 inhibitors nevertheless target also its close homologue BACE2, which potentially causes side effects (Bennett et al. 2000; Alexander et al. 2014; Neumann et al. 2015; Cebers et al. 2017; Hawkes 2017). BACE2 was shown to have no major impact on the development and progression of Alzheimer's disease because its β-secretase activity is only conditional (Wang et al. 2019). Due to its diverse functions in the CNS and the periphery (Bennett et al. 2000; Esterhazy et al. 2011; Rochin et al. 2013; Voytyuk et al. 2018b), unintentional BACE2 inhibition might have severe side effect in human patients. The group of Prof. Dr. Stefan Lichtenthaler at the DZNE e.V. in Munich therefore investigates potential BACE2 substrates in order to find a physiologic marker of BACE2 activity. With this, they aim to predict unintended BACE2 inhibition by newly developed BACE1 inhibitors. During their research they found VEGFR3 to be a potential candidate as a measurable BACE2 substrate and handed parts of the required experiments concerning this hypothesis over to us.

5.2.1 Unspecific BACE inhibition affects VEGFR3 protein and signaling in adult human LECs

In order to evaluate whether VEGFR3 might be a target of one of the BACE family proteases, we started our analyses by use of one of the common BACE1 inhibitors named β-Secretase Inhibitor IV (referred to as 'C3'). C3 blocks the proteolytic activity of BACE1 by binding to its active site, but also targets BACE2 and can therefore be used as a non-specific BACE inhibitor (Stachel et al. 2004; Ben Halima et al. 2016). We treated cultured adult human LECs with C3 for 6 hours. Afterwards, we lysed the LECs and detected total VEGFR3 protein levels in the lysates via Western Blotting (Figure 21A). Interestingly, the total VEGFR3 protein levels were non-significantly upregulated by around 91% upon C3 treatment, when compared to the DMSO control (control) treatment (Figure 21B).

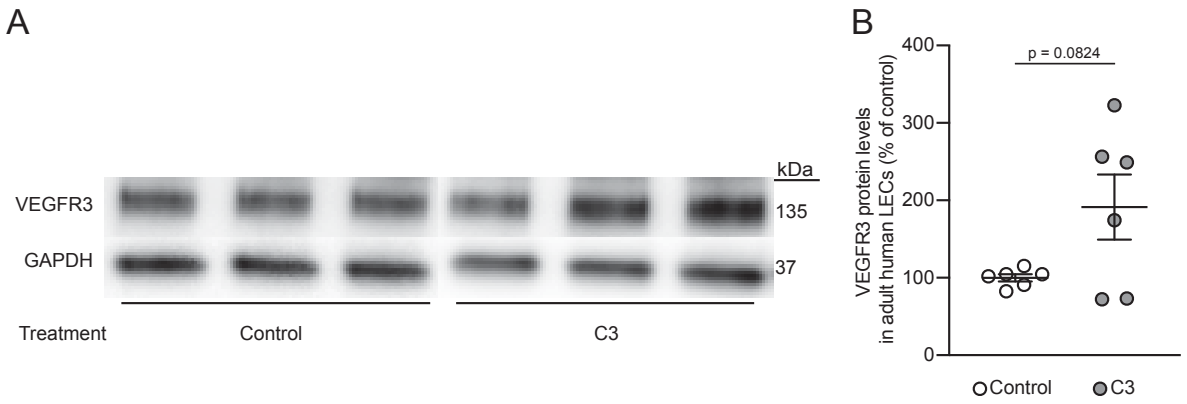

Figure 21: β-Secretase Inhibitor IV (C3) mediated BACE inhibition increases VEGFR3 protein levels in adult human LECs.
(**A**) Representative Western Blot image of adult human LEC lysates after 6 hours of treatment with DMSO control (Control) or the β-Secretase Inhibitor IV (C3) showing protein bands of VEGFR3 and GAPDH serving as loading control. (**B**) Quantification of VEGFR3 protein levels in adult human LECs normalized to respective GAPDH amount after 6 hours of treatment with either DMSO control or C3, shown as percentage of control. All values are shown as means ± SEM with n = 6 independently treated sets of LECs per condition, statistical significance was determined by an unpaired two-tailed Student's t-test. Laura Sophie Hilger performed the presented experiment.

The finding, that unspecific BACE inhibition causes increased VEGFR3 protein levels (Figure 21) already indicates a potential role of one of the proteases in the regulation of VEGFR3 protein content in adult human LECs. Since we are interested in the regulation of VEGFR3 signaling and not only total VEGFR3 protein content, we next questioned whether the C3 treatment also affects VEGFR3 phosphorylation.

Therefore, we repeated the Western Blotting (Figure 22A) and found VEGFR3 phosphorylation to be non-significantly upregulated by around 77% in adult human LECS upon the treatment with the unspecific BACE inhibitor C3 when compared to respective DMSO controls (Figure 22B).

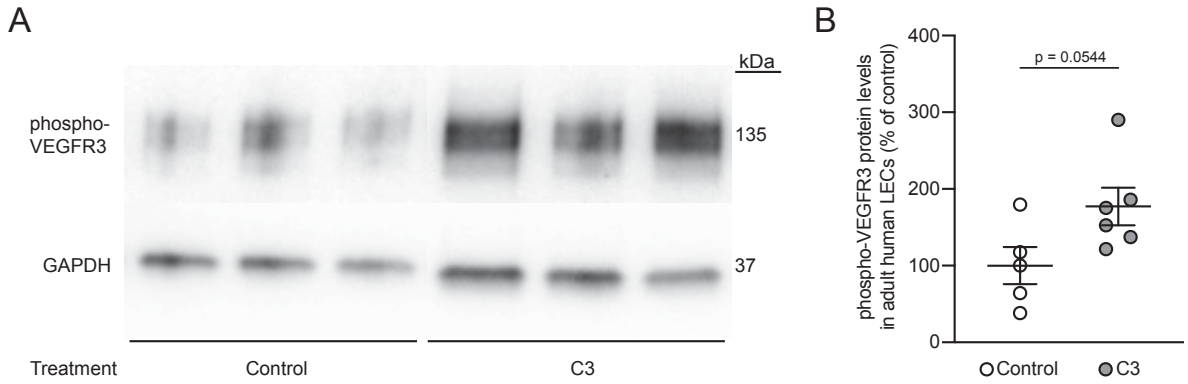

Figure 22: C3 mediated BACE inhibition increases phosphorylated VEGFR3 protein levels in adult human LECs.
(**A**) Representative Western Blot image of adult human LEC lysates after 6 hours of treatment with DMSO control (Control) or the BACE inhibitor C3 (C3) showing protein bands of phospho-VEGFR3 and GAPDH serving as loading control. (**B**) Quantification of phospho-VEGFR3 protein levels normalized to respective GAPDH levels in adult human LECs after 6 hours of treatment with either DMSO control or C3, shown as percentage of control. All values are shown as means ± SEM with $n \geqq 5$ independently treated sets of LECs per condition, statistical significance was determined by an unpaired two-tailed Student's t-test. Laura Sophie Hilger performed the presented experiment.

In parallel, we also used the method of PLA to detect phosphorylated VEGFR3 on adult human LECs. We used this method to label sites on the C3 treated and fixed adult human LECs which were both positive for phosphorylated tyrosine residues (referred to as 'pTyr') and VEGFR3, thus indicating phosphorylated VEGFR3 (referred to as 'pTyr/VEGFR3'). The amount of counted PLA sites was normalized to the cell count of each image. Comparison of the number of pTyr/VEGFR3 PLA sites on DMSO control treated LECs (control) (Figure 23A) and C3 treated LECs (Figure 23B) revealed a significant increase in the number of pTyr/VEGFR3 PLA sites on LECs which were previously treated with the BACE inhibitor C3 by around 194% (Figure 23C).

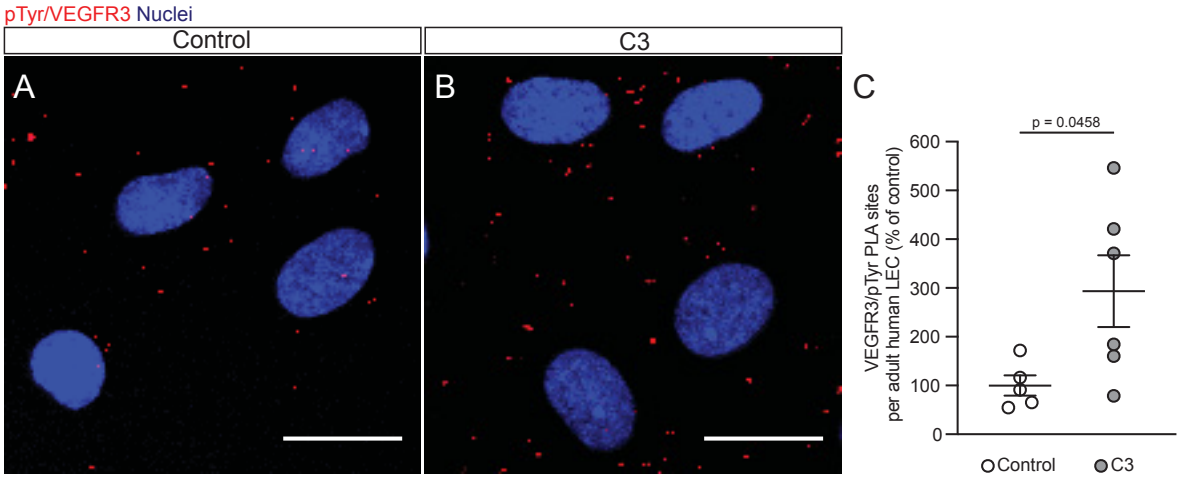

Figure 23: C3 mediated BACE inhibition significantly increases number of pTyr/VEGFR3 PLA sites in adult human LECs.
(**A,B**) Representative LSM images of adult human LECs after 6 hours of treatment with DMSO control (Control) or the BACE inhibitor C3 (C3) showing pTyr/VEGFR3 proximity ligation assay (PLA) sites (red). A co-staining for nuclei (blue) is also shown. Scale bars, 20 µm. (**C**) Quantification of pTyr/VEGFR3 PLA sites per adult human LEC after 6 hours of treatment with either DMSO control or C3, shown as percentage of control. All values are shown as means ± SEM with n ≧ 5 independently treated sets of LECs per condition, statistical significance was determined by an unpaired two-tailed Student's t-test. Laura Sophie Hilger performed the presented experiment.

The quantification of pTyr/VEGFR3 PLA sites on C3 treated adult human LECs (Figure 23) revealed a stronger result than Western Blotting of phosphorylated VEGFR3 in C3 treated adult human LEC lysates (Figure 22). Together, these results indicate that unspecific BACE inhibition by use of inhibitor C3 increases VEGFR3 phosphorylation and therefore at least one of the inhibited proteases of the BACE family might impact VEGFR3 signaling in adult human LECs.

On the other hand, we also analyzed the VEGFR2 phosphorylation in C3 treated adult human LECs. As VEGFR2 and VEGFR3 have been described to be of redundant roles during lymphangiogenesis (Goldman et al. 2007), we aimed to distinguish between the two RTKs. After the C3 treatment we fixed the LECs and detected the number of pTyr/VEGFR2 PLA sites, indicating phosphorylated VEGFR2 on adult human LECs (Figure 24A,B). Upon treatment with the unspecific BACE inhibitor C3 versus DMSO control (control), the number of pTyr/VEGFR2 PLA sites was not significantly altered (Figure 24C).

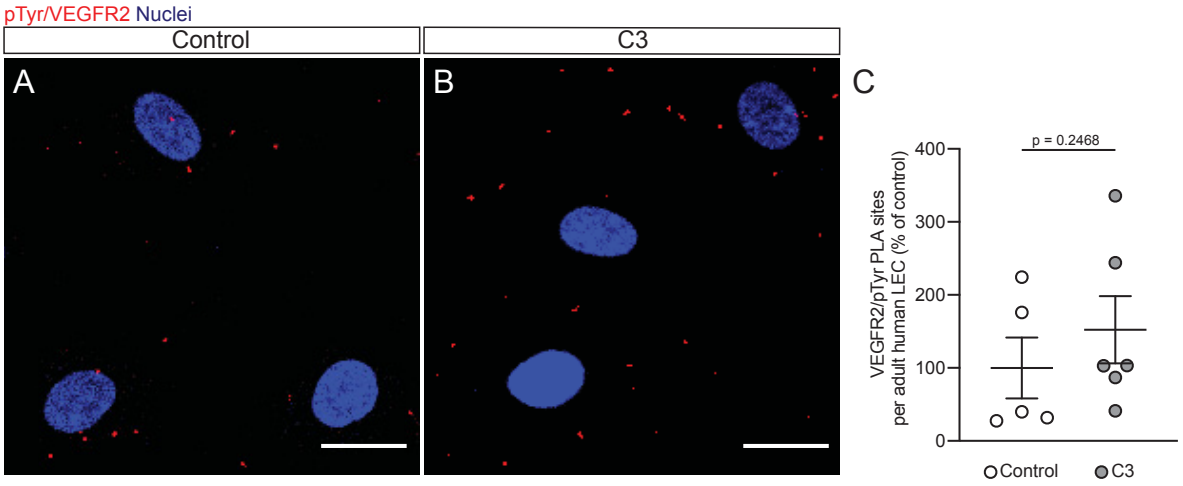

Figure 24: C3 mediated BACE inhibition does not remarkably alter number of pTyr/VEGFR2 PLA sites in adult human LECs.
(**A,B**) Representative LSM images of adult human LECs after 6 hours of treatment with DMSO control (Control) (A) or the BACE inhibitor C3 (C3) (B) showing pTyr/VEGFR2 proximity ligation assay (PLA) sites (red). A co-staining for nuclei (blue) is also shown. Scale bars, 20 µm. (**C**) Quantification of pTyr/VEGFR2 PLA sites per adult human LEC after 6 hours of treatment with either DMSO control or C3, shown as percentage of control. All values are shown as means ± SEM with n ≧ 5 independently treated sets of LECs per condition, statistical significance was determined by a Mann-Whitney test. Laura Sophie Hilger performed the presented experiment.

The obtained results on VEGFR3 and VEGFR2 phosphorylation in adult human LECs upon unspecific BACE inhibition therefore revealed that at least one of the BACE proteases might influence VEGFR3 signaling (Figure 22 and Figure 23) but none of the targeted BACE family members seems to influence VEGFR2 signaling (Figure 24).

5.2.2 C3 mediated BACE inhibition increases adult human LEC proliferation

Increased VEGFR3 signaling in adult human LECs normally correlates with increased LEC proliferation. As we have seen a regulation of VEGFR3 signaling by one of the BACE family members targeted by the unspecific inhibitor C3 (Figure 22 and Figure 23), we next analyzed adult human LEC proliferation upon this treatment. Therefore, we added BrdU to the medium of the LECs in parallel to the treatment with either DMSO control (control) or the BACE inhibitor C3 and incubated the LECs for 6 hours. The immunostaining for BrdU and nuclei (Figure 25A,B) and the normalization of BrdU-positive LECs to the total amount of nuclei revealed a non-significant increase of adult human LEC proliferation by around 21% upon treatment with C3 when compared to respective DMSO controls (Figure 25C).

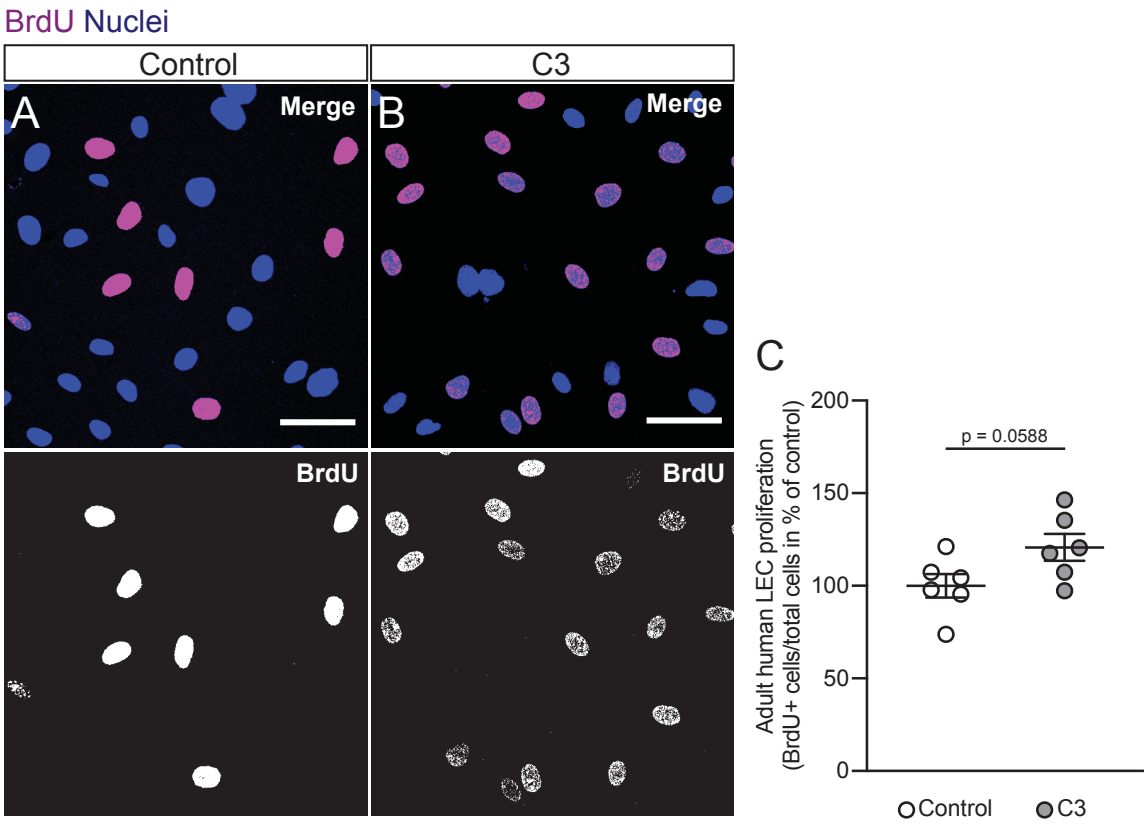

Figure 25: C3 mediated BACE inhibition increases adult human LECs proliferation.
(**A,B**) Representative LSM images of adult human LECs after 6 hours of treatment with either DMSO control (Control) (A) or the BACE inhibitor C3 (C3) (B). The proliferation marker BrdU was added to the medium for the last 3 hours of the respective treatment. Staining shows BrdU (magenta) and nuclei (blue). Scale bars, 50 µm. (**C**) Quantification of BrdU-positive LECs normalized to total cells after 6 hours of treatment with either control or C3, shown as percentage of control. All values are shown as means ± SEM with n = 6 independently treated sets of LECs per condition, statistical significance was determined by an unpaired two-tailed Student's t-test. Laura Sophie Hilger performed the presented experiment.

As a conclusion we can therefore say that the unspecific inhibition of BACE family proteases via the inhibitor C3 results in increased total VEGFR3 protein levels (Figure 21), increased VEGFR3 phosphorylation (Figure 22 and Figure 23) and finally also in increased adult human LEC proliferation (Figure 25), while VEGFR2 phosphorylation was not significantly influenced (Figure 24). Thus, the unspecific inhibitor C3 seems to target at least one of the BACE family proteases which might have a regulating role in VEGFR3 signaling of adult human LECs.

5.2.3 Verubecestat treatment reduces *BACE1* but neither *BACE2*, nor *VEGFR3* mRNA expression levels in adult human LECs

Aiming for a more precise knowledge about which of the BACE proteases possibly contributes to the regulation of VEGFR3 signaling in adult human LECs, we next treated the adult human LECs with the BACE1 inhibitor named verubecestat (Kennedy et al. 2016; Scott et al. 2016). Verubecestat was already used for clinical trials with human patients and turned out to cause severe side effects which might be due to a co-inhibition of BACE2 in addition to the intended inhibition of BACE1 (Hawkes 2017). To determine whether verubecestat targets BACE1 and BACE2 in adult human LECs, we treated the LECs *in vitro* for 6 hours with either a DMSO control (control) or verubecestat and subsequently isolated RNA. The analysis of *BACE1* mRNA expression levels by use of qPCR revealed a significant downregulation of *BACE1* mRNA expression in adult human LECs upon treatment with verubecestat (Figure 26A-C). For a more precise normalization of *BACE1* mRNA levels, we used the mRNA expression levels of three different housekeeping genes. Normalization to the mRNA expression levels of *Ribosomal phosphoprotein P0* (*RPLP0*) revealed a significant downregulation of *BACE1* mRNA expression levels by around 22%, while the normalization of *BACE1* mRNA expression levels to expression levels of the housekeeping gene *Beta-2-microglobulin* (*B2M*) revealed a trend towards downregulation of *BACE1* mRNA expression levels by around 18% (Figure 26B). As a third housekeeping gene, we used the mRNA expression levels of *Hypoxanthine phosphoribosyltransferase* (*HPRT1*) for the normalization of *BACE1* mRNA expression levels and the quantification revealed a significant downregulation of *BACE1* mRNA expression levels by around 26% upon verubecestat treatment in adult human LECs (Figure 26C). The presented analyses of *BACE1* mRNA expression after verubecestat treatment suggest that verubecestat functions as a *BACE1* inhibitor on mRNA expression levels in adult human LECs (Figure 26).

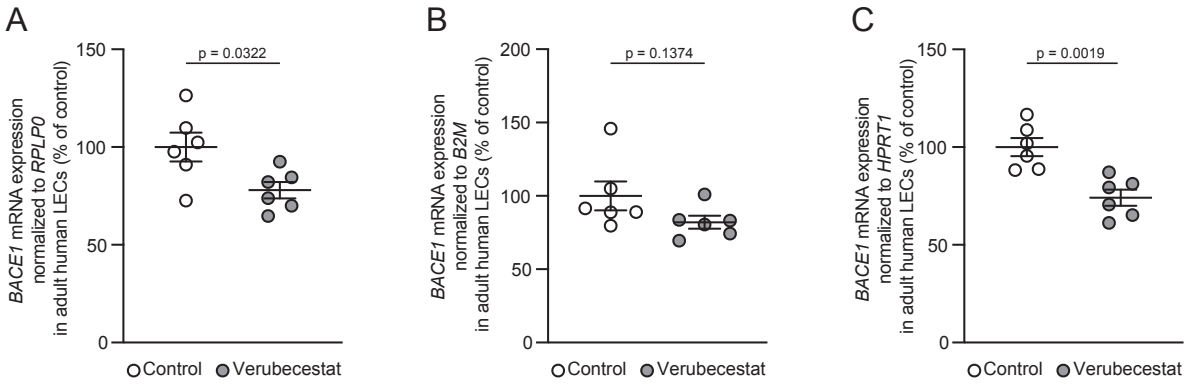

Figure 26: Verubecestat mediated BACE inhibition decreases *BACE1* mRNA expression levels in adult human LECs.
Quantification of *BACE1* mRNA expression levels in lysates of adult human LECs treated for 6 hours with either DMSO control (Control) or the BACE inhibitor verubecestat normalized to three different reference genes; (**A**) *BACE1* mRNA expression normalized to the expression of reference gene *36b4*, (**B**) *BACE1* mRNA expression normalized to the expression of reference gene *B2M*, (**C**) *BACE1* mRNA expression normalized to the expression of reference gene *HPRT1* in adult human LECs. All values are shown as means ± SEM with n ≧ 5 independently treated sets of LECs per condition, statistical significance was determined by unpaired two-tailed Student's t-tests. Laura Sophie Hilger performed the presented experiments.

On the contrary, we also investigated the mRNA expression levels of *BACE2* after 6 hours of treatment with verubecestat in adult human LEC lysates. The normalization to the expression levels of all of the housekeeping genes (*RPLP0, B2M* and *HPRT1)* did not show a significant alteration of *BACE2* mRNA expression levels upon treatment with verubecestat (Figure 27A,C). Nevertheless, the *BACE2* mRNA expression levels upon verubecestat treatment normalized to *B2M* mRNA expression levels were increased by around 18% by trend when compared to control (Figure 27B).

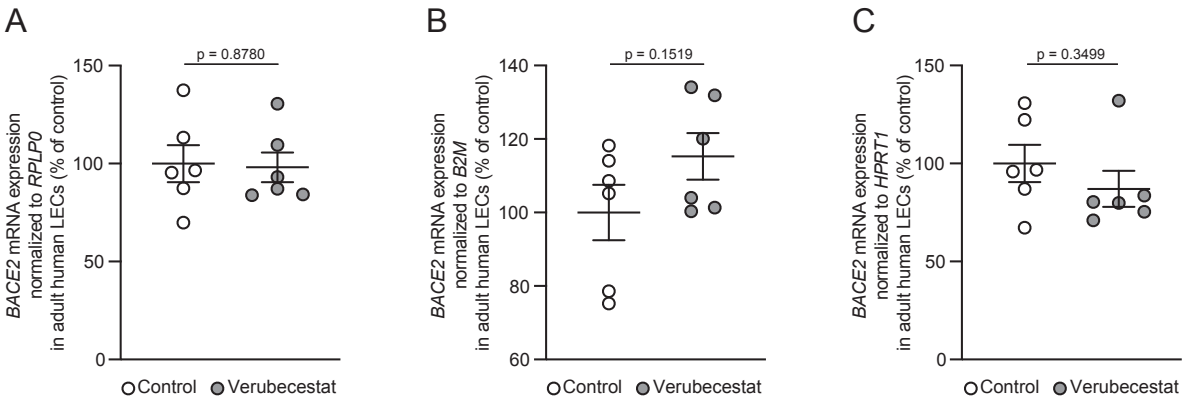

Figure 27: Verubecestat mediated BACE inhibition has no major effect on *BACE2* mRNA expression levels in adult human LECs.
(**A-C**) Quantification of *BACE2* mRNA expression levels in lysates of adult human LECs treated for 6 hours with either DMSO control (Control) or the BACE inhibitor verubecestat normalized to three different reference genes; (A) *BACE2* mRNA expression normalized to the expression of reference gene *36b4*, (B) *BACE2* mRNA expression normalized to the expression of reference gene *B2M*, (C) *BACE2* mRNA expression normalized to the expression of reference gene *HPRT1* in adult human LECs. All values are shown as means ± SEM with n = 6 independently treated sets of LECs per condition, statistical significance was determined by unpaired two-tailed Student's t-tests. Laura Sophie Hilger performed the presented experiments.

To obtain a better understanding of the way verubecestat may possibly affect signaling within adult human LECs, we next analyzed *VEGFR3* mRNA expression patterns in the same LEC lysates as before. We normalized the mRNA expression levels of *VEGFR3* to the ones of three different housekeeping genes (*RPLP0, B2M, HPRT1*) and could not detect a significant alteration of *VEGFR3* mRNA expression levels upon the treatment with verubecestat in adult human LECs (Figure 28A-C). As an exception, the *VEGFR3* mRNA expression upon verubecestat treatment was decreased by around 15% by trend, when normalized to *HPRT1* mRNA expression levels and compared to control (Figure 28C). This finding leads to the suggestion that *VEGFR3* mRNA expression levels are not majorly affected by the treatment with BACE inhibitor verubecestat (Figure 28). Since only *BACE1* mRNA expression levels were significantly altered in adult human LECs upon treatment with verubecestat (Figure 26-28), these results further support the hypothesis that *BACE2* rather than *BACE1* regulates VEGFR3 signaling in adult human LECs.

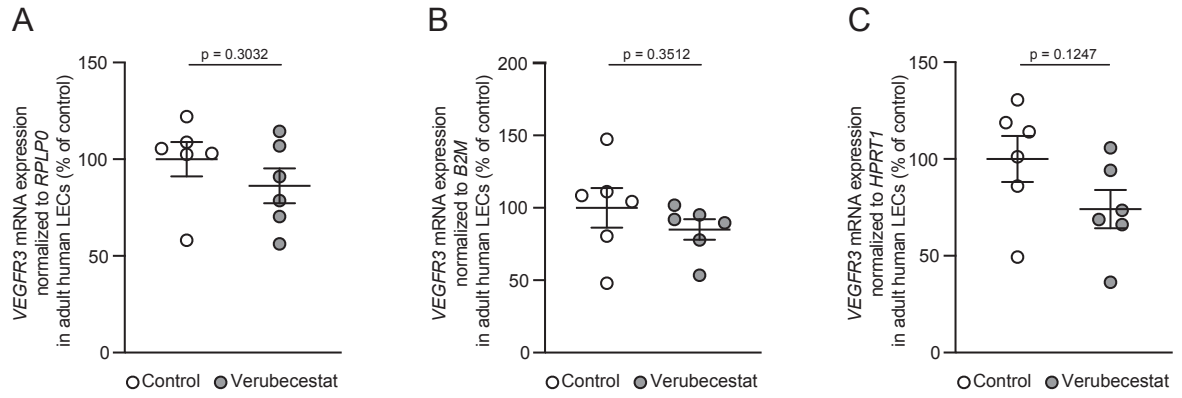

Figure 28: Verubecestat mediated BACE inhibition has no major effect on *VEGFR3* mRNA expression levels in adult human LECs.
(**A-C**) Quantification of *VEGFR3* mRNA expression levels in lysates of adult human LECs treated for 6 hours with either DMSO control (Control) or the BACE inhibitor verubecestat normalized to three different reference genes; (**A**) *VEGFR3* mRNA expression normalized to the expression of reference gene *36b4*, (**B**) *VEGFR3* mRNA expression normalized to the expression of reference gene *B2M*, (**C**) *VEGFR3* mRNA expression normalized to the expression of reference gene *HPRT1* in adult human LECs. All values are shown as means ± SEM with n = 6 independently treated sets of LECs per condition, statistical significance was determined by unpaired two-tailed Student's t-tests. Laura Sophie Hilger performed the presented experiments.

5.2.4 Verubecestat treatment significantly decreases BACE1 protein levels and BACE2 protein levels by trend in adult human LECs

In addition to our analyses on mRNA expression levels, we next analyzed BACE1 and BACE2 protein levels in adult human LECs upon treatment with the BACE1 inhibitor verubecestat. We hypothesized that BACE1 protein levels but not BACE2 protein levels would be reduced upon verubecestat treatment, as indicated on mRNA levels before (Figure 26 and Figure 27). In these experiments we again treated adult human LECs for 6 hours with either the BACE inhibitor verubecestat or the respective DMSO control (control) and lysed the LECs subsequently. Via Western Blotting we could detect the protein bands of BACE1 and GAPDH serving as loading control (Figure 29A). The quantification revealed a significant decrease of BACE1 protein levels by around 82% in adult human LECs after 6 hours of treatment with verubecestat (Figure 29B). The finding of a significant BACE1 protein level decrease in adult human LECs after treatment with the BACE inhibitor verubecestat (Figure 29) matched the previously described result on *BACE1* mRNA levels (Figure 26) and indicates that verubecestat treatment reduces *BACE1* both on mRNA and on protein level.

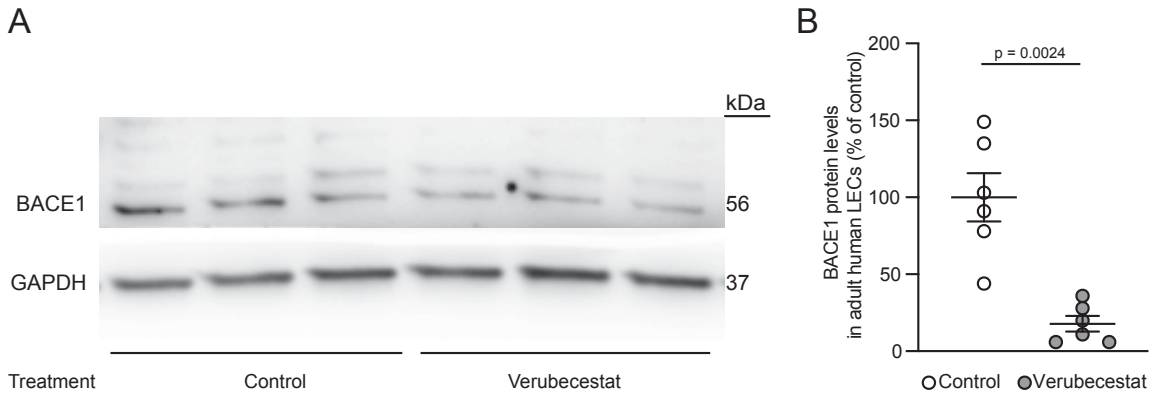

Figure 29: Verubecestat treatment significantly decreases BACE1 protein levels in adult human LECs.
(**A**) Representative Western blot image of human LEC lysates after 6 hours of treatment with DMSO control (Control) or the BACE inhibitor verubecestat showing protein bands of BACE1 and GAPDH serving as loading control. (**B**) Quantification of BACE1 protein levels in adult human LECs normalized to respective GAPDH levels after 6 hours of treatment with either DMSO control (Control) or BACE inhibitor verubecestat, shown as percentage of control. All values are shown as means ± SEM with n = 6 independently treated sets of LECs per condition, statistical significance was determined by an unpaired two-tailed Student's t-test. Laura Sophie Hilger performed the presented experiment.

To test whether the same is true for BACE2 protein levels, we analyzed the lysates of verubecestat treated adult human LECs for BACE2 protein levels via Western Blotting (Figure 30A). The normalization of BACE2 protein levels to the respective GAPDH content revealed a non-significant decrease of BACE2 protein levels by around 46% upon treatment of adult human LECs with verubecestat (Figure 30B).

As it was already indicated on *BACE1* and *BACE2* mRNA expression levels (Figure 26 and Figure 27), the effect of verubecestat treatment on BACE1 protein levels (Figure 29) was more intense, than the effect of verubecestat treatment on BACE2 protein levels (Figure 30). The data on *BACE1* (Figure 26), *BACE2* (Figure 27) and *VEGFR3* (Figure 28) mRNA expression levels as well as on BACE1 (Figure 29) and BACE2 (Figure 30) protein levels suggest that the inhibitory effect of verubecestat is more effective towards BACE1 than towards BACE2. Nevertheless, the result that verubecestat affects BACE2 in adult human LECs fits to previously published studies about the selectivity of verubecestat towards BACE1 (Kennedy et al. 2016; Scott et al. 2016).

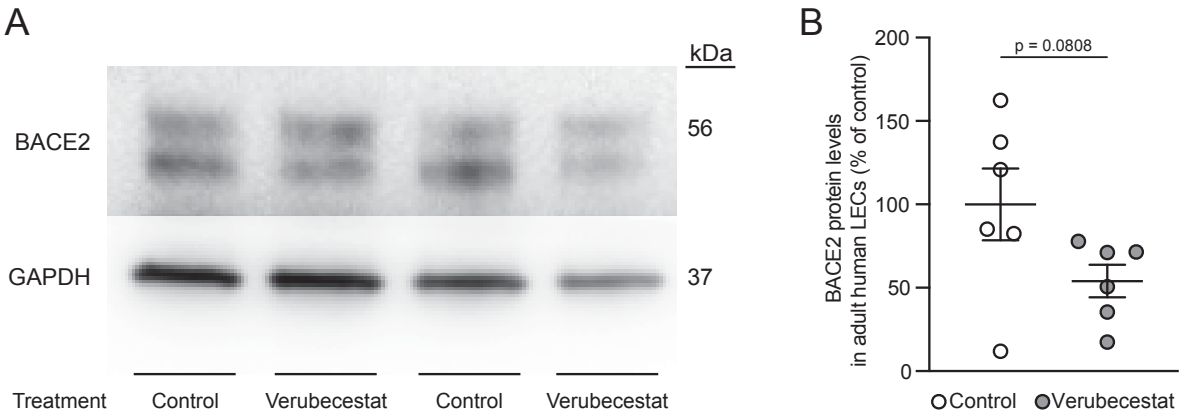

Figure 30: Verubecestat treatment decreases BACE2 protein levels in adult human LECs. (**A**) Representative Western blot image of human LEC lysates after 24 hours of treatment with DMSO control (Control) or the BACE inhibitor verubecestat showing protein bands of BACE2 and GAPDH serving as loading control. (**B**) Quantification of BACE2 protein expression levels in adult human LECs normalized to respective GAPDH expression after 24 hours of treatment with either control or verubecestat, shown as percentage of control. All values are shown as means ± SEM with n = 6 independently treated sets of LECs per condition, statistical significance was determined by an unpaired two-tailed Student's t-test. Laura Sophie Hilger performed the presented experiment.

5.2.5 Verubecestat treatment induces no major changes in VEGFR3 protein levels but decreases VEGFR3 phosphorylation

Since we hypothesized that at least one of the BACE proteases contributes to extracellular VEGFR3 attenuation, we additionally aimed to analyze VEGFR3 protein levels in adult human LECs upon treatment for 24 hours with either verubecestat or DMSO control (control). We suggested total VEGFR3 protein levels to accumulate in the LEC plasma membrane upon inhibition of BACE as proteases which potentially cleave VEGFR3. Via Western Blotting we could detect total VEGFR3 protein bands, while GAPDH was serving as loading control (Figure 31A). The normalization of VEGFR3 protein levels to the respective GAPDH amounts revealed that the verubecestat treatment for 24 hours increased total VEGFR3 protein levels by around 34% by trend (Figure 31B).

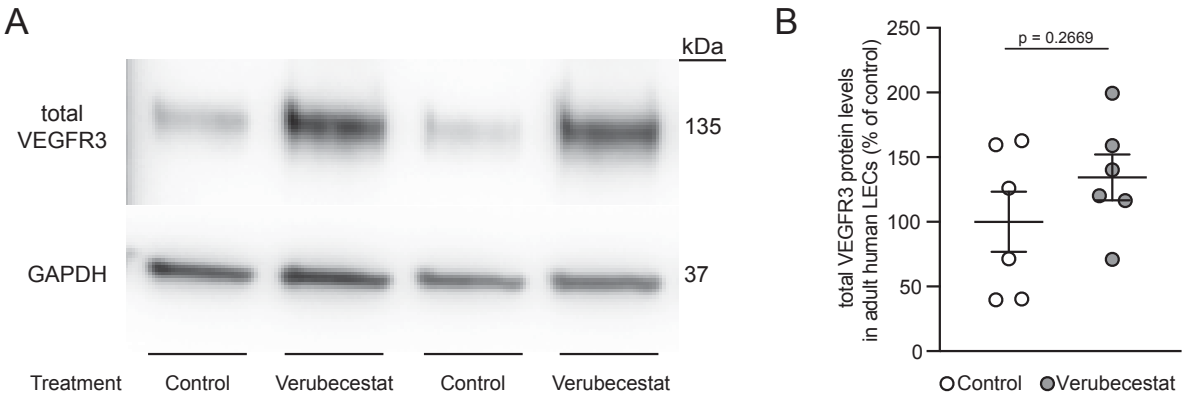

Figure 31: Verubecestat treatment increases VEGFR3 protein levels in adult human LECs by trend.
(**A**) Representative Western blot image of human LEC lysates after 24 hours of treatment with DMSO control (Control) or the BACE inhibitor verubecestat showing protein bands of VEGFR3 and GAPDH serving as loading control. (**B**) Quantification of VEGFR3 protein levels in adult human LECs normalized to respective GAPDH levels after 24 hours of treatment with either control or verubecestat, shown as percentage of control. All values are shown as means ± SEM with n = 6 independently treated sets of LECs per condition, statistical significance was determined by an unpaired two-tailed Student's t-test. Laura Sophie Hilger performed the presented experiments.

We next analyzed the phosphorylated VEGFR3 (phospho-VEGFR3) protein levels in the same adult human LEC lysates by Western Blotting (Figure 32A). When normalized to the respective amounts of GAPDH, the quantification revealed a significant downregulation of VEGFR3 phosphorylation by around 44% after treatment for 24 hours with verubecestat (Figure 32B). The presented results on total VEGFR3 (Figure 31) and phospho-VEGFR3 protein levels (Figure 32) in adult human LECs after 24 hours of treatment with the BACE inhibitor verubecestat indicate that the treatment has no major effect on VEGFR3 protein levels but significantly reduces VEGFR3 phosphorylation.

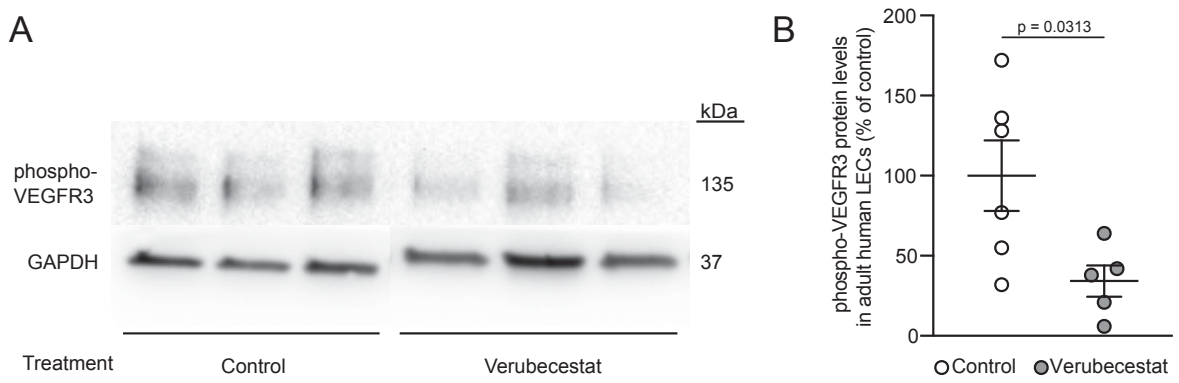

Figure 32: Verubecestat significantly decreases phospho-VEGFR3 protein levels in adult human LECs.
(A) Representative Western blot image of human LEC lysates after 24 hours of treatment with DMSO control (Control) or the BACE inhibitor verubecestat showing protein bands of phospho-VEGFR3 and GAPDH serving as loading control. (B) Quantification of phospho-VEGFR3 protein levels in adult human LECs normalized to respective GAPDH levels after 24 hours of treatment with either DMSO control (Control) or verubecestat, shown as percentage of control. All values are shown as means ± SEM with n = 6 independently treated sets of LECs per condition, statistical significance was determined by an unpaired two-tailed Student's t-test. Laura Sophie Hilger performed the presented experiment.

We further used the pTyr/VEGFR3 PLA (Figure 33) to verify the results concerning VEGFR3 phosphorylation after verubecestat treatment (Figure 32). The result of significantly reduced phosphorylated VEGFR3 protein levels in adult human LECs after 24 hours of treatment with either the BACE inhibitor verubecestat or the respective DMSO control (control) (Figure 32) could be reproduced via PLA by trend (Figure 33A,B). After the treatment, the fixed adult human LECs were immunostained and the counted pTyr/VEGFR3 PLA sites were normalized to the number of nuclei. The quantification resulted in a decrease by trend of VEGFR3 phosphorylation by around 30% after 24 hours of verubecestat treatment (Figure 33C). We therefore concluded that 24 hours of verubecestat treatment was not sufficient to significantly increase total VEGFR3 protein levels (Figure 31), but to decrease VEGFR3 phosphorylation (Figure 32 and Figure 33).

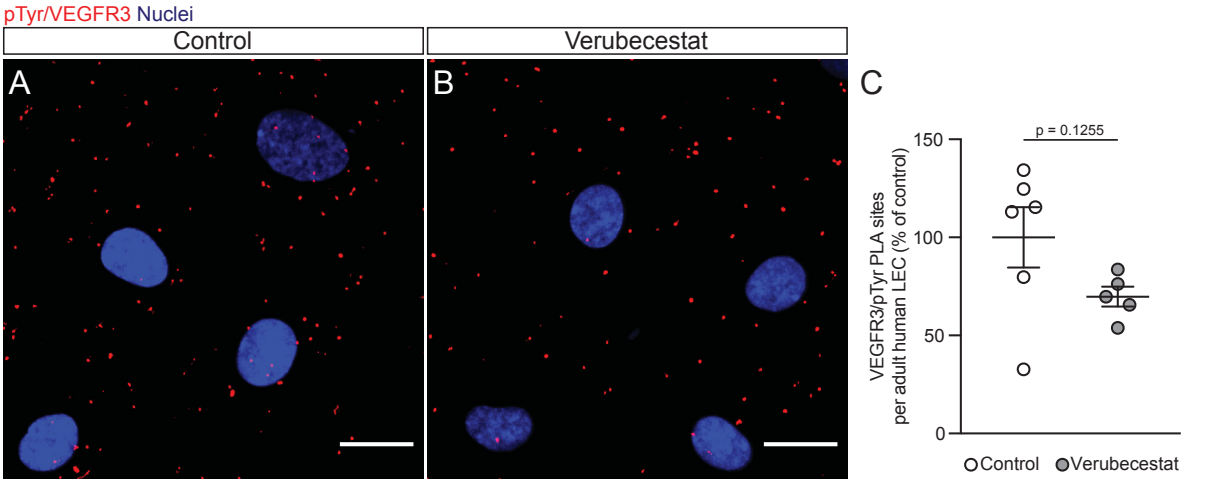

Figure 33: Verubecestat mediated BACE inhibition reduces the number of pTyr/VEGFR3 PLA sites in adult human LECs by trend.
(**A,B**) Representative LSM images of human LECs after 24 hours of treatment with DMSO control (Control) (A) or the BACE inhibitor verubecestat (B) showing pTyr/VEGFR3 proximity ligation assay (PLA) sites (red). A co-staining for nuclei (blue) is also shown. Scale bars, 20 µm. (**B**) Quantification of pTyr/VEGFR3 PLA sites per adult human LEC after 24 hours of treatment with either DMSO control (Control) or verubecestat, shown as percentage of control. All values are shown as means ± SEM with n ≧ 5 independently treated sets of LECs per condition, statistical significance was determined by a Mann-Whitney test. Laura Sophie Hilger and Ida Stöppelkamp performed the presented experiment.

5.2.6 Short-term Verubecestat treatment does not induce major changes in VEGFR3 phosphorylation and adult human LEC proliferation

Changes in VEGFR3 phosphorylation are usually a short-term effect, meaning that this receptor tyrosine kinase (referred to as ‘RTK’) is able to adapt its activity within minutes after a certain stimulus. Therefore, we decided to repeat the verubecestat treatment on adult human LECs again and to use a shorter incubation time. We thus incubated the adult human LECs with either the DMSO control (control) or verubecestat for 20 minutes only and fixed them subsequently. To detect VEGFR3 phosphorylation, we performed a pTyr/VEGFR3 PLA and normalized the number of pTyr/VEGFR3 PLA sites to the cell count of each image (Figure 34A-D). The comparison between the number of pTyr/VEGFR3 PLA sites of verubecestat and control treated adult human LECs revealed an increase in VEGFR3 phosphorylation by around 32% by trend upon treatment with verubecestat for 20 minutes (Figure 34E).

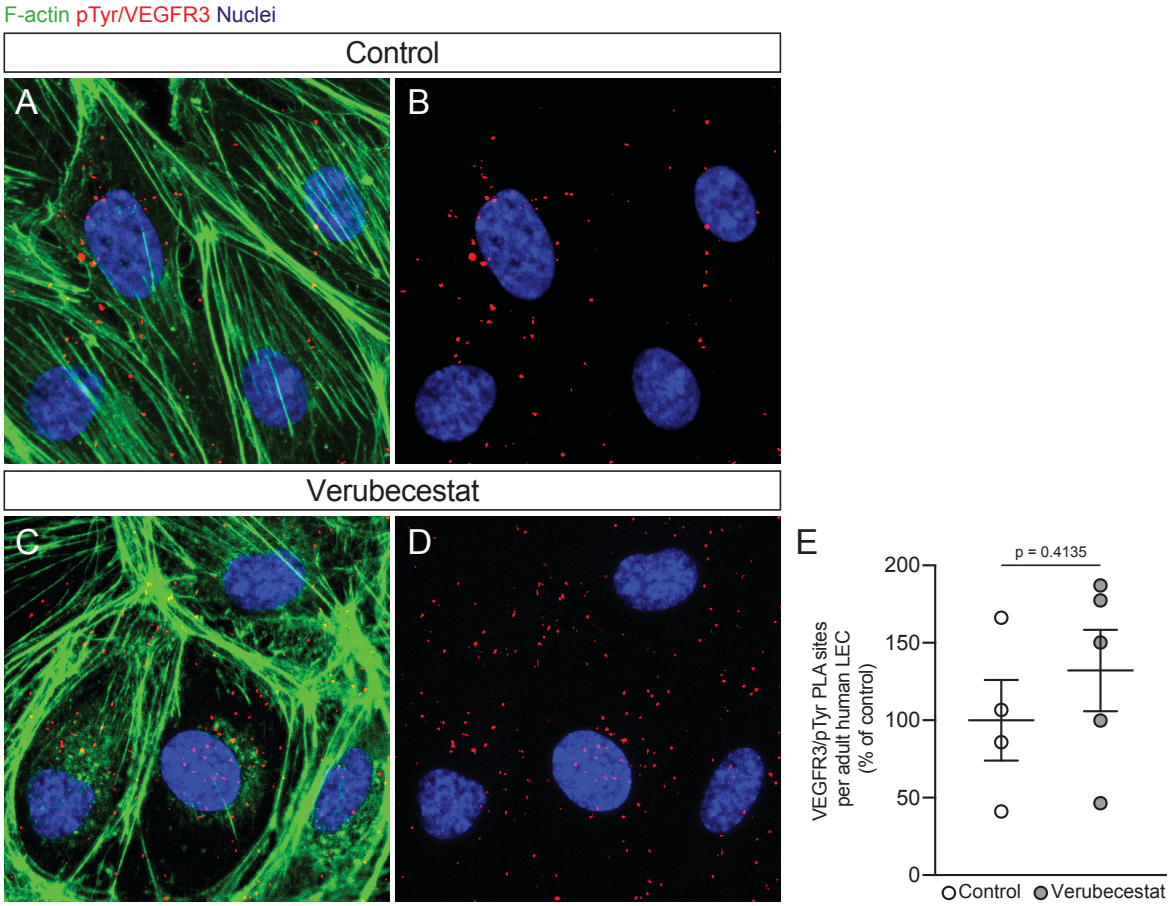

Figure 34: Short-term verubecestat treatment slightly increases the number of pTyr/VEGFR3 PLA sites in adult human LECs.
(**A,B**) Representative LSM images of human LECs after 24 hours of treatment with DMSO control (Control) (A) or the BACE inhibitor verubecestat (B) showing pTyr/VEGFR3 proximity ligation assay (PLA) sites (red). A co-staining for nuclei (blue) is also shown. Scale bars, 20 µm. (**B**) Quantification of pTyr/VEGFR3 PLA sites per adult human LEC after 24 hours of treatment with either DMSO control (Control) or verubecestat, shown as percentage of control. All values are shown as means ± SEM with n ≧ 4 independently treated sets of LECs per condition, statistical significance was determined by an unpaired two-tailed Student's t-test. Laura Sophie Hilger performed the presented experiments in cooperation with Laura Isabelle Hofmann and Andree Schmidt.

Even though the analyses on VEGFR3 phosphorylation did not reveal consistent effects induced by the verubecestat treatment (Figure 32, Figure 33 and Figure 34), we next aimed to analyze adult human LEC proliferation after verubecestat treatment (Figure 35). We did this, because we could detect both a reduction and the tendency towards an increase of VEGFR3 phosphorylation, which might also result in either decreased or increased adult human LEC proliferation. Via BrdU incorporation assay, we visualized the proliferated LECs after 6 hours of DMSO control (Control) or verubecestat treatment (Figure 35A,B) and normalized the BrdU-positive LECs to the total number of nuclei. Thereby, we could not see any changes in adult human LEC proliferation after treatment with verubecestat (Figure 35C).

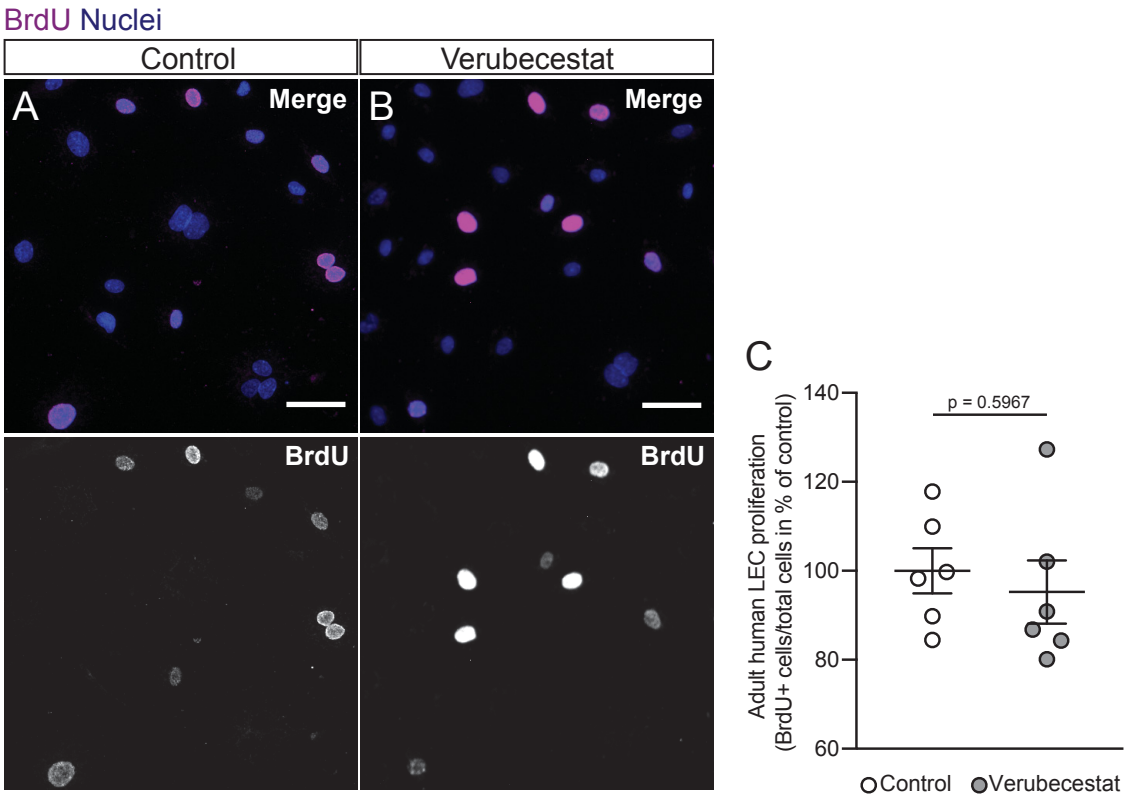

Figure 35: Verubecestat treatment does not affect adult human LEC proliferation.
(**A,B**) Representative LSM images of adult human LECs after 6 hours of treatment with either DMSO control (Control) (A) or the BACE inhibitor Verubecestat (Verubecestat) (B). The proliferation marker BrdU was added to the medium for the last 3 hours of the respective treatment. Staining shows BrdU (magenta) and nuclei (blue). Scale bars, 50 µm. (**C**) Quantification of BrdU-positive LECs normalized to total cells after 6 hours of treatment with either control or Verubecestat, shown as percentage of control. All values are shown as means ± SEM with n = 6 independently treated sets of LECs per condition, statistical significance was determined by an unpaired two-tailed Student's t-test. Laura Sophie Hilger and Ida Stöppelkamp performed the presented experiment.

At this point of the study, we were able to say that verubecestat treatment decreases *BACE1* mRNA and protein levels significantly (Figure 26 and Figure 29) while it only reduces *BACE2* mRNA and protein levels by trend (Figure 27 and Figure 30). Therefore, we could conclude that verubecestat seemed to be more specifically inhibiting BACE1, rather than BACE2. Further analyses could not show significant effects of verubecestat treatment on the total amount of VEGFR3 protein levels (Figure 31), while VEGFR3 phosphorylation was significantly downregulated after 24 hours of treatment with verubecestat (Figure 32, Figure 33) and upregulated by trend upon 20 minutes of verubecestat treatment (Figure 34). Adult human LEC proliferation further remained unchanged upon verubecestat treatment (Figure 35). These findings lead us to the suggestion that rather BACE2 than BACE1 would be contributing to the regulation of VEGFR3 signaling in adult human LECs. Nevertheless, effects of verubecestat treatment on VEGFR3 signaling seem to be time dependent.

5.2.7 Silencing of *BACE1* neither changes VEGFR3 phosphorylation nor adult human LEC proliferation

Since the unspecific BACE inhibition with C3 revealed effects on total VEGFR3 protein content (Figure 21) and its phosphorylation (Figure 22 and Figure 23), as well as on adult human LEC proliferation (Figure 25), while the verubecestat treatment was more specific for BACE1 and did not show consistent effects on VEGFR3 levels and its phosphorylation or LEC proliferation (Figures 26-35), we next aimed to analyze the roles of both BACE1 and BACE2 independently from each other.

Therefore, we chose the method of siRNA mediated silencing and started with silencing of human *BACE1* in adult human LECs. Aiming for a high precision in our results, we decided to use three different BACE1 siRNAs (BACE1 siRNA 1, 2, 3) and a non-targeting control siRNA with a similar GC content (control). We isolated the RNA of adult human LECs 48 hours after the transfections. For the analyses of *BACE1* mRNA expression levels, we normalized to the mRNA expression levels of three different housekeeping genes (*RPLP0, B2M, HPRT1*) (Figure 36A-C). We could detect a significant downregulation of *BACE1* mRNA expression levels by around 37-61% upon transfection with BACE1 siRNA 1, after normalization to all housekeeping genes (Figure 36A-C). When normalized to the mRNA expression levels of *RPLP0*, *B2M* and *HPRT1*, BACE1 siRNA 2 reduced *BACE1* mRNA expression levels by trend by around 20-43% (Figure 36A-C). When normalized to the mRNA expression of housekeeping gene *RPLP0*, BACE1 siRNA 3 silenced *BACE1* mRNA expression levels significantly by around 46% (Figure 36A), while the reduction by 28-36% when normalized to *B2M* or *HPRT1* was only by trend (Figure 36B,C). As we could see a reduction in *BACE1* mRNA expression levels upon transfection with BACE1 siRNAs (Figure 36) we further looked into the protein levels in respective adult human LEC lysates.

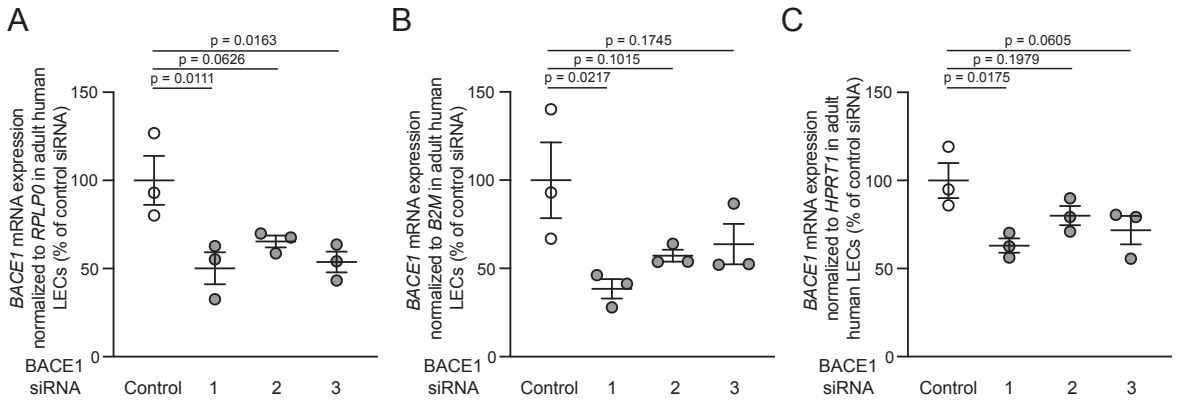

Figure 36: *BACE1* mRNA expression is efficiently silenced in adult human LECs by use of BACE1 siRNA 1.
(A-C) Quantificantions of *BACE1* mRNA levels in adult human LECs 48 hours after transfection with control siRNA (Control) or one of three different siRNAs against *BACE1* (BACE1 siRNA 1, 2, 3), shown as percent of control siRNA. *BACE1* mRNA expression levels were normalized to three different reference genes; in (A) *BACE1* mRNA expression is normalized to *RPLP0* mRNA expression, while in (B) *BACE1* mRNA expression is normalized to *B2M* mRNA expression and in (C) *BACE1* mRNA expression is normalized to *HPRT1* mRNA expression. All values are shown as means ± SEM with n = 3 independent transfections per siRNA; statistical significance was determined by one-way ANOVA and Dunnett's multiple comparisons test. Laura Sophie Hilger and Ida Stöppelkamp performed the presented experiments.

Therefore, we performed Western Blotting with *BACE1* silenced LEC lysates and detected protein bands of VEGFR3, BACE1 and GAPDH serving as loading control (Figure 37A). The quantification of BACE1 protein content after transfection with the three different BACE1 siRNAs and after normalization to the respective GAPDH protein content revealed a decrease in BACE1 protein levels by around 9-54% by trend (Figure 37B). Notably, transfection with BACE1 siRNA 2 was sufficient to significantly decrease BACE2 protein levels by around 54%. We subsequently analyzed the total VEGFR3 protein levels in the same Western Blot (Figure 37A) and did not detect any changes in total VEGFR3 protein levels upon silencing of BACE1 in adult human LECs (Figure 37C).

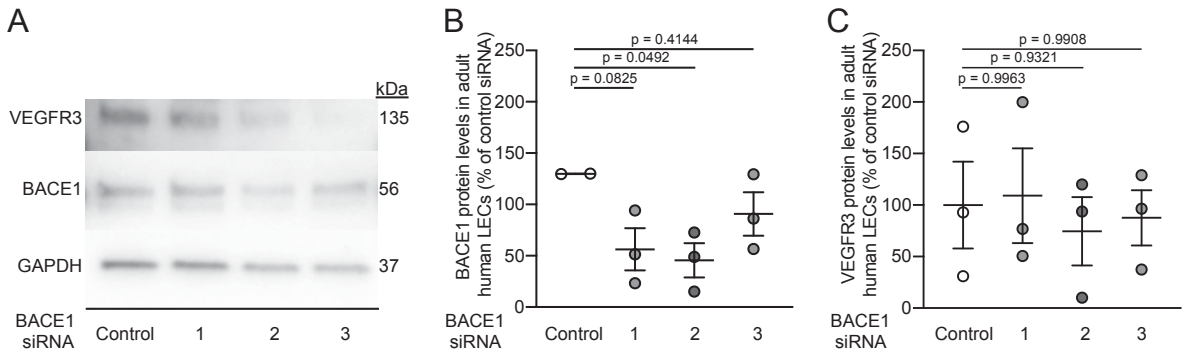

Figure 37: Silencing of *BACE1* does not affect VEGFR3 protein levels in adult human LECs. (**A**) Representative Western Blot image of adult human LEC lysates 48 hours after transfection with either control siRNA (Control) or one of three BACE1 siRNAs (BACE1 siRNA 1, 2, 3) showing protein bands of VEGFR3, BACE1 and GAPDH serving as loading control. (**B**) Quantification of BACE1 protein levels in adult human LECs normalized to respective GAPDH levels 48 hours after transfection with either control siRNA or one of three BACE1 siRNAs, shown as percentage of control. (**C**) Quantifications of VEGFR3 protein levels in LEC lysates 48 hours after transfection with either control or one of three BACE2 siRNAs, shown as percentage of control. All values are shown as means ± SEM with n ≧ 2 independently treated sets of LECs per condition, statistical significance was determined by one-way ANOVA and Dunnett's multiple comparisons test. Laura Sophie Hilger performed the presented experiment.

The unchanged total VEGFR3 protein levels (Figure 37C) upon silencing of *BACE1* (Figure 37B) point to the hypothesis that BACE1 does not regulate VEGFR3 protein content in adult human LECs. To further determine the role of BACE1 in VEGFR3 signaling of adult human LECs, we fixed *BACE1* silenced (referred to as 'BACE1 KD') LECs 48 hours after transfection with the most efficient BACE1 siRNA, which was BACE1 siRNA 1 (Figure 36). We subsequently performed a co-staining for F-actin and used the pTyr/VEGFR3 PLA to visualize sites of phosphorylated VEGFR3 on LECs either transfected with control siRNA (control) or BACE1 siRNA 1 (BACE1 KD) (Figure 38A,B). The normalization of pTyr/VEGFR3 PLA sites to the number of nuclei and the comparison between control treatment and BACE1 KD revealed no major changes in the number of pTyr/VEGFR3 PLA sites after silencing of *BACE1* (Figure 38C).

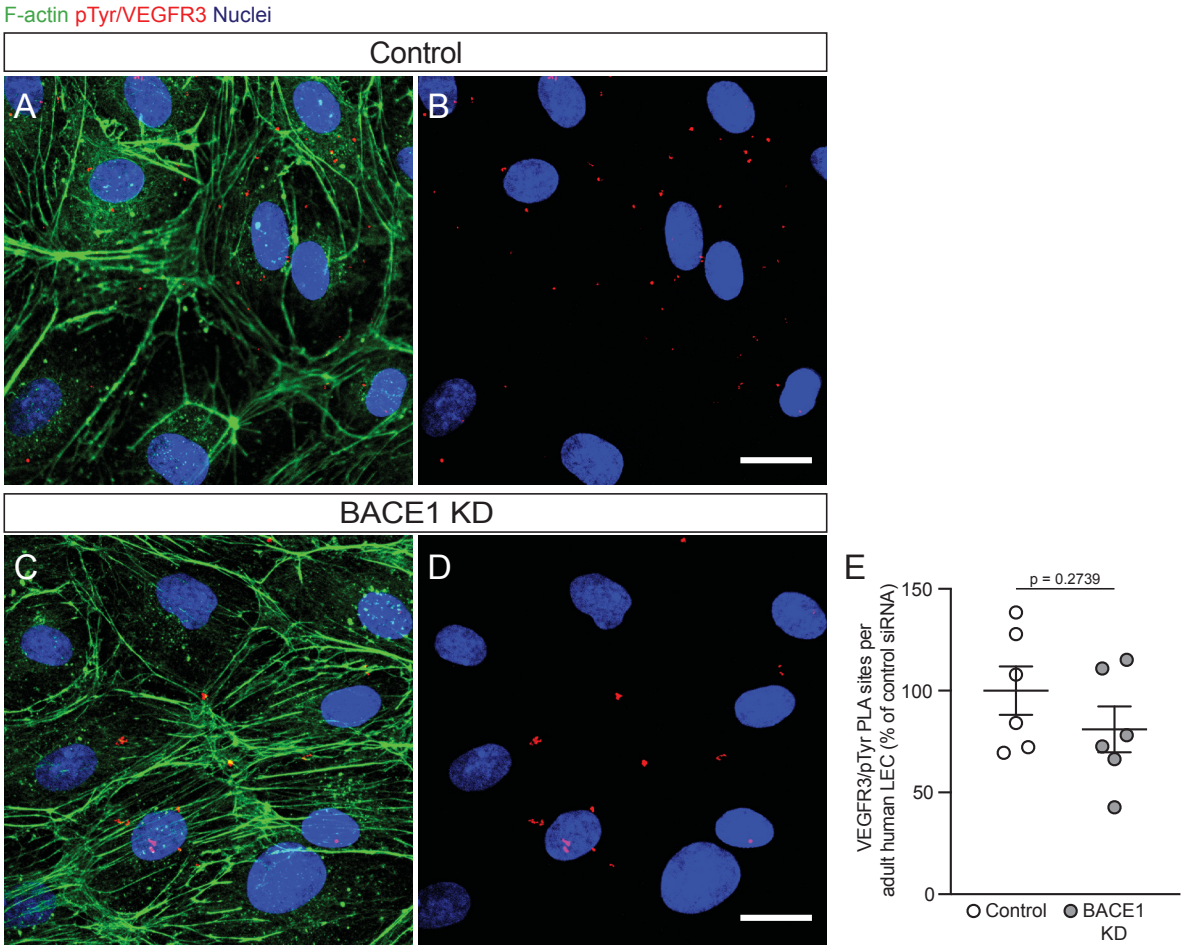

Figure 38: Silencing of *BACE1* induces no major changes in the number of pTyr/VEGFR3 PLA sites in adult human LECs.
(**A,B**) Representative LSM images of adult human LECs 48 hours after transfection with either control siRNA (Control) (A) or BACE1 siRNA 1 (BACE1 KD) (B) showing pTyr/VEGFR3 proximity ligation assay (PLA) sites (red). A co-staining for F-actin (green) and nuclei (blue) is also shown. Scale bars, 20 µm. (**B**) Quantification of pTyr/VEGFR3 PLA sites per adult human LEC 48 hours after transfection with either control or BACE1 siRNA 1 (BACE1 KD), shown as percentage of control. All values are shown as means ± SEM with n = 6 independently transfected sets of LECs per condition, statistical significance was determined by an unpaired two-tailed Student's t-test. Laura Sophie Hilger and Ida Stöppelkamp performed the presented experiment.

Even though *BACE1* silencing did neither result in altered VEGFR3 protein, nor altered VEGFR3 signaling, we next aimed to analyze adult human LEC proliferation upon silencing of *BACE1*. With this, we aimed to exclude the a VEGFR3-independent way by which BACE1 might possibly influence LEC proliferation. We therefore performed BrdU assays with adult human LECs which were transfected with either control siRNA (control) or BACE1 siRNA 1 (BACE1 KD) 48 hours in advance (Figure 39A,B). The normalization of BrdU-positive LECs to the total number of cells and the comparison between the two groups revealed no major changes in adult human LEC proliferation rates of *BACE1* silenced LECs (Figure 39C).

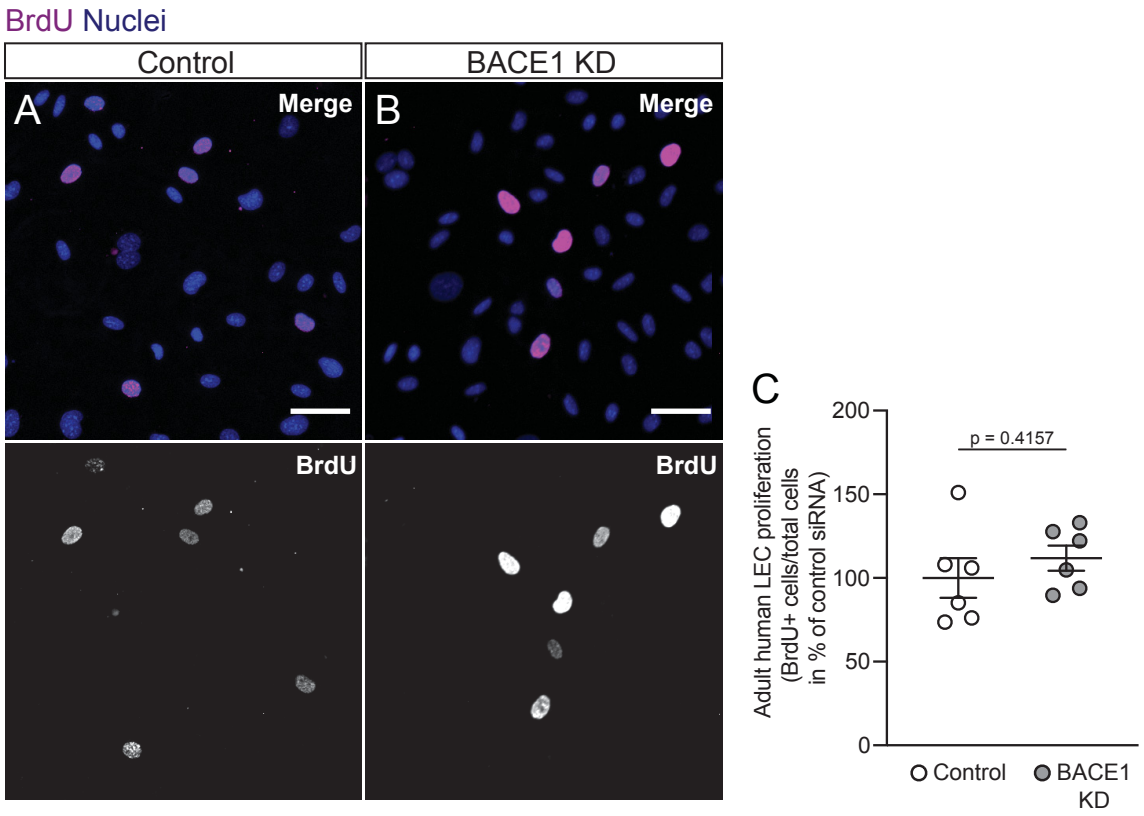

Figure 39: Silencing of *BACE1* does not alter adult human LEC proliferation.
(**A,B**) Representative LSM images of adult human LECs 48 hours after transfection with either control siRNA (Control) (A) or BACE1 siRNA 1 (BACE1 KD) (B). The proliferation marker BrdU was added for 3 hours to the medium of the respective treatment. Staining shows BrdU (magenta) and nuclei (blue). Scale bars, 50 µm. (**C**) Quantification of BrdU-positive LECs normalized to total cells 48 hours after transfection with control or BACE1 siRNA 1 (BACE1 KD), shown as percentage of control. All values are shown as means ± SEM with n = 6 independently transfected sets of LECs per condition, statistical significance was determined by an unpaired two-tailed Student's t-test. Laura Sophie Hilger and Ida Stöppelkamp performed the presented experiment.

The unaltered proliferation rates of *BACE1* silenced adult human LECs compared to control LECs (Figure 39) suggest that BACE1 does not influence adult human LEC proliferation. These results fit to the suggestion we made after the C3 and verubecestat treatment of adult human LECs, in which the more selective BACE1 inhibition by verubecestat had no increasing effect on VEGFR3 signaling (Figure 32, Figure 33 and Figure 34) while the unspecific inhibition of all BACE proteases by C3 increased VEGFR3 phosphorylation (Figure 22 and Figure 23).

5.2.8 Recombinant BACE2 protein addition significantly reduces total VEGFR3 protein levels in adult human LECs

We concluded that BACE1 has no regulatory functions concerning the VEGFR3 signaling in adult human LECs and next aimed to analyze the functions of BACE2. Therefore, we first added recombinant human BACE2 protein to the adult human LEC culture and incubated the LECs for 6 hours. After lysis, LEC lysates were subsequently analyzed via Western Blotting for VEGFR3 and BACE2 protein levels, while GAPDH served as loading control (Figure 40A). Addition of recombinant human BACE2 protein lead to a significant increase in BACE2 protein levels by around 3522% in adult human LEC lysates (Figure 40B) and to a correlating dramatic and also highly significant decrease by around 93% of total VEGFR3 protein levels in the same lysates (Figure 40C).

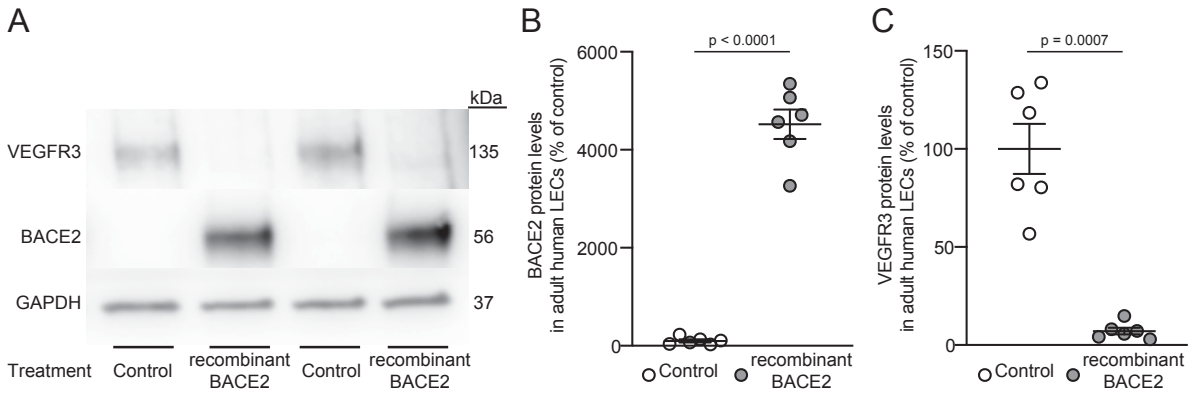

Figure 40: Addition of recombinant BACE2 to adult human LECs decreases VEGFR3 protein levels dramatically.
(**A**) Representative Western Blot image of adult human LEC lysates after 6 hours of treatment with control (Control) or recombinant BACE2 protein (recombinant BACE2), showing protein bands of VEGFR3, BACE2 and GAPDH serving as loading control. (**B**) Quantification of BACE2 protein levels in adult human LECs normalized to respective GAPDH levels after 6 hours of treatment with control or recombinant BACE2 protein shown as percentage of control. (**C**) Quantification of VEGFR3 protein levels in adult human LEC lysates after 6 hours of treatment with control or recombinant BACE2 protein, shown as percentage of control. All values are shown as means ± SEM with n = 6 independently treated sets of LECs per condition, statistical significance was determined by unpaired two-tailed Student's t-test. Laura Sophie Hilger performed the presented experiment.

According to the result, that VEGFR3 protein levels were strongly reduced in adult human LEC lysates treated with recombinant human BACE2 protein (Figure 40), we suggested that VEGFR3 might be a possible substrate of BACE2.

5.2.9 SiRNA mediated silencing of *BACE2* in adult human LECs does not alter VEGFR3 protein levels

In addition to the hint that VEGFR3 might be a substrate of BACE2 (Figure 40), we have also seen altered VEGFR3 signaling upon unspecific inhibition of BACE proteases by C3 treatment (Figure 22 and Figure 23). The decreased or unchanged VEGFR3 signaling after more selective inhibition of BACE1 (Figure 32, Figure 33 and Figure 34) or even BACE1 silencing (Figure 38), also pointed in the direction of rather BACE2 than BACE1 being a possible regulator of VEGFR3 signaling in adult human LECs. To further test this hypothesis, we next aimed to silence human *BACE2* in adult human LECs by transfection with BACE2 siRNAs. To obtain more specific results, we used three different BACE2 siRNAs (BACE2 siRNA 1, 2, 3) and a non-targeting control siRNA (control) and isolated the RNA of these adult human LECs 48 hours after transfection. The mRNA expression levels of *BACE2* were furthermore normalized to the mRNA expression levels of three different housekeeping genes (*RPLP0, B2M, HPRT1*). Our quantifications revealed a (non-)significant downregulation of *BACE2* mRNA expression levels by around 64-71% upon silencing with BACE2 siRNA 2 when normalized to all of the three of housekeeping genes, while the other siRNAs only silenced *BACE2* mRNA expression by trend (Figure 41A-C).

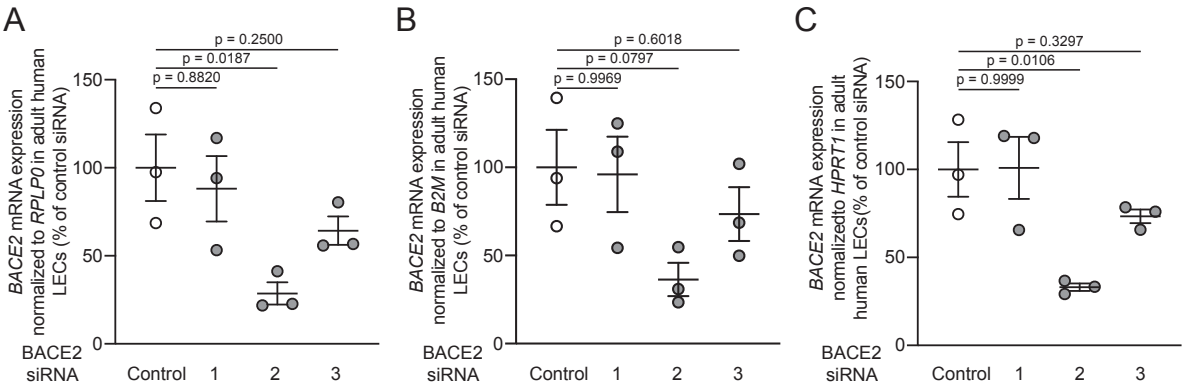

Figure 41: *BACE2* is silenced in adult human LECs by use of BACE2 siRNA 2.
(**A-C**) Quantifications of *BACE2* mRNA expression levels in adult human LECs 48 hours after transfection with control siRNA (Control) or one of three different siRNAs against *BACE2* (BACE2 siRNA 1, 2, 3), shown as percentage of control siRNA. *BACE2* mRNA expression levels were normalized to the mRNA expression levels of three different reference genes; in (A) *BACE2* mRNA expression is normalized to *RPLP0* mRNA expression, while in (B) *BACE2* mRNA expression is normalized to *B2M* mRNA expression and in (C) *BACE2* mRNA expression is normalized to *HPRT1* mRNA expression. All values are shown as means ± SEM with n = 3 independent transfections per siRNA; statistical significance was determined by one-way ANOVA and Dunnett's multiple comparisons test. Laura Sophie Hilger and Ida Stöppelkamp performed the presented experiments.

As the next step, we analyzed BACE2 and VEGFR3 protein content in adult human LECs which were transfected with BACE2 siRNA 2 (referred to as 'BACE2 KD'). We therefore lysed the BACE2 KD LECs and the respective control LECs 48 hours after transfection and performed Western Blotting for total VEGFR3 and BACE2, while GAPDH served as loading control (Figure 42A). According to the Western Blot analysis, BACE2 protein levels were by trend reduced by around 77% when transfected with BACE2 siRNA 2 and compared to control (Figure 42B), while this mild silencing had no major effect on total VEGFR3 protein levels (Figure 42C).

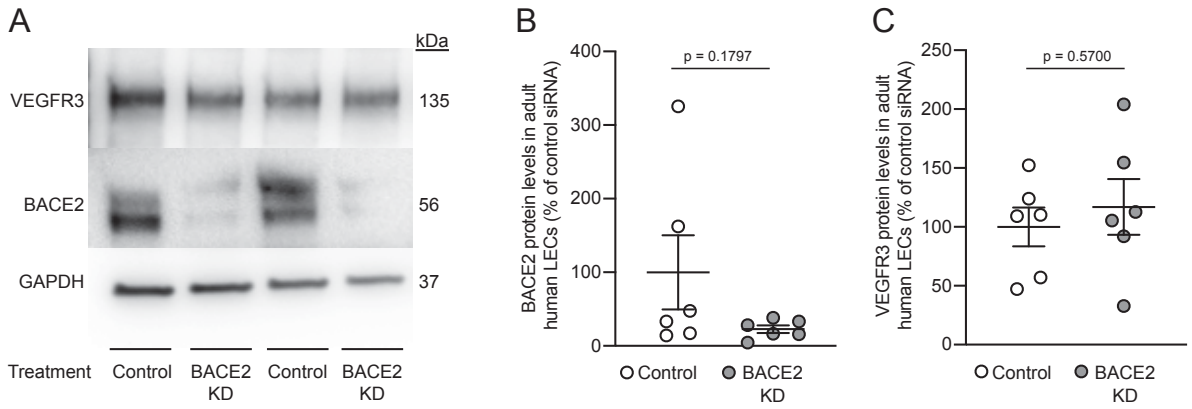

Figure 42: Mild silencing of *BACE2* has no major effect on VEGFR3 protein levels in adult human LECs.
(**A**) Representative Western Blot image of adult human LEC lysates 48 hours after transfection with either control siRNA (Control) or a siRNA against BACE2 (BACE2 KD) showing protein bands of VEGFR3, BACE2 and GAPDH serving as loading control. (**B**) Quantification of BACE2 protein levels in adult human LECs normalized to respective GAPDH levels 48 hours after transfection with either control siRNA or a siRNA against BACE2 (BACE2 KD), shown as percentage of control. (**C**) Quantification of VEGFR3 protein levels in LEC lysates 48 hours after transfection with either control or BACE2 siRNA (BACE2 KD), shown as percentage of control. All values are shown as means ± SEM with n = 6 independently treated sets of LECs per condition, statistical significance of (B) was determined by a Mann-Whitney test, while the statistical significance of (C) was determined by an unpaired two-tailed Student's t-test. Laura Sophie Hilger performed the presented experiment.

5.2.10 BACE2 contributes to the regulation of VEGFR3 phosphorylation and adult human LEC proliferation

Since the total VEGFR3 protein levels do not necessarily give a hint on the VEGFR3 signaling activity, we next aimed to analyze the latter. As the level of VEGFR3 phosphorylation can be used as an indicator for VEGFR3 signaling, we performed a pTyr/VEGFR3 PLA assay on adult human LECs 48 hours after BACE2 KD with BACE2 siRNA 2.

We performed a co-staining for F-actin in addition to the nuclei and pTyr/VEGFR3 PLA sites (Figure 43A,B) and normalized the counted pTyr/VEGFR3 PLA sites to the total nuclei count. The comparison of the amount of pTyr/VEGFR3 PLA sites per nuclei between control and BACE2 KD revealed a non-significant increase in VEGFR3 phosphorylation by 32% upon BACE2 KD in adult human LECs (Figure 43E).

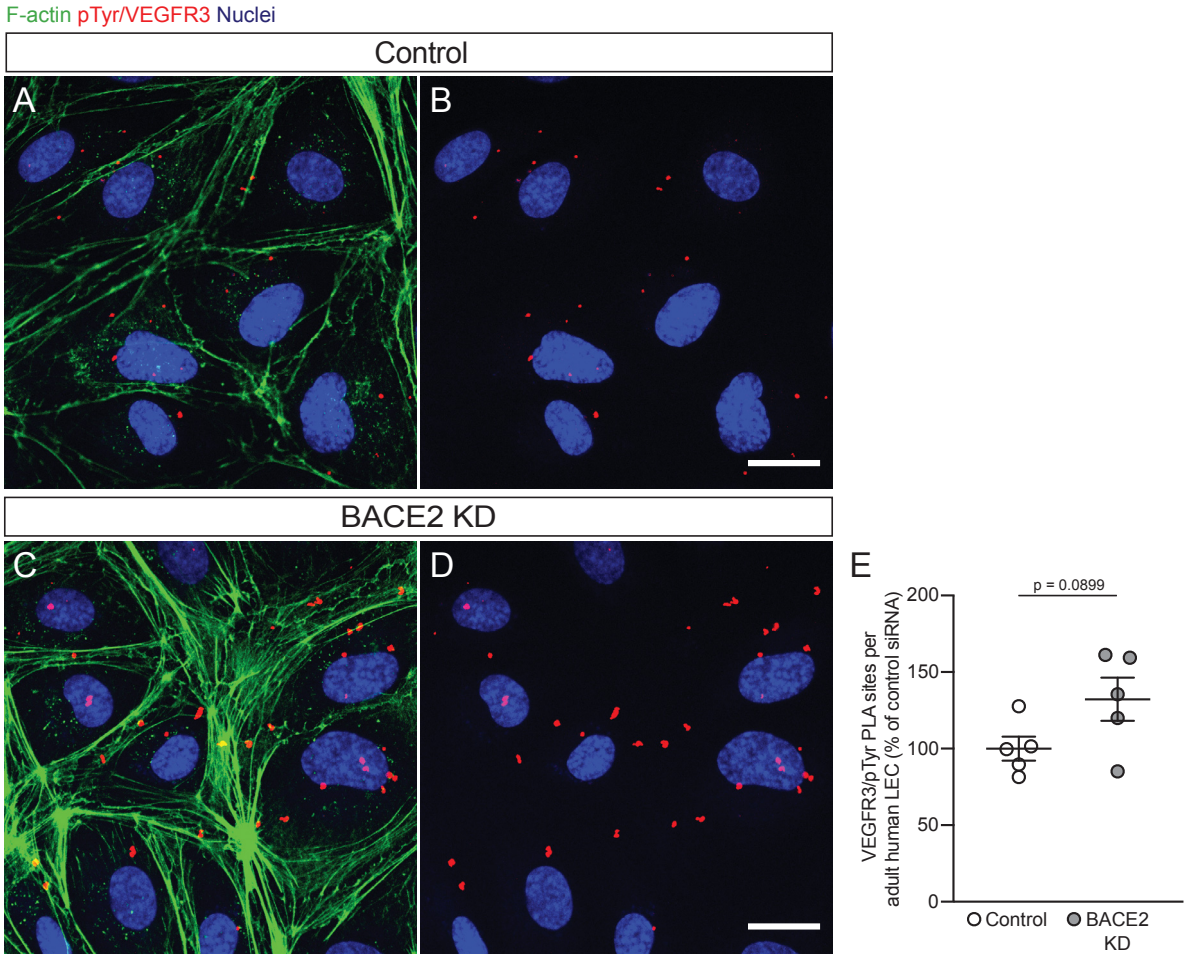

Figure 43: Silencing of *BACE2* increases the number of pTyr/VEGFR3 PLA sites in adult human LECs.
(**A-D**) Representative LSM images of adult human LECs 48 hours after transfection with either control siRNA (Control) (A,B) or a BACE2 siRNA (BACE2 KD) (C,D) showing pTyr/VEGFR3 proximity ligation assay (PLA) sites (red). A co-staining for F-actin (green) and nuclei (blue) is also shown. Scale bars, 20 µm. (**E**) Quantification of pTyr/VEGFR3 PLA sites per adult human LEC 48 hours after transfection with either control or BACE2 siRNA (BACE2 KD), shown as percentage of control. All values are shown as means ± SEM with n = 6 independently transfected sets of LECs per condition, statistical significance was determined by an unpaired two-tailed Student's t-test. Laura Sophie Hilger and Ida Stöppelkamp performed the presented experiment.

As a potential effect of this increased VEGFR3 phosphorylation in BACE2 KD adult human LECs (Figure 43) we next analyzed their proliferation rates. Therefore, we used the BrdU incorporation assay and normalized BrdU-positive LECs to the total number of nuclei per image. In this experiment we again compared adult human LECs transfected with control siRNA (control) to adult human LECs transfected with BACE2 siRNA 2 (BACE2 KD) 48 hours after transfection (Figure 44A,B). The comparison of proliferation rates between control and BACE2 KD LECs revealed a significant increase in adult human LEC proliferation by around 76% upon BACE2 KD (Figure 44C).

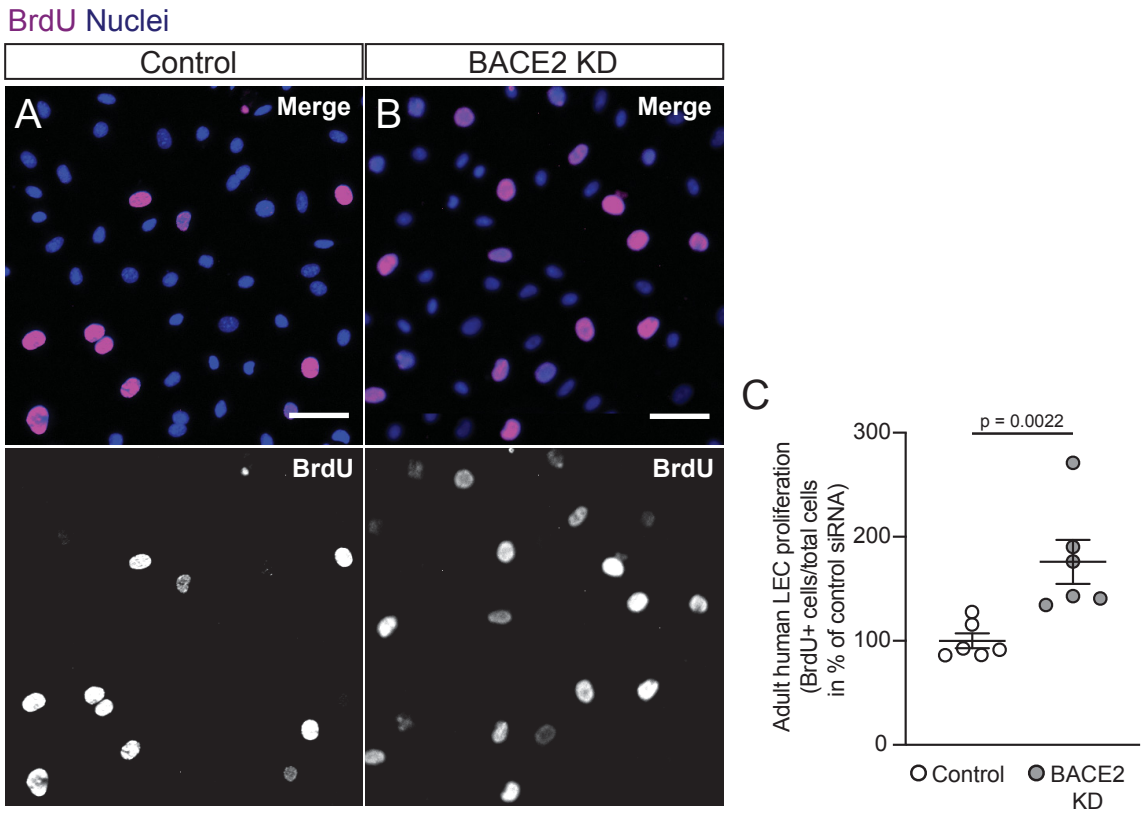

Figure 44: Silencing of *BACE2* significantly increases adult human LEC proliferation.
(**A,B**) Representative LSM images of adult human LECs 48 hours after transfection with either control siRNA (Control) (A) or one BACE2 siRNA (BACE2 KD) (B). The proliferation marker BrdU was added for 3 hours to the medium of the respective treatment. Staining shows BrdU (magenta) and nuclei (blue). Scale bars, 50 µm. (**C**) Quantification of BrdU-positive LECs normalized to total cells 48 hours after transfection with control or BACE2 siRNA, shown as percentage of control. All values are shown as means ± SEM with n = 6 independently transfected sets of LECs per condition, statistical significance was determined by an unpaired two-tailed Student's t-test. Laura Sophie Hilger and Ida Stöppelkamp performed the presented experiment.

Summarizing it is to say that *BACE2* silencing in adult human LECs by use of BACE2 siRNA 2 efficiently decreased *BACE2* mRNA expression levels (Figure 41) and BACE2 protein levels (Figure 42). Further, *BACE2* silencing did not change total VEGFR3 protein levels (Figure 42) but nevertheless increased VEGFR3 phosphorylation (Figure 43) and finally lead to a significantly increased adult human LEC proliferation (Figure 44). In addition to that, the treatment of adult human LECs with recombinant human BACE2 protein dramatically reduced the total VEGFR3 protein content within the LEC lysates (Figure 40) and therefore indicates that VEGFR3 is a substrate of BACE2. Thus, we can conclude that BACE2 might use VEGFR3 as a substrate in adult human LECs and thereby extracellularly contributes to the regulation of VEGFR3 signaling.

6. Discussion

The aim of this study was to examine mechanisms for intracellular versus extracellular attenuation of VEGFR3 activity in adult human LECs. To achieve this, *in vitro* cultured adult human LECs were transfected with siRNAs to silence either *ILK*, *PARVA*, *BACE1* or *BACE2*. Upon these conditions, VEGFR3 phosphorylation and LEC proliferation were quantified and compared to control treated LECs. In addition, mechanical stretch, as well as two different protease inhibitors were applied to support the hypotheses. In this context, treatment of adult human LECs with recombinant BACE2 protein further indicated that VEGFR3 might be a potential BACE2 substrate. In summary, ILK, α-parvin and BACE2 were found to attenuate VEGFR3 activity and LEC proliferation, from which ILK and α-parvin function via an intracellular and BACE2 via an extracellular mechanism.

6.1 Attenuation of VEGFR3 activity by an intracellular mechanism in LECs

6.1.1 ILK attenuates VEGFR3 signaling by preventing its interaction with β1 integrin in adult human LECs

ILK is known to be an intracellular adapter protein of β1 integrin (Hannigan et al. 1996), a mechanoreceptor with critical functions for proper vascular development and VEGFR3 signaling (Planas-Paz et al. 2012). In our previously published research article, we already identified ILK as a critical regulator of VEGFR3 signaling and lymphatic vascular growth in embryonic and adult mouse models (Urner et al. 2019). This thesis hence aimed to transfer the analyses on ILK, obtained in mice, to the adult human system and to extend our knowledge about the underlying mechanism.

In *in vitro* cultured adult human LECs, we first silenced human *ILK* by transfection with ILK siRNAs and analyzed behavior of these LECs in comparison with LECs transfected with non-targeting control siRNAs. VEGFR3 phosphorylation, as an indicator for VEGFR3 signaling activity, was strongly upregulated upon silencing of *ILK*, as determined by ELISA. As a consequence of this increased VEGFR3 signaling, we accordingly found significantly increased LEC proliferation upon silencing of *ILK*. With these results, we obtained first evidence that ILK might regulate VEGFR3 signaling in adult human LECs. Nevertheless,

VEGFR3 activity can be triggered via several axes including ligand binding (Joukov et al. 1996; Achen et al. 1998) and mechanical stimulation transduced via interactions between β1 integrin and VEGFR3 (Wang et al. 2001; Zhang et al. 2005; Planas-Paz et al. 2012).

To gain more insight into the underlying mechanism by which ILK regulates VEGFR3 signaling, we next analyzed the interactions between VEGFR3 and β1 integrin. Interestingly, silencing of *ILK* also resulted in increased interactions between β1 integrin and VEGFR3. ILK hence seems to have an attenuating effect on VEGFR3 signaling and LEC proliferation along the β1 integrin axis. We could support this conclusion via experimental stimulation of LECs *in vitro* by use of mechanical stretch. With this, we induced a mechanical stimulation of LECs which is comparable with increased interstitial fluid pressure *in vivo*. In mouse embryos, increased interstitial fluid pressure applied by fluid injections notably stretched the LECs of jugular lymph sacs (jls) or primordial thoracic ducts (pTD) as the first lymphatic structures and thereby increased their VEGFR3 phosphorylation and proliferation to adjust lymphatic function (Planas-Paz et al. 2012). In the lysates of mechanically stretched adult human LECs, ILK could here be shown to lose its connection to β1 integrin (performed by Dr. Sofia Urner), while the interactions between β1 integrin and VEGFR3 increased significantly upon the same conditions.

The presented results in adult human LECs indicate that ILK attenuates interactions between β1 integrin and VEGFR3 and thus β1 integrin mediated VEGFR3 signaling in a quiescent, physiological state. Mechanical stretch however stimulates the LECs and thereby disrupts the connection between ILK an β1 integrin, resulting in increased β1 integrin and VEGFR3 interactions, followed by increased VEGFR3 activity and LEC proliferation. Earlier *in vitro* studies e.g. in vascular smooth muscle cells also described silencing of *ILK* as a pro-proliferative trigger (Ho et al. 2008) and especially for angiogenesis in cancer development and progression ILK has been described as an important player (Tan et al. 2004; Zheng et al. 2019).

6.1.2 α-parvin contributes to the intracellular attenuation of VEGFR3 signaling in adult human LECs

For a more detailed analysis of the mechanism by which ILK facilitates the intracellular attenuation of VEGFR3 signaling in adult human LECs, we had a closer look on ILK's complex partner α-parvin (Tu et al. 2001; Legate et al. 2006; Fukuda et al. 2009). The latter (in)directly connects β1 integrin to the F-actin cytoskeleton and thereby contributes to the inside-out and

outside-in signaling of the mechanoreceptor (Nikolopoulos and Turner 2000). Mechanical stimuli from the ECM can be translated into the cell via this axis, as well as in the opposite direction (Maniotis et al. 1997). The F-actin cytoskeleton is responsible for cell shape and adhesion processes and is therefore highly impacted upon mechanical stimulation such as mechanical stretching (Z. Sun et al. 2016). Accordingly, mechanical stimuli which induce β1 integrin mediated VEGFR3 activation might also impact α-parvin due to its (in)direct connection to the F-actin cytoskeleton. In general, α-parvin's functions are associated with cell survival, adhesion, migration, as well as cellular junctions, vascular integrity and mural cell recruitment (Nikolopoulos and Turner 2000; Fukuda et al. 2003b; Montanez et al. 2009; Fraccaroli et al. 2015). Endothelial cell-specific deletion of *Parva* in mouse embryos was further shown to induce VEGFR3 phosphorylation, LEC proliferation and lymphatic vascular expansion (Urner et al. 2019).

The decreased interactions between β1 integrin and ILK in adult human LECs upon mechanical stretching indicated changes in the whole IPP complex upon mechanical stimulation, which is why we also analyzed the total protein levels of ILK and α-parvin in these cell lysates. Whilst the total protein levels of ILK were only tendentially reduced upon mechanical stretching, α-parvin protein levels were significantly reduced. Thus, the same stimulus which decreases the interactions between ILK and β1 integrin and thereby increases interactions between β1 integrin and VEGFR3, finally causing increased VEGFR3 signaling and LEC proliferation, is sufficient to significantly reduce α-parvin protein levels. In our *in vitro* system we furthermore found silencing of *ILK* to cause a significant reduction of α-parvin protein levels in adult human LECs, highlighting a potential interdependency between the complex partners in this cell type. We furthermore noticed ILK protein levels to not being majorly altered upon silencing of *PARVA*, while silencing of *ILK* caused a significant decrease in α-parvin protein levels. This uneven interdependency between the two complex partners lead us to the assumption that ILK, as the central component of the IPP complex (Qin and Wu 2012), functions upstream of α-parvin.

This interdependency between the IPP complex partners has been described before in studies concerning focal adhesion assembly. The assembly requires IPP complex localization at the cell surface, a process which is only successful upon fully completed IPP complex formation. It could be shown that IPP complex formation is disturbed upon silencing of one of the complex partners (Xu et al. 2005), which consequently impacts focal adhesion assembly (Zhang et al. 2002b; Fukuda et al. 2003a; Fukuda et al. 2009). Hence, a mechanical stimulus which is sufficient to alter the protein levels of IPP complex members and the ILK/β1 integrin connection might consequently also impact the LEC focal adhesion assembly and therefore

the cell's adaption to the initial stimulus. In addition to that, failed IPP complex formation might also impair the negative regulation of VEGFR3 signaling by its association with caveolin-1. It has been reported that impaired IPP complex formation also disturbs the correct localization of caveolin-1 to the so called caveolae which are lipid rafts in endothelial cells. As the association of caveolin-1 with VEGFR3 at this lipid rafts inhibits VEGFR3 activation, the impaired localization of caveolin-1 thus might exaggerate VEGFR3 activation (Malan et al. 2013).

For all of these reasons, we suggested α-parvin to potentially contribute to regulation of VEGFR3 activity in adult human LECs, as our previously described *in vivo* findings already indicated (Urner et al. 2019). In *PARVA* silenced adult human LECs, VEGFR3 phosphorylation was significantly upregulated upon use of siRNA 3, even though silencing of *PARVA* did not majorly change ILK protein expression levels. Interestingly, also the LEC proliferation was upregulated in these LECs by trend. The described effects were therefore comparable, but less relevant than the effects we noticed upon silencing of *ILK* in adult human LECs. Nevertheless, the results demonstrate that α-parvin is involved in the intracellular attenuation of VEGFR3 activity by ILK in adult human LECs and therefore also to ILK's regulation of physiologic LEC proliferation. Physiologic LEC proliferation is e.g. required for lymphatic vessels to adapt to increased fluid pressure and thus ensure proper lymphatic drainage (Planas-Paz et al. 2012).

6.1.3 Simplified model of an intracellular mechanism for attenuation of VEGFR3 signaling in adult human LECs

We here propose a model of how ILK and α-parvin intracellularly attenuate VEGFR3 activity (Figure 45). According to our model, ILK and its IPP complex members PINCH and α-parvin bind to β1 integrin intracellularly, thereby preventing interactions between the ECM bound mechanoreceptor β1 integrin and VEGFR3 in quiescent LECs. With this, the IPP complex intracellularly attenuates β1 integrin mediated VEGFR3 signaling (Figure 45A). Furthermore, the IPP complex connects β1 integrin to the F-actin cytoskeleton and therefore facilitates the cellular inside-out and outside-in signaling. Upon mechanical stimulation such as increased interstitial fluid pressure or mechanical stretch by use of *in vitro* stretching chambers, the connection between β1 integrin and ILK, as well as the IPP complex, disrupts (Figure 45B). Therefore, β1 integrin is free to interact with VEGFR3 and the subsequently increased interactions between β1 integrin and VEGFR3 induce VEGFR3 activity, finally stimulating LEC proliferation and physiologic lymphatic growth. As a result of the IPP complex

disruption, α-parvin loses its stability ensured by IPP complex formation and gets degraded (Figure 45C). Artificial silencing of *ILK* mimics the effect of mechanical stretching on the interactions between β1 integrin and VEGFR3, as well as it causes the degradation of α-parvin. In contrast to the physiologic stimulus of mechanical stretch, which does not majorly impact the protein levels of ILK in LECs, silencing of *ILK* of course diminishes the ILK protein content and therefore induces an excessive LEC reaction as manifested by strongly increased VEGFR3 signaling and non-physiologic lymphatic overgrowth (Figure 45D).

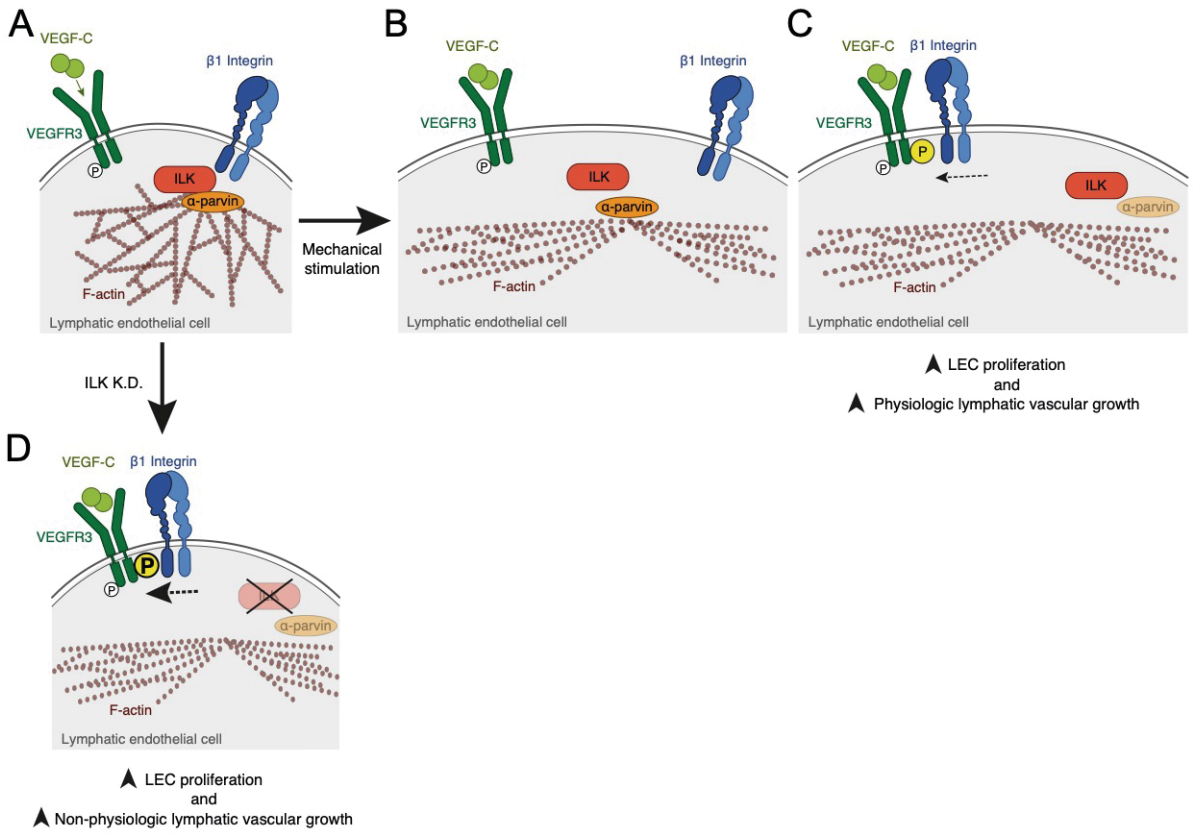

Figure 45: Simplified model of an intracellular mechanism to attenuate VEGFR3 activity.
(**A**) In quiescent LECs, ILK and α-parvin (as members of the IPP complex) are intracellularly bound to β1 integrin. With this, the IPP complex links β1 integrin to the F-actin cytoskeleton to facilitate inside-out and outside-in transduction of mechanical stimuli. (**B**) Upon mechanical stimulation such as LEC stretching due to increased interstitial fluid pressure, the connection between ILK and β1 integrin disrupts, releasing both β1 integrin and the IPP complex members. (**C**) While α-parvin gets degraded, β1 integrin interacts increasingly with VEGFR3 and thereby causes its autophosphorylation, which subsequently activates VEGFR3 signaling for LEC proliferation and physiologic lymphatic vascular growth. (**D**) Artificial silencing of *ILK* in LECs diminishes ILK protein from LECs and thereby enables excessive interactions between β1 integrin and VEGFR3, finally causing strongly increased LEC proliferation and non-physiologic lymphatic vascular growth. Modified from Urner et al., 2019 with permission from John Wiley and Sons provided by Rightslink® Copyright Clearance Center (License Number 4926991273484).

6.2 Extracellular mechanism for attenuation of VEGFR3 activity in LECs

The second part of my thesis focused on the investigation of a potential candidate, which might be part of an extracellular mechanism for the attenuation of VEGFR3 signaling in adult human LECs. By now, little is known about extracellular mechanisms which regulate VEGFR3 signaling in LECs. The most prominent extracellular mechanism which attenuates VEGFR3 activity in lymphatic vessels of the limbus is the presence of soluble VEGFRs in the cornea, which capture VEGF-C in the same tissue and therefore prevent the growth factor from binding to VEGFR3 on LECs of the limbus. Thereby, the soluble VEGFRs attenuate VEGFR3 activity and thus lymphangiogenesis from the limbus into the cornea to maintain a clear vision (Albuquerque et al. 2009; Singh et al. 2013). Despite of this, the matrix metalloproteinase (MMP)-9 has also been described as a potential extracellular regulator of VEGFR3 activity, as MMP-9 inhibition reduced VEGFR3 expression levels and corneal lymphangiogenesis in abundance of corneal inflammation as a pro-lymphangiogenic trigger (Du et al. 2017).

This part of the project was initiated by our cooperation partner, the Institute of Neuroproteomics at the DZNE in Munich and its head Prof. Dr. Lichtenthaler during a study on Alzheimer's disease (AD) and the included screening of potential inhibitors to attenuate the progression of this neurological disease. The candidates were developed to inhibit the activity of β-secretases or β-site of amyloid precursor protein cleaving enzyme 1 (BACE1). BACE1 is involved in the development and worsening of AD, as it is crucial for the development of dementia causing amyloid plaques (Wisniewski and Silverman 1997; Selkoe and Hardy 2016; Kang et al. 2017). However, in the past years several phase III trials with inhibitors targeting BACE1 have been quit due to multiple reasons (Mullard 2017). It is known that most of the common BACE1 inhibitors also target BACE1's close homologue BACE2 (Bennett et al. 2000; Alexander et al. 2014; Neumann et al. 2015; Cebers et al. 2017), which has no major impact on AD development (Farzan et al. 2000; Sun et al. 2006) but is described to have important functions in the periphery (Bennett et al. 2000; Esterhazy et al. 2011; Alcarraz-Vizan et al. 2017; Rochin et al. 2013). Consequently, research groups are now both trying to develop more specific inhibitors for BACE1 which do not target BACE2 and also screen for potential BACE2 substrates causing the adverse effects due to BACE2 inhibition. With this, potential adverse effects of BACE1 inhibition will be more easily to predict.

Screening of blood plasma from BACE inhibitor treated AD patients and *Bace2* deficient mice uncovered cleaved VEGFR3 levels to be altered upon BACE2 impairment, which labels VEGFR3 as a potential substrate of BACE2. Notably, plasma levels of VEGFR3 in *Bace1* deficient mice were not changed, when compared to controls (unpublished data). Due to these findings and the knowledge, that adult VEGFR3 expression is mainly restricted to LECs, we analyzed in how far BACE inhibition impacts VEGFR3 signaling and LEC behavior in this thesis.

6.2.1 Effects of BACE inhibitor treatments in VEGFR3 activity

6.2.1.1 β-Secretase Inhibitor IV (C3)

As a first step, we treated cultured adult human LECs with the general BACE inhibitor 'β-Secretase Inhibitor IV' (Stachel et al. 2004) (referred to as 'C3'). As VEGFR3 expression in the adult is mainly restricted to LECs and AD occurs in the adult system, this cell type was our favorite choice. Treatment of adult human LECs with C3 resulted in increased total VEGFR3 protein levels, indicating that either a protease which usually cleaves VEGFR3 has been successfully inhibited, or VEGFR3 expression has been increased. Increased VEGFR3 protein levels were accompanied by increased VEGFR3 phosphorylation as a marker for VEGFR3 activity. Notably, VEGFR3 phosphorylation of each sample has been normalized to the respective VEGFR3 protein content, excluding the suggestion that increased VEGFR3 activity was due to its increased protein level. This conclusion was further supported by increased LEC proliferation upon C3 treatment, a consequence usually triggered by VEGFR3 signaling in LECs (Makinen et al. 2001). We further excluded a potential contribution of the VEGFR2 axis, whose activation was reported to induce lymphangiogenesis independently from VEGFR3 signaling (Hong et al. 2004; Kunstfeld et al. 2004; Goldman et al. 2007), by demonstrating no major effects of C3 treatment on VEGFR2 phosphorylation in adult human LECs. This is why we concluded that the inhibition of at least one BACE protease causes changes in VEGFR3 protein levels and also in the receptor's signaling. Thus, at least one of the targeted proteases might be involved in an extracellular mechanism which usually attenuates VEGFR3 signaling in adult human LECs.

6.2.1.2 Verubecestat

Keeping in mind that one of the initial questions was to identify possible BACE2 substrates to predict potential adverse effects caused by BACE1 inhibition, we next aimed to distinguish between the different proteases and their effects on VEGFR3. Hence, we used a more specific BACE1 inhibitor, which has already been used in phase III trials and was shown to reduce β-amyloid amounts in CNS of treated animals and AD patients – Merck's verubecestat or MK-8931. Even though the trials needed to be stopped due to no improvement of patient's clinical ratings and occurring side effects, the inhibitor is still a proper tool for examination of our hypothesis (Scott et al. 2016; Kennedy et al. 2016; Egan et al. 2018; Egan et al. 2019b; Egan et al. 2019a). Treatment of cultured adult human LECs with verubecestat significantly decreased *BACE1* mRNA expression but not *BACE2* mRNA expression, while also the *VEGFR3* mRNA expression remained stable upon the treatment. The latter finding seems to be reasonable, since BACE proteases cleave proteins and a reduction of protease activity due to application of an inhibitor such as verubecestat might rather cause increased substrate levels due to decreased cleavage than due to increased mRNA expression of the respective substrate. For confirmation of this hypothesis, analysis of the supernatants of treated LECs for cleaved VEGFR3 protein was considered but yet technically impossible as we could not detect measurable amounts of VEGFR3 in supernatants at all. On mRNA levels, these results suggest that BACE1 but not BACE2 is a target of verubecestat, speaking for its BACE1 selectivity. To evaluate whether the reduced *BACE1* mRNA expression upon the treatment with verubecestat also alters BACE1 protein levels, we next performed Western Blots. Interestingly, 6 hours of verubecestat treatment decreased both BACE1 and BACE2 protein levels, indicating that also BACE2 might be targeted by verubecestat in adult human LECs. Nevertheless, BACE1 protein levels were more strongly decreased than BACE2 protein levels. This cross-targeting has already been described as a potential cause for adverse effects of verubecestat treatment (Scott et al. 2016; Egan et al. 2019b).

For the analysis of verubecestat treatment effects on VEGFR3 protein levels, we decided to increase the duration of treatment from 6 to 24 hours, as we assumed VEGFR3 protein to accumulate in the LEC's plasma membrane over time once potential BACE mediated cleavage was inhibited. Notably, VEGFR3 protein levels remained stable even after this longer period of treatment. The protein levels of phosphorylated VEGFR3 protein however were significantly decreased in this setting. To verify the reliability of this strong result, we repeated the treatment and used a proximity ligation assay (PLA) instead of Western Blotting to determine the level of VEGFR3 phosphorylation in adult human LECs. The results of these

PLA experiments were comparable with the results of Western Blotting, as the relative VEGFR3 phosphorylation was decreased by trend in comparison to DMSO control treated adult human LECs.

As phosphorylation of RTKs such as VEGFR3 occurs subsequently after stimulation, we also tested a much shorter treatment of adult human LECs with verubecestat. This short-term treatment was restricted to a verubecestat incubation for 20 minutes and did not result in decreased VEGFR3 phosphorylation, but in more or less unchanged VEGFR3 phosphorylation levels. As a more downstream indicator of VEGFR3 signaling activity, we additionally quantified adult human LEC proliferation after 6 hours of incubation with verubecestat and could not find changes in LEC proliferation when compared to DMSO control treated LECs. We therefore conclude that even in the early time points of verubecestat treatment, VEGFR3 signaling is not sufficiently activated to increase LEC proliferation and therefore will most probably have no major effect on lymphatic vascular growth. The significant decline in VEGFR3 phosphorylation after 24 hours of verubecestat treatment together with the unchanged VEGFR3 protein levels hint towards the assumption that verubecestat treatment does not induce VEGFR3 activity in adult human LECs.

6.2.2 Effects of separately silenced *BACE1* and *BACE2* expression

Verubecestat treatment affected both BACE1 and BACE2 protein levels, and therefore it was not possible to distinguish between the proteases and describe the potential role of BACE1 in this context. This is why we decided to specify the analyses by use of transfection with siRNAs against *BACE1* and *BACE2* in separate experiments. The mild siRNA mediated BACE1 knockdown (BACE1 KD) we achieved thereby neither affected VEGFR3 protein expression, nor VEGFR3 phosphorylation or LEC proliferation. This is why we conclude that BACE1 has no major role in the potential extracellular mechanism of VEGFR3 attenuation in adult human LECs.

On the other hand, siRNA mediated BACE2 knockdown (BACE2 KD) increased VEGFR3 phosphorylation in adult human LECs and the respective LEC proliferation was further significantly increased. These findings suggest that BACE2 plays a role in the attenuation of VEGFR3 activity in adult human LECs. Interestingly, the effects on VEGFR3 activity occurred without affected total VEGFR3 protein levels, which might be due to the weak BACE2 KD efficiency in some of the samples. In contrast to the more or less unchanged total VEGFR3 protein levels upon BACE2 KD, the addition of recombinant human BACE2 protein to adult

human LECs dramatically reduced VEGFR3 protein levels. Since the addition of recombinant BACE2 protein increased BACE2 protein levels within the LEC lysates to more than 3000%, the observed effect on VEGFR3 protein levels might also be due to these unphysiological protein amounts. Therefore, a controlled overexpression of *BACE2* might be a more reliable tool for future experiments.

6.2.3 Potential extracellular mechanism to attenuate VEGFR3 activity

Taken together with the results obtained from C3 treatment, the results on *BACE2* silencing might indicate a proteolytic activity of BACE2 with VEGFR3 being a potential substrate in adult human LECs. According to this hypothesis, BACE2 inhibition would stop proteolytic cleavage of VEGFR3 on the plasma membrane and the accumulated amounts of VEGFR3 then would be more likely to be activated upon both ligand binding by VEGF-C and via β1 integrin due to mechanical stimuli. Nevertheless, this hypothesis must be further tested in the future by analysis of the VEGFR3 content in supernatants of *BACE2* silenced or inhibited LECs. According to the current hypothesis, cleaved VEGFR3 amounts should be drastically decreased in the supernatants of BACE2 inhibited LECs, because of the inhibited proteolytic BACE2 activity.

It should also be considered that the mechanism by which BACE2 potentially attenuates VEGFR3 activity might be a secondary effect. As BACE2 substrates in adult human LECs are yet fairly unknown, one cannot exclude that a processed BACE2 substrate or the respective product might be the direct cause for the attenuation of VEGFR3 activity in a physiological state. According to this, BACE2 inhibition or silencing attenuates this substrate processing and therefore the decreasing amounts of the respective product or the increasing amounts of the substrate might stop the attenuation of VEGFR3 signaling. As an example, it has been described that in diabetic pancreatic β-cells, BACE2 produces the islet amyloid polypeptide (IAPP) via a similar amyloidogenic pathway like BACE1 produces β-amyloid in the brain during AD (Clark et al. 1996; Cooper et al. 1987; Rulifson et al. 2016). IAPP does not only form pancreatic plaques which are comparable to amyloid plaques in the brain, but also induces the production of reactive oxygen species (ROS) (Zraika et al. 2009). The latter in turn triggers the expression and activity of epsin-1 and epsin-2, which are known to be involved endocytosis (reviewed in (Sen et al. 2012)) and bind to VEGFR3 in LECs (Wu et al. 2018). By this, epsins induce VEGFR3 internalization and degradation, hence attenuating VEGFR3 signaling by restricting its availability at the plasma membrane (Liu et al. 2014). This pathway is considered to be responsible for the diabetic condition of impaired lymphangiogenesis (Wu et al. 2018)

and it is likely that, apart from the pancreatic tissue, a comparable mechanism attenuates VEGFR3 activity via BACE2.

In addition to the proposed *in vitro* supernatant analysis for reduced VEGFR3 levels, we also consider the analysis of lymphatic vessel in *Bace2* deficient (BACE2 K.O.) mice. According to our hypothesis, the global deletion of *Bace2* should lead to significantly increased VEGFR3 activity and thus also increased lymphangiogenesis. Potential tissues for these analyses can e.g. be the inner ear skin, as it allows a beautiful view on complete lymphatic and blood vessels across its whole surface, but also corneas which are usually avascular and therefore are perfect for the analysis of lymphangiogenesis. As meningeal lymphatics also play an important role for the detoxification of the brain, analyses of these vessels are also interesting. Preliminary data obtained from one *Bace2* deficient mouse cohort in cooperation with the Lichtenthaler group already revealed interesting results. Furthermore, analysis of blood and lymphatic vasculature in mouse embryos might also to be promising, since VEGFR3 is expressed in both vessel types during embryonic development (Kaipainen et al. 1995). Genetical deletion of *Bace2* or pharmacological inhibition of BACE2 in wildtype mouse embryos during whole embryo culture might reveal effects of VEGFR3 activation during development.

6.3 Conclusion

Based on the results we obtained during my thesis, two different mechanisms could be identified, which both contribute to the attenuation of VEGFR3 activity in adult human LECs. On the one hand, the IPP complex intracellularly prevents interactions between VEGFR3 and β1 integrin and thereby attenuates β1 integrin induced VEGFR3 activity. Under physiological conditions, only a sufficient mechanical stimulus overcomes this blockage and thereby removes the IPP complex from β1 integrin, followed by subsequent interactions between β1 integrin and VEGFR3, as well as VEGFR3 activity and physiologic LEC proliferation. Extracellularly, we could find indications for the assumption that BACE2 is involved in the attenuation of VEGFR3 activity. In its function as a protease, BACE2 probably cleaves certain amounts of VEGFR3 from the plasma membrane and releases the cleaved part into the extracellular space. Upon inhibition of BACE2 activity by use of BACE inhibitors such as C3 and to a lower extent also verubecestat, the VEGFR3 protein levels hence increase at the plasma membrane and are therefore more likely to be activated by ligand binding or mechanical stimuli.

7. Publications

2018/2019 Parts of this study were presented in:

Urner S*, Planas-Paz L*, Hilger LS, Henning C, Branopolski A, Kelly-Goss M, Stanczuk L, Peirce SM, Mäkinen T, Flögel U and Lammert E (* equally contributed).
Identification of ILK as a critical regulator of VEGFR3 signaling and lymphatic vascular growth.
EMBO J. 2019 Jan 15;38(2):e99322. doi: 10.15252/embj.201899322.
Epub 2018 Dec 5.

2020/2021 Parts of this study will be used for a publication in cooperation with the Institute for Neuroproteomics at the DZNE eV. in Munich, headed by Prof. Dr. Lichtenthaler:
Identification of VEGFR3 as a novel BACE2 substrate. Publication under preparation (2020).

Other publications:

2019: Hilger LS, Lammert E.
Der Einfluss mechanischer Kräfte auf das sich entwickelnde Lymphgefäßsystem.
LymphForsch. 2019 Dec;23(2):99-103. ISSN 1433-5255
Invited Review article.

8. References

Achen, M. G., Jeltsch, M., Kukk, E., Makinen, T., Vitali, A., Wilks, A. F., Alitalo, K., and Stacker, S. A. 1998. 'Vascular endothelial growth factor D (VEGF-D) is a ligand for the tyrosine kinases VEGF receptor 2 (Flk1) and VEGF receptor 3 (Flt4)', *Proc Natl Acad Sci U S A*, 95: 548-53.

Akiyama, H., Barger, S., Barnum, S., Bradt, B., Bauer, J., Cole, G. M., Cooper, N. R., Eikelenboom, P., Emmerling, M., Fiebich, B. L., et al. 2000. 'Inflammation and Alzheimer's disease', *Neurobiology of Aging*, 21: 383-421.

Albuquerque, R. J., Hayashi, T., Cho, W. G., Kleinman, M. E., Dridi, S., Takeda, A., Baffi, J. Z., Yamada, K., Kaneko, H., Green, M. G., et al. 2009. 'Alternatively spliced vascular endothelial growth factor receptor-2 is an essential endogenous inhibitor of lymphatic vessel growth', *Nat Med*, 15: 1023-30.

Alcarraz-Vizan, G., Castano, C., Visa, M., Montane, J., Servitja, J. M., and Novials, A. 2017. 'BACE2 suppression promotes beta-cell survival and function in a model of type 2 diabetes induced by human islet amyloid polypeptide overexpression', *Cell Mol Life Sci*, 74: 2827-38.

Alexander, R., Budd, S., Russell, M., Kugler, A., Cebers, G., Ye, N., Olsson, T., Burdette, D., Maltby, J., Paraskos, J., et al. 2014. 'AZD3293 A NOVEL BACE1 INHIBITOR: SAFETY, TOLERABILITY, AND EFFECTS ON PLASMA AND CSF A beta PEPTIDES FOLLOWING SINGLE- AND MULTIPLE-DOSE ADMINISTRATION', *Neurobiology of Aging*, 35: S2-S2.

Alvarez-Aznar, A., Muhl, L., and Gaengel, K. 2017. 'VEGF Receptor Tyrosine Kinases: Key Regulators of Vascular Function', *Curr Top Dev Biol*, 123: 433-82.

Aschen, S. Z., Farias-Eisner, G., Cuzzone, D. A., Albano, N. J., Ghanta, S., Weitman, E. S., Ortega, S., and Mehrara, B. J. 2014. 'Lymph node transplantation results in spontaneous lymphatic reconnection and restoration of lymphatic flow', *Plast Reconstr Surg*, 133: 301-10.

Aspelund, A., Antila, S., Proulx, S. T., Karlsen, T. V., Karaman, S., Detmar, M., Wiig, H., and Alitalo, K. 2015. 'A dural lymphatic vascular system that drains brain interstitial fluid and macromolecules', *J Exp Med*, 212: 991-9.

Au, A. C., Hernandez, P. A., Lieber, E., Nadroo, A. M., Shen, Y. M., Kelley, K. A., Gelb, B. D., and Diaz, G. A. 2010. 'Protein tyrosine phosphatase PTPN14 is a regulator of lymphatic function and choanal development in humans', *Am J Hum Genet*, 87: 436-44.

Bahram, F., and Claesson-Welsh, L. 2010. 'VEGF-mediated signal transduction in lymphatic endothelial cells', *Pathophysiology*, 17: 253-61.

Baluk, P., Fuxe, J., Hashizume, H., Romano, T., Lashnits, E., Butz, S., Vestweber, D., Corada, M., Molendini, C., Dejana, E., et al. 2007. 'Functionally specialized junctions between endothelial cells of lymphatic vessels', *J Exp Med*, 204: 2349-62.

Barao, S., Moechars, D., Lichtenthaler, S. F., and De Strooper, B. 2016. 'BACE1 Physiological Functions May Limit Its Use as Therapeutic Target for Alzheimer's Disease', *Trends Neurosci*, 39: 158-69.

Basi, G., Frigon, N., Barbour, R., Doan, T., Gordon, G., McConlogue, L., Sinha, S., and Zeller, M. 2003. 'Antagonistic effects of beta-site amyloid precursor protein-cleaving enzymes 1 and 2 on beta-amyloid peptide production in cells', *J Biol Chem*, 278: 31512-20.

Beeg, M., Stravalaci, M., Romeo, M., Carra, A. D., Cagnotto, A., Rossi, A., Diomede, L., Salmona, M., and Gobbi, M. 2016. 'Clusterin Binds to Abeta1-42 Oligomers with High Affinity and Interferes with Peptide Aggregation by Inhibiting Primary and Secondary Nucleation', *J Biol Chem*, 291: 6958-66.

Ben Halima, S., Mishra, S., Raja, K. M. P., Willem, M., Baici, A., Simons, K., Brustle, O., Koch, P., Haass, C., Caflisch, A., et al. 2016. 'Specific Inhibition of beta-Secretase

Processing of the Alzheimer Disease Amyloid Precursor Protein', *Cell Rep*, 14: 2127-41.

Bennett, B. D., Babu-Khan, S., Loeloff, R., Louis, J. C., Curran, E., Citron, M., and Vassar, R. 2000. 'Expression analysis of BACE2 in brain and peripheral tissues', *J Biol Chem*, 275: 20647-51.

Benoit, J. N., Zawieja, D. C., Goodman, A. H., and Granger, H. J. 1989. 'Characterization of intact mesenteric lymphatic pump and its responsiveness to acute edemagenic stress', *Am J Physiol*, 257: H2059-69.

Bhattacharjee, S., Lee, Y., Zhu, B., Wu, H., Chen, Y., and Chen, H. 2020. 'Epsins in vascular development, function and disease', *Cell Mol Life Sci*.

Boudeau, J., Miranda-Saavedra, D., Barton, G. J., and Alessi, D. R. 2006. 'Emerging roles of pseudokinases', *Trends Cell Biol*, 16: 443-52.

Brakenhielm, E., Gonzalez, A., and Diez, J. 2020. 'Role of Cardiac Lymphatics in Myocardial Edema and Fibrosis: JACC Review Topic of the Week', *J Am Coll Cardiol*, 76: 735-44.

Braun, A., Bordoy, R., Stanchi, F., Moser, M., Kostka, G. G., Ehler, E., Brandau, O., and Fassler, R. 2003. 'PINCH2 is a new five LIM domain protein, homologous to PINCHand localized to focal adhesions', *Exp Cell Res*, 284: 239-50.

Breslin, J. W. 2014. 'Mechanical forces and lymphatic transport', *Microvasc Res*, 96: 46-54.

Cai, H., Wang, Y., McCarthy, D., Wen, H., Borchelt, D. R., Price, D. L., and Wong, P. C. 2001. 'BACE1 is the major beta-secretase for generation of Abeta peptides by neurons', *Nat Neurosci*, 4: 233-4.

Cebers, G., Alexander, R. C., Haeberlein, S. B., Han, D., Goldwater, R., Ereshefsky, L., Olsson, T., Ye, N. D., Rosen, L., Russell, M., et al. 2017. 'AZD3293: Pharmacokinetic and Pharmacodynamic Effects in Healthy Subjects and Patients with Alzheimer's Disease', *Journal of Alzheimers Disease*, 55: 1039-53.

Cebers, G., Lejeune, T., Attalla, B., Soderberg, M., Alexander, R. C., Budd Haeberlein, S., Kugler, A. R., Ingersoll, E. W., Platz, S., and Scott, C. W. 2016. 'Reversible and Species-Specific Depigmentation Effects of AZD3293, a BACE Inhibitor for the Treatment of Alzheimer's Disease, Are Related to BACE2 Inhibition and Confined to Epidermis and Hair', *J Prev Alzheimers Dis*, 3: 202-18.

Chen, C. H., Zhou, W., Liu, S., Deng, Y., Cai, F., Tone, M., Tone, Y., Tong, Y., and Song, W. 2012. 'Increased NF-kappaB signalling up-regulates BACE1 expression and its therapeutic potential in Alzheimer's disease', *Int J Neuropsychopharmacol*, 15: 77-90.

Choe, K., Jang, J. Y., Park, I., Kim, Y., Ahn, S., Park, D. Y., Hong, Y. K., Alitalo, K., Koh, G. Y., and Kim, P. 2015. 'Intravital imaging of intestinal lacteals unveils lipid drainage through contractility', *J Clin Invest*, 125: 4042-52.

Clark, A., Charge, S. B., Badman, M. K., MacArthur, D. A., and de Koning, E. J. 1996. 'Islet amyloid polypeptide: actions and role in the pathogenesis of diabetes', *Biochem Soc Trans*, 24: 594-9.

Cole, S. L., and Vassar, R. 2007. 'The Basic Biology of BACE1: A Key Therapeutic Target for Alzheimer's Disease', *Curr Genomics*, 8: 509-30.

Cooper, G. J., Willis, A. C., Clark, A., Turner, R. C., Sim, R. B., and Reid, K. B. 1987. 'Purification and characterization of a peptide from amyloid-rich pancreases of type 2 diabetic patients', *Proc Natl Acad Sci U S A*, 84: 8628-32.

Da Mesquita, S., Louveau, A., Vaccari, A., Smirnov, I., Cornelison, R. C., Kingsmore, K. M., Contarino, C., Onengut-Gumuscu, S., Farber, E., Raper, D., et al. 2018. 'Functional aspects of meningeal lymphatics in ageing and Alzheimer's disease', *Nature*, 560: 185-91.

Daems, M., Peacock, H. M., and Jones, E. A. V. 2020. 'Fluid flow as a driver of embryonic morphogenesis', *Development*, 147.

Davis, M. J., Rahbar, E., Gashev, A. A., Zawieja, D. C., and Moore, J. E., Jr. 2011. 'Determinants of valve gating in collecting lymphatic vessels from rat mesentery', *Am J Physiol Heart Circ Physiol*, 301: H48-60.

De Strooper, B. 2014. 'Lessons from a failed gamma-secretase Alzheimer trial', *Cell*, 159: 721-6.

De Strooper, B., and Chavez Gutierrez, L. 2015. 'Learning by failing: ideas and concepts to tackle gamma-secretases in Alzheimer's disease and beyond', *Annu Rev Pharmacol Toxicol*, 55: 419-37.

De Strooper, B., Saftig, P., Craessaerts, K., Vanderstichele, H., Guhde, G., Annaert, W., Von Figura, K., and Van Leuven, F. 1998. 'Deficiency of presenilin-1 inhibits the normal cleavage of amyloid precursor protein', *Nature*, 391: 387-90.

Deane, R., Wu, Z., Sagare, A., Davis, J., Du Yan, S., Hamm, K., Xu, F., Parisi, M., LaRue, B., Hu, H. W., et al. 2004. 'LRP/amyloid beta-peptide interaction mediates differential brain efflux of Abeta isoforms', *Neuron*, 43: 333-44.

Deng, Y., Wang, Z., Wang, R., Zhang, X., Zhang, S., Wu, Y., Staufenbiel, M., Cai, F., and Song, W. 2013. 'Amyloid-beta protein (Abeta) Glu11 is the major beta-secretase site of beta-site amyloid-beta precursor protein-cleaving enzyme 1(BACE1), and shifting the cleavage site to Abeta Asp1 contributes to Alzheimer pathogenesis', *Eur J Neurosci*, 37: 1962-9.

Deng, Y., Zhang, X., and Simons, M. 2015. 'Molecular controls of lymphatic VEGFR3 signaling', *Arterioscler Thromb Vasc Biol*, 35: 421-9.

Devraj, K., Poznanovic, S., Spahn, C., Schwall, G., Harter, P. N., Mittelbronn, M., Antoniello, K., Paganetti, P., Muhs, A., Heilemann, M., et al. 2016. 'BACE-1 is expressed in the blood-brain barrier endothelium and is upregulated in a murine model of Alzheimer's disease', *J Cereb Blood Flow Metab*, 36: 1281-94.

Dieterich, L. C., and Detmar, M. 2016. 'Tumor lymphangiogenesis and new drug development', *Adv Drug Deliv Rev*, 99: 148-60.

Dislich, B., Wohlrab, F., Bachhuber, T., Muller, S. A., Kuhn, P. H., Hogl, S., Meyer-Luehmann, M., and Lichtenthaler, S. F. 2015. 'Label-free Quantitative Proteomics of Mouse Cerebrospinal Fluid Detects beta-Site APP Cleaving Enzyme (BACE1) Protease Substrates In Vivo', *Mol Cell Proteomics*, 14: 2550-63.

Dixelius, J., Makinen, T., Wirzenius, M., Karkkainen, M. J., Wernstedt, C., Alitalo, K., and Claesson-Welsh, L. 2003. 'Ligand-induced vascular endothelial growth factor receptor-3 (VEGFR-3) heterodimerization with VEGFR-2 in primary lymphatic endothelial cells regulates tyrosine phosphorylation sites', *J Biol Chem*, 278: 40973-9.

Dixon, J. B. 2010. 'Lymphatic lipid transport: sewer or subway?', *Trends Endocrinol Metab*, 21: 480-7.

Dobreva, I., Fielding, A., Foster, L. J., and Dedhar, S. 2008. 'Mapping the integrin-linked kinase interactome using SILAC', *J Proteome Res*, 7: 1740-9.

Dominguez, D., Tournoy, J., Hartmann, D., Huth, T., Cryns, K., Deforce, S., Serneels, L., Camacho, I. E., Marjaux, E., Craessaerts, K., et al. 2005. 'Phenotypic and biochemical analyses of BACE1- and BACE2-deficient mice', *J Biol Chem*, 280: 30797-806.

Doody, R. S., Raman, R., Farlow, M., Iwatsubo, T., Vellas, B., Joffe, S., Kieburtz, K., He, F., Sun, X., Thomas, R. G., et al. 2013. 'A phase 3 trial of semagacestat for treatment of Alzheimer's disease', *N Engl J Med*, 369: 341-50.

Drayton, D. L., Liao, S., Mounzer, R. H., and Ruddle, N. H. 2006. 'Lymphoid organ development: from ontogeny to neogenesis', *Nat Immunol*, 7: 344-53.

Du, H. T., Du, L. L., Tang, X. L., Ge, H. Y., and Liu, P. 2017. 'Blockade of MMP-2 and MMP-9 inhibits corneal lymphangiogenesis', *Graefes Arch Clin Exp Ophthalmol*, 255: 1573-79.

Du, X., Wang, X., and Geng, M. 2018. 'Alzheimer's disease hypothesis and related therapies', *Transl Neurodegener*, 7: 2.

Egan, M. F., Kost, J., Tariot, P. N., Aisen, P. S., Cummings, J. L., Vellas, B., Sur, C., Mukai, Y., Voss, T., Furtek, C., et al. 2018. 'Randomized Trial of Verubecestat for Mild-to-Moderate Alzheimer's Disease', *N Engl J Med*, 378: 1691-703.

Egan, M. F., Kost, J., Voss, T., Mukai, Y., Aisen, P. S., Cummings, J. L., Tariot, P. N., Vellas, B., van Dyck, C. H., Boada, M., et al. 2019a. 'Randomized Trial of Verubecestat for Prodromal Alzheimer's Disease', *N Engl J Med*, 380: 1408-20.

Egan, M. F., Mukai, Y., Voss, T., Kost, J., Stone, J., Furtek, C., Mahoney, E., Cummings, J. L., Tariot, P. N., Aisen, P. S., et al. 2019b. 'Further analyses of the safety of

verubecestat in the phase 3 EPOCH trial of mild-to-moderate Alzheimer's disease', *Alzheimers Res Ther*, 11: 68.

Escobedo, N., Proulx, S. T., Karaman, S., Dillard, M. E., Johnson, N., Detmar, M., and Oliver, G. 2016. 'Restoration of lymphatic function rescues obesity in Prox1-haploinsufficient mice', *JCI Insight*, 1.

Esposito, E., Ahn, B. J., Shi, J., Nakamura, Y., Park, J. H., Mandeville, E. T., Yu, Z., Chan, S. J., Desai, R., Hayakawa, A., et al. 2019. 'Brain-to-cervical lymph node signaling after stroke', *Nat Commun*, 10: 5306.

Esterhazy, D., Stutzer, I., Wang, H., Rechsteiner, M. P., Beauchamp, J., Dobeli, H., Hilpert, H., Matile, H., Prummer, M., Schmidt, A., et al. 2011. 'Bace2 is a beta cell-enriched protease that regulates pancreatic beta cell function and mass', *Cell Metab*, 14: 365-77.

Farzan, M., Schnitzler, C. E., Vasilieva, N., Leung, D., and Choe, H. 2000. 'BACE2, a beta -secretase homolog, cleaves at the beta site and within the amyloid-beta region of the amyloid-beta precursor protein', *Proc Natl Acad Sci U S A*, 97: 9712-7.

Fassler, R., and Meyer, M. 1995. 'Consequences of lack of beta 1 integrin gene expression in mice', *Genes Dev*, 9: 1896-908.

Favier, B., Alam, A., Barron, P., Bonnin, J., Laboudie, P., Fons, P., Mandron, M., Herault, J. P., Neufeld, G., Savi, P., et al. 2006. 'Neuropilin-2 interacts with VEGFR-2 and VEGFR-3 and promotes human endothelial cell survival and migration', *Blood*, 108: 1243-50.

Feng, D., Nagy, J. A., Brekken, R. A., Pettersson, A., Manseau, E. J., Pyne, K., Mulligan, R., Thorpe, P. E., Dvorak, H. F., and Dvorak, A. M. 2000. 'Ultrastructural localization of the vascular permeability factor/vascular endothelial growth factor (VPF/VEGF) receptor-2 (FLK-1, KDR) in normal mouse kidney and in the hyperpermeable vessels induced by VPF/VEGF-expressing tumors and adenoviral vectors', *J Histochem Cytochem*, 48: 545-56.

Fernandez, C., Clark, K., Burrows, L., Schofield, N. R., and Humphries, M. J. 1998. 'Regulation of the extracellular ligand binding activity of integrins', *Front Biosci*, 3: d684-700.

Fluhrer, R., Capell, A., Westmeyer, G., Willem, M., Hartung, B., Condron, M. M., Teplow, D. B., Haass, C., and Walter, J. 2002. 'A non-amyloidogenic function of BACE-2 in the secretory pathway', *J Neurochem*, 81: 1011-20.

Fong, G. H., Rossant, J., Gertsenstein, M., and Breitman, M. L. 1995. 'Role of the Flt-1 receptor tyrosine kinase in regulating the assembly of vascular endothelium', *Nature*, 376: 66-70.

Forster, R., Schubel, A., Breitfeld, D., Kremmer, E., Renner-Muller, I., Wolf, E., and Lipp, M. 1999. 'CCR7 coordinates the primary immune response by establishing functional microenvironments in secondary lymphoid organs', *Cell*, 99: 23-33.

Fournier, E., Dubreuil, P., Birnbaum, D., and Borg, J. P. 1995. 'Mutation at tyrosine residue 1337 abrogates ligand-dependent transforming capacity of the FLT4 receptor', *Oncogene*, 11: 921-31.

Fraccaroli, A., Pitter, B., Taha, A. A., Seebach, J., Huveneers, S., Kirsch, J., Casaroli-Marano, R. P., Zahler, S., Pohl, U., Gerhardt, H., et al. 2015. 'Endothelial alpha-parvin controls integrity of developing vasculature and is required for maintenance of cell-cell junctions', *Circ Res*, 117: 29-40.

Fukuda, K., Gupta, S., Chen, K., Wu, C., and Qin, J. 2009. 'The pseudoactive site of ILK is essential for its binding to alpha-Parvin and localization to focal adhesions', *Mol Cell*, 36: 819-30.

Fukuda, T., Chen, K., Shi, X., and Wu, C. 2003a. 'PINCH-1 is an obligate partner of integrin-linked kinase (ILK) functioning in cell shape modulation, motility, and survival', *J Biol Chem*, 278: 51324-33.

Fukuda, T., Guo, L., Shi, X., and Wu, C. 2003b. 'CH-ILKBP regulates cell survival by facilitating the membrane translocation of protein kinase B/Akt', *J Cell Biol*, 160: 1001-8.

Fukumoto, H., Rosene, D. L., Moss, M. B., Raju, S., Hyman, B. T., and Irizarry, M. C. 2004. 'Beta-secretase activity increases with aging in human, monkey, and mouse brain', *Am J Pathol*, 164: 719-25.

Galbraith, C. G., Yamada, K. M., and Galbraith, J. A. 2007. 'Polymerizing actin fibers position integrins primed to probe for adhesion sites', *Science*, 315: 992-5.

Galvagni, F., Anselmi, F., Salameh, A., Orlandini, M., Rocchigiani, M., and Oliviero, S. 2007. 'Vascular endothelial growth factor receptor-3 activity is modulated by its association with caveolin-1 on endothelial membrane', *Biochemistry*, 46: 3998-4005.

Galvagni, F., Pennacchini, S., Salameh, A., Rocchigiani, M., Neri, F., Orlandini, M., Petraglia, F., Gotta, S., Sardone, G. L., Matteucci, G., et al. 2010. 'Endothelial cell adhesion to the extracellular matrix induces c-Src-dependent VEGFR-3 phosphorylation without the activation of the receptor intrinsic kinase activity', *Circ Res*, 106: 1839-48.

Geng, X., Yanagida, K., Akwii, R. G., Choi, D., Chen, L., Ho, Y., Cha, B., Mahamud, M. R., Berman de Ruiz, K., Ichise, H., et al. 2020. 'S1PR1 regulates the quiescence of lymphatic vessels by inhibiting laminar shear stress-dependent VEGF-C signaling', *JCI Insight*, 5.

Gerli, R., Solito, R., Weber, E., and Agliano, M. 2000. 'Specific adhesion molecules bind anchoring filaments and endothelial cells in human skin initial lymphatics', *Lymphology*, 33: 148-57.

Ghannam, Jack Y., and Al Kharazi, Khalid A. 2019. "Neuroanatomy, Cranial Meninges." In.: StatPearls Publishing, Treasure Island (FL).

Ghanta, S., Cuzzone, D. A., Torrisi, J. S., Albano, N. J., Joseph, W. J., Savetsky, I. L., Gardenier, J. C., Chang, D., Zampell, J. C., and Mehrara, B. J. 2015. 'Regulation of inflammation and fibrosis by macrophages in lymphedema', *Am J Physiol Heart Circ Physiol*, 308: H1065-77.

Giancotti, F. G., and Ruoslahti, E. 1999. 'Integrin signaling', *Science*, 285: 1028-32.

Girard, J. P., Moussion, C., and Forster, R. 2012. 'HEVs, lymphatics and homeostatic immune cell trafficking in lymph nodes', *Nat Rev Immunol*, 12: 762-73.

Goldman, J., Rutkowski, J. M., Shields, J. D., Pasquier, M. C., Cui, Y., Schmokel, H. G., Willey, S., Hicklin, D. J., Pytowski, B., and Swartz, M. A. 2007. 'Cooperative and redundant roles of VEGFR-2 and VEGFR-3 signaling in adult lymphangiogenesis', *FASEB J*, 21: 1003-12.

Gousopoulos, E., Proulx, S. T., Scholl, J., Uecker, M., and Detmar, M. 2016. 'Prominent Lymphatic Vessel Hyperplasia with Progressive Dysfunction and Distinct Immune Cell Infiltration in Lymphedema', *Am J Pathol*, 186: 2193-203.

Haniu, M., Denis, P., Young, Y., Mendiaz, E. A., Fuller, J., Hui, J. O., Bennett, B. D., Kahn, S., Ross, S., Burgess, T., et al. 2000. 'Characterization of Alzheimer's beta -secretase protein BACE. A pepsin family member with unusual properties', *J Biol Chem*, 275: 21099-106.

Hanks, S. K., Quinn, A. M., and Hunter, T. 1988. 'The protein kinase family: conserved features and deduced phylogeny of the catalytic domains', *Science*, 241: 42-52.

Hannigan, G. E., Leung-Hagesteijn, C., Fitz-Gibbon, L., Coppolino, M. G., Radeva, G., Filmus, J., Bell, J. C., and Dedhar, S. 1996. 'Regulation of cell adhesion and anchorage-dependent growth by a new beta 1-integrin-linked protein kinase', *Nature*, 379: 91-6.

Hardy, J., and Selkoe, D. J. 2002. 'The amyloid hypothesis of Alzheimer's disease: progress and problems on the road to therapeutics', *Science*, 297: 353-6.

Harvey, N. L., Srinivasan, R. S., Dillard, M. E., Johnson, N. C., Witte, M. H., Boyd, K., Sleeman, M. W., and Oliver, G. 2005. 'Lymphatic vascular defects promoted by Prox1 haploinsufficiency cause adult-onset obesity', *Nat Genet*, 37: 1072-81.

Hattori, K., Heissig, B., Wu, Y., Dias, S., Tejada, R., Ferris, B., Hicklin, D. J., Zhu, Z., Bohlen, P., Witte, L., et al. 2002. 'Placental growth factor reconstitutes hematopoiesis by recruiting VEGFR1(+) stem cells from bone-marrow microenvironment', *Nat Med*, 8: 841-9.

Hawkes, N. 2017. 'Merck ends trial of potential Alzheimer's drug verubecestat', *BMJ*, 356: j845.

He, Y., Rajantie, I., Ilmonen, M., Makinen, T., Karkkainen, M. J., Haiko, P., Salven, P., and Alitalo, K. 2004. 'Preexisting lymphatic endothelium but not endothelial progenitor cells

are essential for tumor lymphangiogenesis and lymphatic metastasis', *Cancer Res*, 64: 3737-40.

Heldin, C. H. 1995. 'Dimerization of cell surface receptors in signal transduction', *Cell*, 80: 213-23.

Hilger, L. S., and Lammert, E. 2019. 'Der Einfluss mechanischer Kräfte auf das sich entwickelnde Lymphgefäßsystem.', *LymphForsch*, 23: 99-103.

Hiratsuka, S., Minowa, O., Kuno, J., Noda, T., and Shibuya, M. 1998. 'Flt-1 lacking the tyrosine kinase domain is sufficient for normal development and angiogenesis in mice', *Proc Natl Acad Sci U S A*, 95: 9349-54.

Ho, B., Hou, G., Pickering, J. G., Hannigan, G., Langille, B. L., and Bendeck, M. P. 2008. 'Integrin-linked kinase in the vascular smooth muscle cell response to injury', *Am J Pathol*, 173: 278-88.

Holler, C. J., Webb, R. L., Laux, A. L., Beckett, T. L., Niedowicz, D. M., Ahmed, R. R., Liu, Y., Simmons, C. R., Dowling, A. L., Spinelli, A., et al. 2012. 'BACE2 expression increases in human neurodegenerative disease', *Am J Pathol*, 180: 337-50.

Hong, Y. K., Lange-Asschenfeldt, B., Velasco, P., Hirakawa, S., Kunstfeld, R., Brown, L. F., Bohlen, P., Senger, D. R., and Detmar, M. 2004. 'VEGF-A promotes tissue repair-associated lymphatic vessel formation via VEGFR-2 and the alpha1beta1 and alpha2beta1 integrins', *FASEB J*, 18: 1111-3.

Hutzschenreuter, P., Brummer, H., and Ebberfeld, K. 1989. '[Experimental and clinical studies of the mechanism of effect of manual lymph drainage therapy]', *Z Lymphol*, 13: 62-4.

Iliff, J. J., and Nedergaard, M. 2013. 'Is there a cerebral lymphatic system?', *Stroke*, 44: S93-5.

Iliff, J. J., Wang, M., Liao, Y., Plogg, B. A., Peng, W., Gundersen, G. A., Benveniste, H., Vates, G. E., Deane, R., Goldman, S. A., et al. 2012. 'A paravascular pathway facilitates CSF flow through the brain parenchyma and the clearance of interstitial solutes, including amyloid beta', *Sci Transl Med*, 4: 147ra11.

Jessen, N. A., Munk, A. S., Lundgaard, I., and Nedergaard, M. 2015. 'The Glymphatic System: A Beginner's Guide', *Neurochem Res*, 40: 2583-99.

Jiang, X., Tian, W., Granucci, E. J., Tu, A. B., Kim, D., Dahms, P., Pasupneti, S., Peng, G., Kim, Y., Lim, A. H., et al. 2020. 'Decreased lymphatic HIF-2alpha accentuates lymphatic remodeling in lymphedema', *J Clin Invest*, 130: 5562-75.

Joukov, V., Pajusola, K., Kaipainen, A., Chilov, D., Lahtinen, I., Kukk, E., Saksela, O., Kalkkinen, N., and Alitalo, K. 1996. 'A novel vascular endothelial growth factor, VEGF-C, is a ligand for the Flt4 (VEGFR-3) and KDR (VEGFR-2) receptor tyrosine kinases', *EMBO J*, 15: 290-98.

Kaipainen, A., Korhonen, J., Mustonen, T., van Hinsbergh, V. W., Fang, G. H., Dumont, D., Breitman, M., and Alitalo, K. 1995. 'Expression of the fms-like tyrosine kinase 4 gene becomes restricted to lymphatic endothelium during development', *Proc Natl Acad Sci U S A*, 92: 3566-70.

Kang, Y., Zhang, Y., Feng, Z., Liu, M., Li, Y., Yang, H., Wang, D., Zheng, L., Lou, D., Cheng, L., et al. 2017. 'Nutritional Deficiency in Early Life Facilitates Aging-Associated Cognitive Decline', *Curr Alzheimer Res*, 14: 841-49.

Karaman, S., and Detmar, M. 2014. 'Mechanisms of lymphatic metastasis', *J Clin Invest*, 124: 922-8.

Karkkainen, M. J., Haiko, P., Sainio, K., Partanen, J., Taipale, J., Petrova, T. V., Jeltsch, M., Jackson, D. G., Talikka, M., Rauvala, H., et al. 2004. 'Vascular endothelial growth factor C is required for sprouting of the first lymphatic vessels from embryonic veins', *Nat Immunol*, 5: 74-80.

Katoh, O., Tauchi, H., Kawaishi, K., Kimura, A., and Satow, Y. 1995. 'Expression of the vascular endothelial growth factor (VEGF) receptor gene, KDR, in hematopoietic cells and inhibitory effect of VEGF on apoptotic cell death caused by ionizing radiation', *Cancer Res*, 55: 5687-92.

Kennedy, M. E., Stamford, A. W., Chen, X., Cox, K., Cumming, J. N., Dockendorf, M. F., Egan, M., Ereshefsky, L., Hodgson, R. A., Hyde, L. A., et al. 2016. 'The BACE1 inhibitor

verubecestat (MK-8931) reduces CNS beta-amyloid in animal models and in Alzheimer's disease patients', *Sci Transl Med*, 8: 363ra150.

Keskin, A. D., Kekus, M., Adelsberger, H., Neumann, U., Shimshek, D. R., Song, B., Zott, B., Peng, T., Forstl, H., Staufenbiel, M., et al. 2017. 'BACE inhibition-dependent repair of Alzheimer's pathophysiology', *Proc Natl Acad Sci U S A*, 114: 8631-36.

Kida, E., Choi-Miura, N. H., and Wisniewski, K. E. 1995. 'Deposition of apolipoproteins E and J in senile plaques is topographically determined in both Alzheimer's disease and Down's syndrome brain', *Brain Res*, 685: 211-6.

Koh, L., Zakharov, A., and Johnston, M. 2005. 'Integration of the subarachnoid space and lymphatics: is it time to embrace a new concept of cerebrospinal fluid absorption?', *Cerebrospinal Fluid Res*, 2: 6.

Korenbaum, E., Olski, T. M., and Noegel, A. A. 2001. 'Genomic organization and expression profile of the parvin family of focal adhesion proteins in mice and humans', *Gene*, 279: 69-79.

Kress, B. T., Iliff, J. J., Xia, M., Wang, M., Wei, H. S., Zeppenfeld, D., Xie, L., Kang, H., Xu, Q., Liew, J. A., et al. 2014. 'Impairment of paravascular clearance pathways in the aging brain', *Ann Neurol*, 76: 845-61.

Kuhn, P. H., Koroniak, K., Hogl, S., Colombo, A., Zeitschel, U., Willem, M., Volbracht, C., Schepers, U., Imhof, A., Hoffmeister, A., et al. 2012. 'Secretome protein enrichment identifies physiological BACE1 protease substrates in neurons', *EMBO J*, 31: 3157-68.

Kunstfeld, R., Hirakawa, S., Hong, Y. K., Schacht, V., Lange-Asschenfeldt, B., Velasco, P., Lin, C., Fiebiger, E., Wei, X., Wu, Y., et al. 2004. 'Induction of cutaneous delayed-type hypersensitivity reactions in VEGF-A transgenic mice results in chronic skin inflammation associated with persistent lymphatic hyperplasia', *Blood*, 104: 1048-57.

Lai, K. S. P., Liu, C. S., Rau, A., Lanctot, K. L., Kohler, C. A., Pakosh, M., Carvalho, A. F., and Herrmann, N. 2017. 'Peripheral inflammatory markers in Alzheimer's disease: a systematic review and meta-analysis of 175 studies', *J Neurol Neurosurg Psychiatry*, 88: 876-82.

Lampugnani, M. G., Orsenigo, F., Gagliani, M. C., Tacchetti, C., and Dejana, E. 2006. 'Vascular endothelial cadherin controls VEGFR-2 internalization and signaling from intracellular compartments', *J Cell Biol*, 174: 593-604.

Le Bras, B., Barallobre, M. J., Homman-Ludiye, J., Ny, A., Wyns, S., Tammela, T., Haiko, P., Karkkainen, M. J., Yuan, L., Muriel, M. P., et al. 2006. 'VEGF-C is a trophic factor for neural progenitors in the vertebrate embryonic brain', *Nat Neurosci*, 9: 340-8.

Leak, L. V. 1970. 'Electron microscopic observations on lymphatic capillaries and the structural components of the connective tissue-lymph interface', *Microvasc Res*, 2: 361-91.

Leak, L. V., and Burke, J. F. 1968. 'Ultrastructural studies on the lymphatic anchoring filaments', *J Cell Biol*, 36: 129-49.

Lee, J., Gray, A., Yuan, J., Luoh, S. M., Avraham, H., and Wood, W. I. 1996. 'Vascular endothelial growth factor-related protein: a ligand and specific activator of the tyrosine kinase receptor Flt4', *Proc Natl Acad Sci U S A*, 93: 1988-92.

Legate, K. R., Montanez, E., Kudlacek, O., and Fassler, R. 2006. 'ILK, PINCH and parvin: the tIPP of integrin signalling', *Nat Rev Mol Cell Biol*, 7: 20-31.

Lemmon, M. A., and Schlessinger, J. 2010. 'Cell signaling by receptor tyrosine kinases', *Cell*, 141: 1117-34.

Leppanen, V. M., Tvorogov, D., Kisko, K., Prota, A. E., Jeltsch, M., Anisimov, A., Markovic-Mueller, S., Stuttfeld, E., Goldie, K. N., Ballmer-Hofer, K., et al. 2013. 'Structural and mechanistic insights into VEGF receptor 3 ligand binding and activation', *Proc Natl Acad Sci U S A*, 110: 12960-5.

Li, F., Zhang, Y., and Wu, C. 1999. 'Integrin-linked kinase is localized to cell-matrix focal adhesions but not cell-cell adhesion sites and the focal adhesion localization of integrin-linked kinase is regulated by the PINCH-binding ANK repeats', *J Cell Sci*, 112 (Pt 24): 4589-99.

Li, S., Bordoy, R., Stanchi, F., Moser, M., Braun, A., Kudlacek, O., Wewer, U. M., Yurchenco, P. D., and Fassler, R. 2005. 'PINCH1 regulates cell-matrix and cell-cell adhesions, cell polarity and cell survival during the peri-implantation stage', *J Cell Sci*, 118: 2913-21.

Liang, X., Zhou, Q., Li, X., Sun, Y., Lu, M., Dalton, N., Ross, J., Jr., and Chen, J. 2005. 'PINCH1 plays an essential role in early murine embryonic development but is dispensable in ventricular cardiomyocytes', *Mol Cell Biol*, 25: 3056-62.

Lidstrom, A. M., Bogdanovic, N., Hesse, C., Volkman, I., Davidsson, P., and Blennow, K. 1998. 'Clusterin (apolipoprotein J) protein levels are increased in hippocampus and in frontal cortex in Alzheimer's disease', *Exp Neurol*, 154: 511-21.

Lin, X., Koelsch, G., Wu, S., Downs, D., Dashti, A., and Tang, J. 2000. 'Human aspartic protease memapsin 2 cleaves the beta-secretase site of beta-amyloid precursor protein', *Proc Natl Acad Sci U S A*, 97: 1456-60.

Liu, X., Pasula, S., Song, H., Tessneer, K. L., Dong, Y., Hahn, S., Yago, T., Brophy, M. L., Chang, B., Cai, X., et al. 2014. 'Temporal and spatial regulation of epsin abundance and VEGFR3 signaling are required for lymphatic valve formation and function', *Sci Signal*, 7: ra97.

Livak, K. J., and Schmittgen, T. D. 2001. 'Analysis of relative gene expression data using real-time quantitative PCR and the 2(-Delta Delta C(T)) Method', *Methods*, 25: 402-8.

Louveau, A., Da Mesquita, S., and Kipnis, J. 2016. 'Lymphatics in Neurological Disorders: A Neuro-Lympho-Vascular Component of Multiple Sclerosis and Alzheimer's Disease?', *Neuron*, 91: 957-73.

Louveau, A., Smirnov, I., Keyes, T. J., Eccles, J. D., Rouhani, S. J., Peske, J. D., Derecki, N. C., Castle, D., Mandell, J. W., Lee, K. S., et al. 2015. 'Structural and functional features of central nervous system lymphatic vessels', *Nature*, 523: 337-41.

Luo, B. H., Carman, C. V., and Springer, T. A. 2007. 'Structural basis of integrin regulation and signaling', *Annu Rev Immunol*, 25: 619-47.

Luo, Y., Bolon, B., Kahn, S., Bennett, B. D., Babu-Khan, S., Denis, P., Fan, W., Kha, H., Zhang, J., Gong, Y., et al. 2001. 'Mice deficient in BACE1, the Alzheimer's beta-secretase, have normal phenotype and abolished beta-amyloid generation', *Nat Neurosci*, 4: 231-2.

Ly, C. L., Kataru, R. P., and Mehrara, B. J. 2017. 'Inflammatory Manifestations of Lymphedema', *Int J Mol Sci*, 18.

Ly, P. T., Wu, Y., Zou, H., Wang, R., Zhou, W., Kinoshita, A., Zhang, M., Yang, Y., Cai, F., Woodgett, J., et al. 2013. 'Inhibition of GSK3beta-mediated BACE1 expression reduces Alzheimer-associated phenotypes', *J Clin Invest*, 123: 224-35.

Maeda, T., Yamamoto, Y., Iwasaki, D., Hayashi, T., Funayama, E., Oyama, A., Murao, N., and Furukawa, H. 2018. 'Lymphatic Reconnection and Restoration of Lymphatic Flow by Nonvascularized Lymph Node Transplantation: Real-Time Fluorescence Imaging Using Indocyanine Green and Fluorescein Isothiocyanate-Dextran', *Lymphat Res Biol*, 16: 165-73.

Makinen, T., Veikkola, T., Mustjoki, S., Karpanen, T., Catimel, B., Nice, E. C., Wise, L., Mercer, A., Kowalski, H., Kerjaschki, D., et al. 2001. 'Isolated lymphatic endothelial cells transduce growth, survival and migratory signals via the VEGF-C/D receptor VEGFR-3', *EMBO J*, 20: 4762-73.

Malan, D., Elischer, A., Hesse, M., Wickstrom, S. A., Fleischmann, B. K., and Bloch, W. 2013. 'Deletion of integrin linked kinase in endothelial cells results in defective RTK signaling caused by caveolin 1 mislocalization', *Development*, 140: 987-95.

Maniotis, A. J., Chen, C. S., and Ingber, D. E. 1997. 'Demonstration of mechanical connections between integrins, cytoskeletal filaments, and nucleoplasm that stabilize nuclear structure', *Proc Natl Acad Sci U S A*, 94: 849-54.

May, P. C., Lampert-Etchells, M., Johnson, S. A., Poirier, J., Masters, J. N., and Finch, C. E. 1990. 'Dynamics of gene expression for a hippocampal glycoprotein elevated in Alzheimer's disease and in response to experimental lesions in rat', *Neuron*, 5: 831-9.

Mayerson, H. S. 1963. 'On Lymph and Lymphatics', *Circulation*, 28: 839-42.

McGeer, P. L., Kawamata, T., and Walker, D. G. 1992. 'Distribution of clusterin in Alzheimer brain tissue', *Brain Res*, 579: 337-41.

Min, Y., Ghose, S., Boelte, K., Li, J., Yang, L., and Lin, P. C. 2011. 'C/EBP-delta regulates VEGF-C autocrine signaling in lymphangiogenesis and metastasis of lung cancer through HIF-1alpha', *Oncogene*, 30: 4901-9.

Mislin, H. 1976. 'Active contractility of the lymphangion and coordination of lymphangion chains', *Experientia*, 32: 820-2.

Montanez, E., Wickstrom, S. A., Altstatter, J., Chu, H., and Fassler, R. 2009. 'Alpha-parvin controls vascular mural cell recruitment to vessel wall by regulating RhoA/ROCK signalling', *EMBO J*, 28: 3132-44.

Mortimer, P. S., and Rockson, S. G. 2014. 'New developments in clinical aspects of lymphatic disease', *J Clin Invest*, 124: 915-21.

Mukherjee, A., Morales-Scheihing, D., Butler, P. C., and Soto, C. 2015. 'Type 2 diabetes as a protein misfolding disease', *Trends Mol Med*, 21: 439-49.

Mullard, A. 2017. 'BACE inhibitor bust in Alzheimer trial', *Nat Rev Drug Discov*, 16: 155.

Murfee, W. L., Rappleye, J. W., Ceballos, M., and Schmid-Schonbein, G. W. 2007. 'Discontinuous expression of endothelial cell adhesion molecules along initial lymphatic vessels in mesentery: the primary valve structure', *Lymphat Res Biol*, 5: 81-9.

Musiek, E. S., and Holtzman, D. M. 2015. 'Three dimensions of the amyloid hypothesis: time, space and 'wingmen'', *Nat Neurosci*, 18: 800-6.

Nagy, J. A., Vasile, E., Feng, D., Sundberg, C., Brown, L. F., Detmar, M. J., Lawitts, J. A., Benjamin, L., Tan, X., Manseau, E. J., et al. 2002. 'Vascular permeability factor/vascular endothelial growth factor induces lymphangiogenesis as well as angiogenesis', *J Exp Med*, 196: 1497-506.

Nakao, S., Hafezi-Moghadam, A., and Ishibashi, T. 2012. 'Lymphatics and lymphangiogenesis in the eye', *J Ophthalmol*, 2012: 783163.

Nakayama, M., Nakayama, A., van Lessen, M., Yamamoto, H., Hoffmann, S., Drexler, H. C., Itoh, N., Hirose, T., Breier, G., Vestweber, D., et al. 2013. 'Spatial regulation of VEGF receptor endocytosis in angiogenesis', *Nat Cell Biol*, 15: 249-60.

Neumann, U., Rueeger, H., Machauer, R., Veenstra, S. J., Lueoend, R. M., Tintelnot-Blomley, M., Laue, G., Beltz, K., Vogg, B., Schmid, P., et al. 2015. 'A novel BACE inhibitor NB-360 shows a superior pharmacological profile and robust reduction of amyloid-beta and neuroinflammation in APP transgenic mice', *Mol Neurodegener*, 10: 44.

Nikolopoulos, S. N., and Turner, C. E. 2000. 'Actopaxin, a new focal adhesion protein that binds paxillin LD motifs and actin and regulates cell adhesion', *J Cell Biol*, 151: 1435-48.

Olski, T. M., Noegel, A. A., and Korenbaum, E. 2001. 'Parvin, a 42 kDa focal adhesion protein, related to the alpha-actinin superfamily', *J Cell Sci*, 114: 525-38.

Olszewski, W., Engeset, A., Jaeger, P. M., Sokolowski, J., and Theodorsen, L. 1977. 'Flow and composition of leg lymph in normal men during venous stasis, muscular activity and local hyperthermia', *Acta Physiol Scand*, 99: 149-55.

Orlandini, M., Spreafico, A., Bardelli, M., Rocchigiani, M., Salameh, A., Nucciotti, S., Capperucci, C., Frediani, B., and Oliviero, S. 2006. 'Vascular endothelial growth factor-D activates VEGFR-3 expressed in osteoblasts inducing their differentiation', *J Biol Chem*, 281: 17961-7.

Pajusola, K., Aprelikova, O., Korhonen, J., Kaipainen, A., Pertovaara, L., Alitalo, R., and Alitalo, K. 1992. 'FLT4 receptor tyrosine kinase contains seven immunoglobulin-like loops and is expressed in multiple human tissues and cell lines', *Cancer Res*, 52: 5738-43.

Pajusola, K., Aprelikova, O., Pelicci, G., Weich, H., Claesson Welsh, L., and Alitalo, K. 1994. 'Signalling properties of FLT4, a proteolytically processed receptor tyrosine kinase related to two VEGF receptors', *Oncogene*, 9: 3545-55.

Partanen, T. A., Arola, J., Saaristo, A., Jussila, L., Ora, A., Miettinen, M., Stacker, S. A., Achen, M. G., and Alitalo, K. 2000. 'VEGF-C and VEGF-D expression in neuroendocrine cells

and their receptor, VEGFR-3, in fenestrated blood vessels in human tissues', *FASEB J*, 14: 2087-96.
Pepper, M. S., and Skobe, M. 2003. 'Lymphatic endothelium: morphological, molecular and functional properties', *J Cell Biol*, 163: 209-13.
Planas-Paz, L., Strilic, B., Goedecke, A., Breier, G., Fassler, R., and Lammert, E. 2012. 'Mechanoinduction of lymph vessel expansion', *EMBO J*, 31: 788-804.
Podgrabinska, S., Braun, P., Velasco, P., Kloos, B., Pepper, M. S., and Skobe, M. 2002. 'Molecular characterization of lymphatic endothelial cells', *Proc Natl Acad Sci U S A*, 99: 16069-74.
Pollay, M. 2010. 'The function and structure of the cerebrospinal fluid outflow system', *Cerebrospinal Fluid Res*, 7: 9.
Potente, M., and Makinen, T. 2017. 'Vascular heterogeneity and specialization in development and disease', *Nat Rev Mol Cell Biol*, 18: 477-94.
Qin, J., and Wu, C. 2012. 'ILK: a pseudokinase in the center stage of cell-matrix adhesion and signaling', *Curr Opin Cell Biol*, 24: 607-13.
Rahbar, E., Akl, T., Cote, G. L., Moore, J. E., Jr., and Zawieja, D. C. 2014. 'Lymph transport in rat mesenteric lymphatics experiencing edemagenic stress', *Microcirculation*, 21: 359-67.
Randall, T. D., Carragher, D. M., and Rangel-Moreno, J. 2008. 'Development of secondary lymphoid organs', *Annu Rev Immunol*, 26: 627-50.
Randolph, G. J., Ivanov, S., Zinselmeyer, B. H., and Scallan, J. P. 2017. 'The Lymphatic System: Integral Roles in Immunity', *Annu Rev Immunol*, 35: 31-52.
Revesz, T., Holton, J. L., Lashley, T., Plant, G., Frangione, B., Rostagno, A., and Ghiso, J. 2009. 'Genetics and molecular pathogenesis of sporadic and hereditary cerebral amyloid angiopathies', *Acta Neuropathol*, 118: 115-30.
Rochin, L., Hurbain, I., Serneels, L., Fort, C., Watt, B., Leblanc, P., Marks, M. S., De Strooper, B., Raposo, G., and van Niel, G. 2013. 'BACE2 processes PMEL to form the melanosome amyloid matrix in pigment cells', *Proc Natl Acad Sci U S A*, 110: 10658-63.
Rockson, S. G. 2001. 'Lymphedema', *Am J Med*, 110: 288-95.
Rulifson, I. C., Cao, P., Miao, L., Kopecky, D., Huang, L., White, R. D., Samayoa, K., Gardner, J., Wu, X., Chen, K., et al. 2016. 'Identification of Human Islet Amyloid Polypeptide as a BACE2 Substrate', *PLoS One*, 11: e0147254.
Rutkowski, J. M., Moya, M., Johannes, J., Goldman, J., and Swartz, M. A. 2006. 'Secondary lymphedema in the mouse tail: Lymphatic hyperplasia, VEGF-C upregulation, and the protective role of MMP-9', *Microvasc Res*, 72: 161-71.
Sabine, A., Agalarov, Y., Maby-El Hajjami, H., Jaquet, M., Hagerling, R., Pollmann, C., Bebber, D., Pfenniger, A., Miura, N., Dormond, O., et al. 2012. 'Mechanotransduction, PROX1, and FOXC2 cooperate to control connexin37 and calcineurin during lymphatic-valve formation', *Dev Cell*, 22: 430-45.
Sacchi, G., Weber, E., Agliano, M., Raffaelli, N., and Comparini, L. 1997. 'The structure of superficial lymphatics in the human thigh: precollectors', *Anat Rec*, 247: 53-62.
Saharinen, P., Tammela, T., Karkkainen, M. J., and Alitalo, K. 2004. 'Lymphatic vasculature: development, molecular regulation and role in tumor metastasis and inflammation', *Trends Immunol*, 25: 387-95.
Saito, Y., Nakagami, H., Kaneda, Y., and Morishita, R. 2013. 'Lymphedema and therapeutic lymphangiogenesis', *Biomed Res Int*, 2013: 804675.
Sakai, T., Li, S., Docheva, D., Grashoff, C., Sakai, K., Kostka, G., Braun, A., Pfeifer, A., Yurchenco, P. D., and Fassler, R. 2003. 'Integrin-linked kinase (ILK) is required for polarizing the epiblast, cell adhesion, and controlling actin accumulation', *Genes Dev*, 17: 926-40.
Salameh, A., Galvagni, F., Bardelli, M., Bussolino, F., and Oliviero, S. 2005. 'Direct recruitment of CRK and GRB2 to VEGFR-3 induces proliferation, migration, and survival of endothelial cells through the activation of ERK, AKT, and JNK pathways', *Blood*, 106: 3423-31.

Sastre, M., Klockgether, T., and Heneka, M. T. 2006. 'Contribution of inflammatory processes to Alzheimer's disease: molecular mechanisms', *Int J Dev Neurosci*, 24: 167-76.

Scallan, J. P., Wolpers, J. H., Muthuchamy, M., Zawieja, D. C., Gashev, A. A., and Davis, M. J. 2012. 'Independent and interactive effects of preload and afterload on the pump function of the isolated lymphangion', *Am J Physiol Heart Circ Physiol*, 303: H809-24.

Schenk, D. B., Rydel, R. E., May, P., Little, S., Panetta, J., Lieberburg, I., and Sinha, S. 1995. 'Therapeutic approaches related to amyloid-beta peptide and Alzheimer's disease', *J Med Chem*, 38: 4141-54.

Schindewolffs, L., Breves, G., Buettner, M., Hadamitzky, C., and Pabst, R. 2014. 'VEGF-C improves regeneration and lymphatic reconnection of transplanted autologous lymph node fragments: An animal model for secondary lymphedema treatment', *Immun Inflamm Dis*, 2: 152-61.

Schlessinger, J. 2003. 'Signal transduction. Autoinhibition control', *Science*, 300: 750-2.

Schmeisser, A., Christoph, M., Augstein, A., Marquetant, R., Kasper, M., Braun-Dullaeus, R. C., and Strasser, R. H. 2006. 'Apoptosis of human macrophages by Flt-4 signaling: implications for atherosclerotic plaque pathology', *Cardiovasc Res*, 71: 774-84.

Schmittgen, T. D., and Livak, K. J. 2008. 'Analyzing real-time PCR data by the comparative C(T) method', *Nat Protoc*, 3: 1101-8.

Schulte-Merker, S., Sabine, A., and Petrova, T. V. 2011. 'Lymphatic vascular morphogenesis in development, physiology, and disease', *J Cell Biol*, 193: 607-18.

Scott, J. D., Li, S. W., Brunskill, A. P., Chen, X., Cox, K., Cumming, J. N., Forman, M., Gilbert, E. J., Hodgson, R. A., Hyde, L. A., et al. 2016. 'Discovery of the 3-Imino-1,2,4-thiadiazinane 1,1-Dioxide Derivative Verubecestat (MK-8931)-A beta-Site Amyloid Precursor Protein Cleaving Enzyme 1 Inhibitor for the Treatment of Alzheimer's Disease', *J Med Chem*, 59: 10435-50.

Selkoe, D. J. 1994. 'Alzheimer's disease: a central role for amyloid', *J Neuropathol Exp Neurol*, 53: 438-47.

Selkoe, D. J., and Hardy, J. 2016. 'The amyloid hypothesis of Alzheimer's disease at 25 years', *EMBO Mol Med*, 8: 595-608.

Selkoe, D. J., Yamazaki, T., Citron, M., Podlisny, M. B., Koo, E. H., Teplow, D. B., and Haass, C. 1996. 'The role of APP processing and trafficking pathways in the formation of amyloid beta-protein', *Ann N Y Acad Sci*, 777: 57-64.

Sen, A., Madhivanan, K., Mukherjee, D., and Aguilar, R. C. 2012. 'The epsin protein family: coordinators of endocytosis and signaling', *Biomol Concepts*, 3: 117-26.

Shalaby, F., Rossant, J., Yamaguchi, T. P., Gertsenstein, M., Wu, X. F., Breitman, M. L., and Schuh, A. C. 1995. 'Failure of blood-island formation and vasculogenesis in Flk-1-deficient mice', *Nature*, 376: 62-6.

Shawber, C. J., Funahashi, Y., Francisco, E., Vorontchikhina, M., Kitamura, Y., Stowell, S. A., Borisenko, V., Feirt, N., Podgrabinska, S., Shiraishi, K., et al. 2007. 'Notch alters VEGF responsiveness in human and murine endothelial cells by direct regulation of VEGFR-3 expression', *J Clin Invest*, 117: 3369-82.

Shimshek, D. R., Jacobson, L. H., Kolly, C., Zamurovic, N., Balavenkatraman, K. K., Morawiec, L., Kreutzer, R., Schelle, J., Jucker, M., Bertschi, B., et al. 2016. 'Pharmacological BACE1 and BACE2 inhibition induces hair depigmentation by inhibiting PMEL17 processing in mice', *Sci Rep*, 6: 21917.

Simons, M., Gordon, E., and Claesson-Welsh, L. 2016. 'Mechanisms and regulation of endothelial VEGF receptor signalling', *Nat Rev Mol Cell Biol*, 17: 611-25.

Singh, N., Tiem, M., Watkins, R., Cho, Y. K., Wang, Y., Olsen, T., Uehara, H., Mamalis, C., Luo, L., Oakey, Z., et al. 2013. 'Soluble vascular endothelial growth factor receptor 3 is essential for corneal alymphaticity', *Blood*, 121: 4242-9.

Slavin, S. A., Van den Abbeele, A. D., Losken, A., Swartz, M. A., and Jain, R. K. 1999. 'Return of lymphatic function after flap transfer for acute lymphedema', *Ann Surg*, 229: 421-7.

Sohn, J., Brick, R. M., and Tuan, R. S. 2016. 'From embryonic development to human diseases: The functional role of caveolae/caveolin', *Birth Defects Res C Embryo Today*, 108: 45-64.

Stachel, S. J., Coburn, C. A., Steele, T. G., Jones, K. G., Loutzenhiser, E. F., Gregro, A. R., Rajapakse, H. A., Lai, M. T., Crouthamel, M. C., Xu, M., et al. 2004. 'Structure-based design of potent and selective cell-permeable inhibitors of human beta-secretase (BACE-1)', *J Med Chem*, 47: 6447-50.

Stanchi, F., Bordoy, R., Kudlacek, O., Braun, A., Pfeifer, A., Moser, M., and Fassler, R. 2005. 'Consequences of loss of PINCH2 expression in mice', *J Cell Sci*, 118: 5899-910.

Stephens, L. E., Sutherland, A. E., Klimanskaya, I. V., Andrieux, A., Meneses, J., Pedersen, R. A., and Damsky, C. H. 1995. 'Deletion of beta 1 integrins in mice results in inner cell mass failure and peri-implantation lethality', *Genes Dev*, 9: 1883-95.

Stutzer, I., Selevsek, N., Esterhazy, D., Schmidt, A., Aebersold, R., and Stoffel, M. 2013. 'Systematic proteomic analysis identifies beta-site amyloid precursor protein cleaving enzyme 2 and 1 (BACE2 and BACE1) substrates in pancreatic beta-cells', *J Biol Chem*, 288: 10536-47.

Su, Y., Xia, W., Li, J., Walz, T., Humphries, M. J., Vestweber, D., Cabanas, C., Lu, C., and Springer, T. A. 2016. 'Relating conformation to function in integrin alpha5beta1', *Proc Natl Acad Sci U S A*, 113: E3872-81.

Sun, X., Fu, Y., Gu, M., Zhang, L., Li, D., Li, H., Chien, S., Shyy, J. Y., and Zhu, Y. 2016. 'Activation of integrin alpha5 mediated by flow requires its translocation to membrane lipid rafts in vascular endothelial cells', *Proc Natl Acad Sci U S A*, 113: 769-74.

Sun, X., He, G., and Song, W. 2006. 'BACE2, as a novel APP theta-secretase, is not responsible for the pathogenesis of Alzheimer's disease in Down syndrome', *FASEB J*, 20: 1369-76.

Sun, Z., Guo, S. S., and Fassler, R. 2016. 'Integrin-mediated mechanotransduction', *J Cell Biol*, 215: 445-56.

Sweeney, M. D., and Zlokovic, B. V. 2018. 'A lymphatic waste-disposal system implicated in Alzheimer's disease', *Nature*, 560: 172-74.

Szaruga, M., Munteanu, B., Lismont, S., Veugelen, S., Horre, K., Mercken, M., Saido, T. C., Ryan, N. S., De Vos, T., Savvides, S. N., et al. 2017. 'Alzheimer's-Causing Mutations Shift Abeta Length by Destabilizing gamma-Secretase-Abetan Interactions', *Cell*, 170: 443-56 e14.

Takahashi, H., and Shibuya, M. 2005. 'The vascular endothelial growth factor (VEGF)/VEGF receptor system and its role under physiological and pathological conditions', *Clin Sci (Lond)*, 109: 227-41.

Tammela, T., and Alitalo, K. 2010. 'Lymphangiogenesis: Molecular mechanisms and future promise', *Cell*, 140: 460-76.

Tammela, T., Zarkada, G., Wallgard, E., Murtomaki, A., Suchting, S., Wirzenius, M., Waltari, M., Hellstrom, M., Schomber, T., Peltonen, R., et al. 2008. 'Blocking VEGFR-3 suppresses angiogenic sprouting and vascular network formation', *Nature*, 454: 656-60.

Tan, C., Cruet-Hennequart, S., Troussard, A., Fazli, L., Costello, P., Sutton, K., Wheeler, J., Gleave, M., Sanghera, J., and Dedhar, S. 2004. 'Regulation of tumor angiogenesis by integrin-linked kinase (ILK)', *Cancer Cell*, 5: 79-90.

Tarasoff-Conway, J. M., Carare, R. O., Osorio, R. S., Glodzik, L., Butler, T., Fieremans, E., Axel, L., Rusinek, H., Nicholson, C., Zlokovic, B. V., et al. 2016. 'Clearance systems in the brain--implications for Alzheimer diseaser', *Nat Rev Neurol*, 12: 248.

Terman, B. I., Carrion, M. E., Kovacs, E., Rasmussen, B. A., Eddy, R. L., and Shows, T. B. 1991. 'Identification of a new endothelial cell growth factor receptor tyrosine kinase', *Oncogene*, 6: 1677-83.

Terman, B. I., Dougher-Vermazen, M., Carrion, M. E., Dimitrov, D., Armellino, D. C., Gospodarowicz, D., and Bohlen, P. 1992. 'Identification of the KDR tyrosine kinase as a receptor for vascular endothelial cell growth factor', *Biochem Biophys Res Commun*, 187: 1579-86.

Thomas, J. L., Baker, K., Han, J., Calvo, C., Nurmi, H., Eichmann, A. C., and Alitalo, K. 2013. 'Interactions between VEGFR and Notch signaling pathways in endothelial and neural cells', *Cell Mol Life Sci*, 70: 1779-92.

Thomson, B. R., Heinen, S., Jeansson, M., Ghosh, A. K., Fatima, A., Sung, H. K., Onay, T., Chen, H., Yamaguchi, S., Economides, A. N., et al. 2014. 'A lymphatic defect causes ocular hypertension and glaucoma in mice', *J Clin Invest*, 124: 4320-4.

Tu, Y., Huang, Y., Zhang, Y., Hua, Y., and Wu, C. 2001. 'A new focal adhesion protein that interacts with integrin-linked kinase and regulates cell adhesion and spreading', *J Cell Biol*, 153: 585-98.

Ullrich, A., and Schlessinger, J. 1990. 'Signal transduction by receptors with tyrosine kinase activity', *Cell*, 61: 203-12.

Urner, S. 2018. 'Role of integrin-linked kinase (ILK) in VEGFR3 signaling and lymphatic vascular growth'.

Urner, S., Kelly-Goss, M., Peirce, S. M., and Lammert, E. 2018. 'Mechanotransduction in Blood and Lymphatic Vascular Development and Disease', *Adv Pharmacol*, 81: 155-208.

Urner, S., Planas-Paz, L., Hilger, L. S., Henning, C., Branopolski, A., Kelly-Goss, M., Stanczuk, L., Pitter, B., Montanez, E., Peirce, S. M., et al. 2019. 'Identification of ILK as a critical regulator of VEGFR3 signalling and lymphatic vascular growth', *EMBO J*, 38.

Vassar, R., Bennett, B. D., Babu-Khan, S., Kahn, S., Mendiaz, E. A., Denis, P., Teplow, D. B., Ross, S., Amarante, P., Loeloff, R., et al. 1999. 'Beta-secretase cleavage of Alzheimer's amyloid precursor protein by the transmembrane aspartic protease BACE', *Science*, 286: 735-41.

Vassar, R., Kuhn, P. H., Haass, C., Kennedy, M. E., Rajendran, L., Wong, P. C., and Lichtenthaler, S. F. 2014. 'Function, therapeutic potential and cell biology of BACE proteases: current status and future prospects', *J Neurochem*, 130: 4-28.

Velyvis, A., Yang, Y., Wu, C., and Qin, J. 2001. 'Solution structure of the focal adhesion adaptor PINCH LIM1 domain and characterization of its interaction with the integrin-linked kinase ankyrin repeat domain', *J Biol Chem*, 276: 4932-9.

Vieira, J. M., Norman, S., Villa Del Campo, C., Cahill, T. J., Barnette, D. N., Gunadasa-Rohling, M., Johnson, L. A., Greaves, D. R., Carr, C. A., Jackson, D. G., et al. 2018. 'The cardiac lymphatic system stimulates resolution of inflammation following myocardial infarction', *J Clin Invest*, 128: 3402-12.

von der Weid, P. Y., and Zawieja, D. C. 2004. 'Lymphatic smooth muscle: the motor unit of lymph drainage', *Int J Biochem Cell Biol*, 36: 1147-53.

Voytyuk, I., De Strooper, B., and Chavez-Gutierrez, L. 2018a. 'Modulation of gamma- and beta-Secretases as Early Prevention Against Alzheimer's Disease', *Biol Psychiatry*, 83: 320-27.

Voytyuk, I., Mueller, S. A., Herber, J., Snellinx, A., Moechars, D., van Loo, G., Lichtenthaler, S. F., and De Strooper, B. 2018b. 'BACE2 distribution in major brain cell types and identification of novel substrates', *Life Sci Alliance*, 1: e201800026.

Vuorio, T., Tirronen, A., and Yla-Herttuala, S. 2017. 'Cardiac Lymphatics - A New Avenue for Therapeutics?', *Trends Endocrinol Metab*, 28: 285-96.

Wang, J. F., Zhang, X. F., and Groopman, J. E. 2001. 'Stimulation of beta 1 integrin induces tyrosine phosphorylation of vascular endothelial growth factor receptor-3 and modulates cell migration', *J Biol Chem*, 276: 41950-7.

Wang, W. Y., Tan, M. S., Yu, J. T., and Tan, L. 2015. 'Role of pro-inflammatory cytokines released from microglia in Alzheimer's disease', *Ann Transl Med*, 3: 136.

Wang, Y., Nakayama, M., Pitulescu, M. E., Schmidt, T. S., Bochenek, M. L., Sakakibara, A., Adams, S., Davy, A., Deutsch, U., Luthi, U., et al. 2010. 'Ephrin-B2 controls VEGF-induced angiogenesis and lymphangiogenesis', *Nature*, 465: 483-6.

Wang, Z., Xu, Q., Cai, F., Liu, X., Wu, Y., and Song, W. 2019. 'BACE2, a conditional beta-secretase, contributes to Alzheimer's disease pathogenesis', *JCI Insight*, 4.

Weller, R. O., Djuanda, E., Yow, H. Y., and Carare, R. O. 2009. 'Lymphatic drainage of the brain and the pathophysiology of neurological disease', *Acta Neuropathol*, 117: 1-14.

Wickstrom, S. A., Lange, A., Montanez, E., and Fassler, R. 2010. 'The ILK/PINCH/parvin complex: the kinase is dead, long live the pseudokinase!', *EMBO J*, 29: 281-91.

Widmaier, M., Rognoni, E., Radovanac, K., Azimifar, S. B., and Fassler, R. 2012. 'Integrin-linked kinase at a glance', *J Cell Sci*, 125: 1839-43.

Wiig, H., and Swartz, M. A. 2012. 'Interstitial fluid and lymph formation and transport: physiological regulation and roles in inflammation and cancer', *Physiol Rev*, 92: 1005-60.

Wisniewski, H. M., and Silverman, W. 1997. 'Diagnostic criteria for the neuropathological assessment of Alzheimer's disease: current status and major issues', *Neurobiology of Aging*, 18: S43-50.

Wu, H., Rahman, H. N. A., Dong, Y., Liu, X., Lee, Y., Wen, A., To, K. H., Xiao, L., Birsner, A. E., Bazinet, L., et al. 2018. 'Epsin deficiency promotes lymphangiogenesis through regulation of VEGFR3 degradation in diabetes', *J Clin Invest*, 128: 4025-43.

Xie, L., Kang, H., Xu, Q., Chen, M. J., Liao, Y., Thiyagarajan, M., O'Donnell, J., Christensen, D. J., Nicholson, C., Iliff, J. J., et al. 2013. 'Sleep drives metabolite clearance from the adult brain', *Science*, 342: 373-7.

Xu, Z., Fukuda, T., Li, Y., Zha, X., Qin, J., and Wu, C. 2005. 'Molecular dissection of PINCH-1 reveals a mechanism of coupling and uncoupling of cell shape modulation and survival', *J Biol Chem*, 280: 27631-7.

Yamaji, S., Suzuki, A., Kanamori, H., Mishima, W., Yoshimi, R., Takasaki, H., Takabayashi, M., Fujimaki, K., Fujisawa, S., Ohno, S., et al. 2004. 'Affixin interacts with alpha-actinin and mediates integrin signaling for reorganization of F-actin induced by initial cell-substrate interaction', *J Cell Biol*, 165: 539-51.

Yamaji, S., Suzuki, A., Sugiyama, Y., Koide, Y., Yoshida, M., Kanamori, H., Mohri, H., Ohno, S., and Ishigatsubo, Y. 2001. 'A novel integrin-linked kinase-binding protein, affixin, is involved in the early stage of cell-substrate interaction', *J Cell Biol*, 153: 1251-64.

Yan, R., Bienkowski, M. J., Shuck, M. E., Miao, H., Tory, M. C., Pauley, A. M., Brashier, J. R., Stratman, N. C., Mathews, W. R., Buhl, A. E., et al. 1999. 'Membrane-anchored aspartyl protease with Alzheimer's disease beta-secretase activity', *Nature*, 402: 533-7.

Yan, R., Munzner, J. B., Shuck, M. E., and Bienkowski, M. J. 2001. 'BACE2 functions as an alternative alpha-secretase in cells', *J Biol Chem*, 276: 34019-27.

Yan, R., and Vassar, R. 2014. 'Targeting the beta secretase BACE1 for Alzheimer's disease therapy', *Lancet Neurol*, 13: 319-29.

Yang, G. L., and Li, L. Y. 2018. 'Counterbalance: modulation of VEGF/VEGFR activities by TNFSF15', *Signal Transduct Target Ther*, 3: 21.

Yang, L. B., Lindholm, K., Yan, R., Citron, M., Xia, W., Yang, X. L., Beach, T., Sue, L., Wong, P., Price, D., et al. 2003. 'Elevated beta-secretase expression and enzymatic activity detected in sporadic Alzheimer disease', *Nat Med*, 9: 3-4.

Yang, Y., and Oliver, G. 2014. 'Development of the mammalian lymphatic vasculature', *J Clin Invest*, 124: 888-97.

Yao, L. C., Baluk, P., Srinivasan, R. S., Oliver, G., and McDonald, D. M. 2012. 'Plasticity of button-like junctions in the endothelium of airway lymphatics in development and inflammation', *Am J Pathol*, 180: 2561-75.

Zawieja, D. C. 2009. 'Contractile physiology of lymphatics', *Lymphat Res Biol*, 7: 87-96.

Zhang, S., Wang, Z., Cai, F., Zhang, M., Wu, Y., Zhang, J., and Song, W. 2017. 'BACE1 Cleavage Site Selection Critical for Amyloidogenesis and Alzheimer's Pathogenesis', *J Neurosci*, 37: 6915-25.

Zhang, X., Groopman, J. E., and Wang, J. F. 2005. 'Extracellular matrix regulates endothelial functions through interaction of VEGFR-3 and integrin alpha5beta1', *J Cell Physiol*, 202: 205-14.

Zhang, Y., Chen, K., Guo, L., and Wu, C. 2002a. 'Characterization of PINCH-2, a new focal adhesion protein that regulates the PINCH-1-ILK interaction, cell spreading, and migration', *J Biol Chem*, 277: 38328-38.

Zhang, Y., Chen, K., Tu, Y., Velyvis, A., Yang, Y., Qin, J., and Wu, C. 2002b. 'Assembly of the PINCH-ILK-CH-ILKBP complex precedes and is essential for localization of each component to cell-matrix adhesion sites', *J Cell Sci*, 115: 4777-86.

Zhang, Y., Guo, L., Chen, K., and Wu, C. 2002c. 'A critical role of the PINCH-integrin-linked kinase interaction in the regulation of cell shape change and migration', *J Biol Chem*, 277: 318-26.

Zhang, Y., and Song, W. 2017. 'Islet amyloid polypeptide: Another key molecule in Alzheimer's pathogenesis?', *Prog Neurobiol*, 153: 100-20.

Zheng, C. C., Hu, H. F., Hong, P., Zhang, Q. H., Xu, W. W., He, Q. Y., and Li, B. 2019. 'Significance of integrin-linked kinase (ILK) in tumorigenesis and its potential implication as a biomarker and therapeutic target for human cancer', *Am J Cancer Res*, 9: 186-97.

Zhou, L., Barao, S., Laga, M., Bockstael, K., Borgers, M., Gijsen, H., Annaert, W., Moechars, D., Mercken, M., Gevaert, K., et al. 2012. 'The neural cell adhesion molecules L1 and CHL1 are cleaved by BACE1 protease in vivo', *J Biol Chem*, 287: 25927-40.

Zinchenko, E., Navolokin, N., Shirokov, A., Khlebtsov, B., Dubrovsky, A., Saranceva, E., Abdurashitov, A., Khorovodov, A., Terskov, A., Mamedova, A., et al. 2019. 'Pilot study of transcranial photobiomodulation of lymphatic clearance of beta-amyloid from the mouse brain: breakthrough strategies for non-pharmacologic therapy of Alzheimer's disease', *Biomed Opt Express*, 10: 4003-17.

Zraika, S., Hull, R. L., Udayasankar, J., Aston-Mourney, K., Subramanian, S. L., Kisilevsky, R., Szarek, W. A., and Kahn, S. E. 2009. 'Oxidative stress is induced by islet amyloid formation and time-dependently mediates amyloid-induced beta cell apoptosis', *Diabetologia*, 52: 626-35.

9. Supplementary information

Fully unedited gel images used for representative Western Blot images in this thesis:

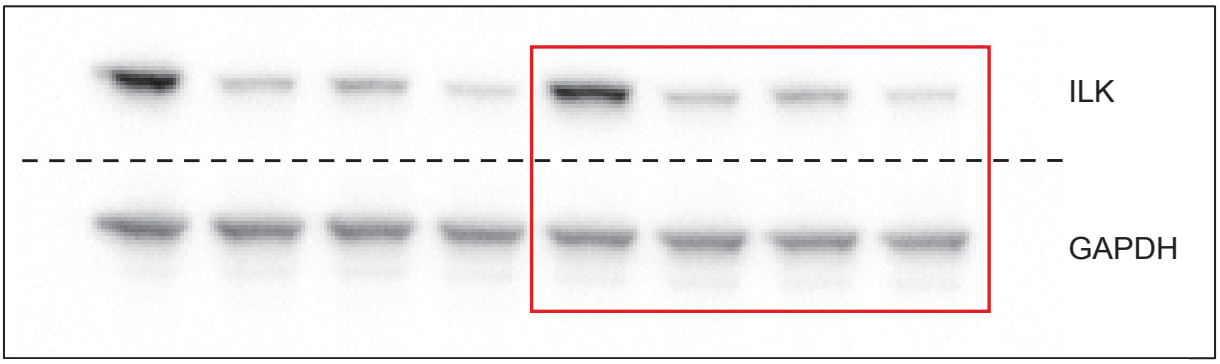

Supplementary Figure 1: Unedited gel images used for Figure 10. Cropped region used for representative image is indicated by red framing.

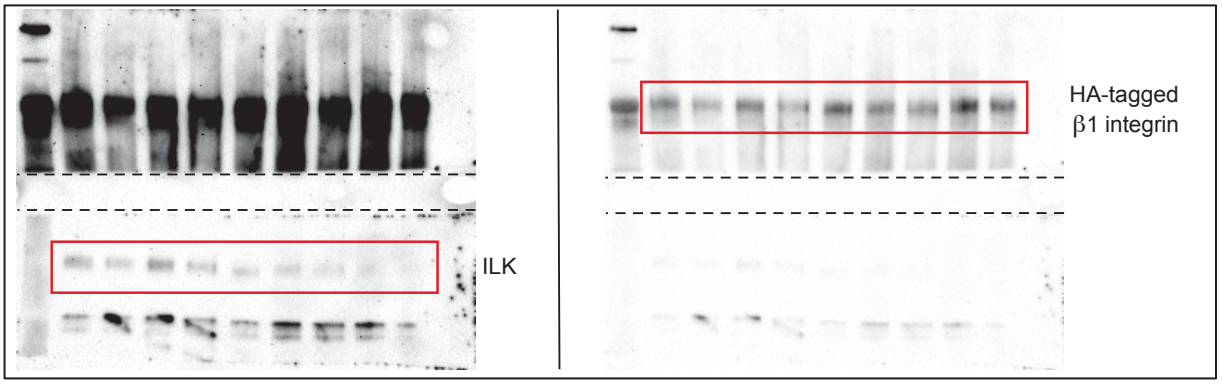

Supplementary Figure 2: Unedited gel images used for Figure 14. Cropped regions used for representative image are indicated by red framing.

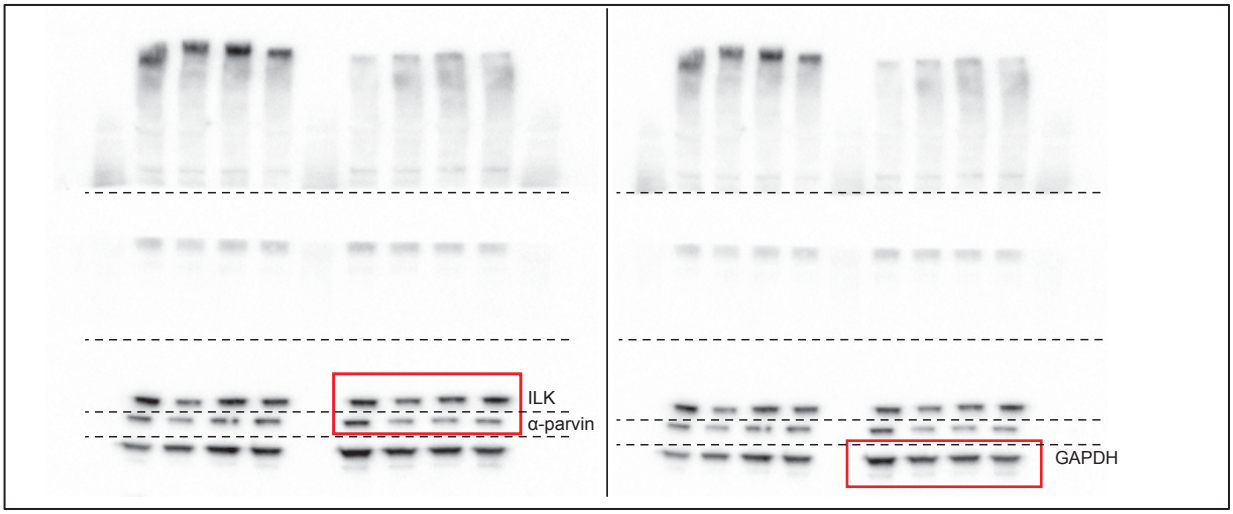

Supplementary Figure 3: Unedited gel images used for Figure 15. Cropped regions used for representative image are indicated by red framing.

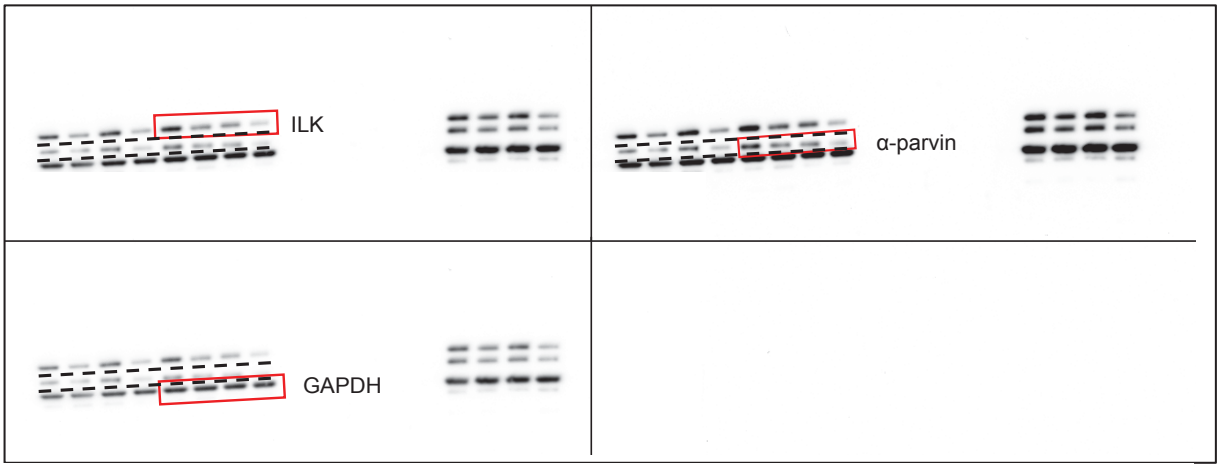

Supplementary Figure 4: Unedited gel images used for Figure 16. Cropped regions used for representative image are indicated by red framing.

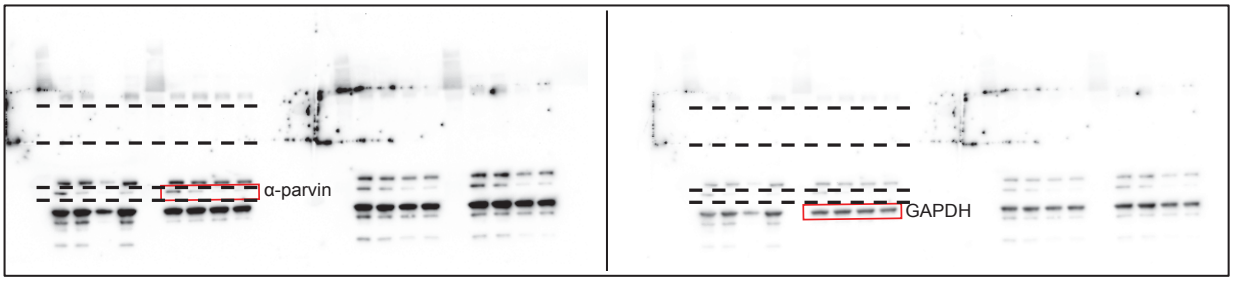

Supplementary Figure 5: Unedited gel images used for Figure 17. Cropped regions used for representative image are indicated by red framing.

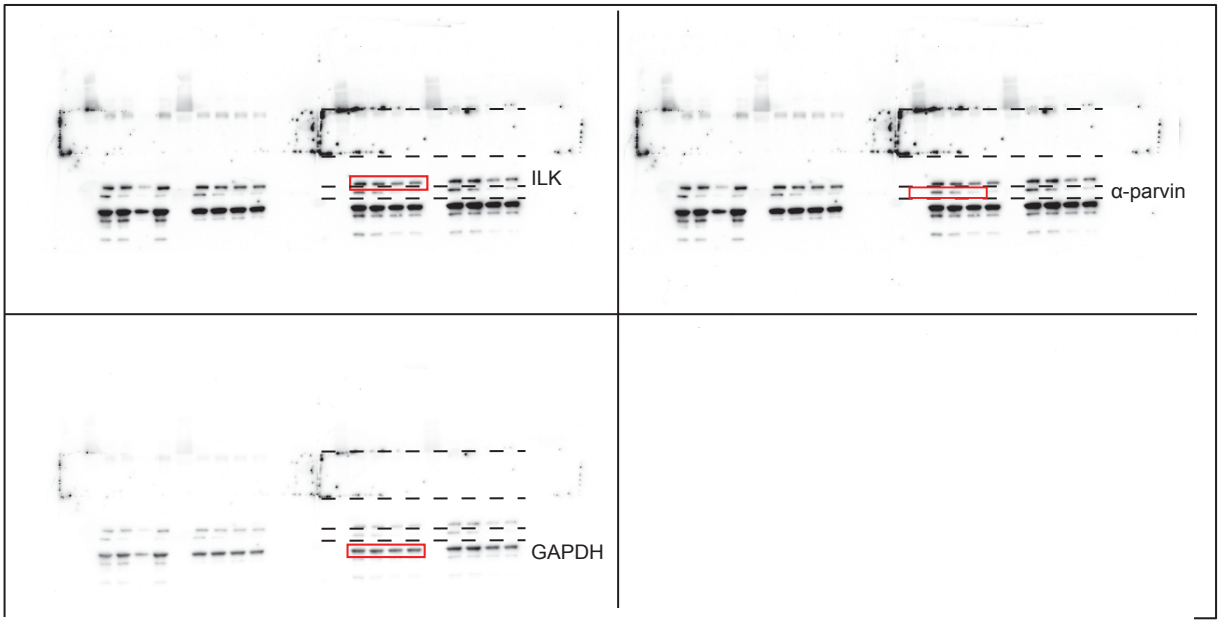

Supplementary Figure 6: Unedited gel images used for Figure 18. Cropped regions used for representative image are indicated by red framing.

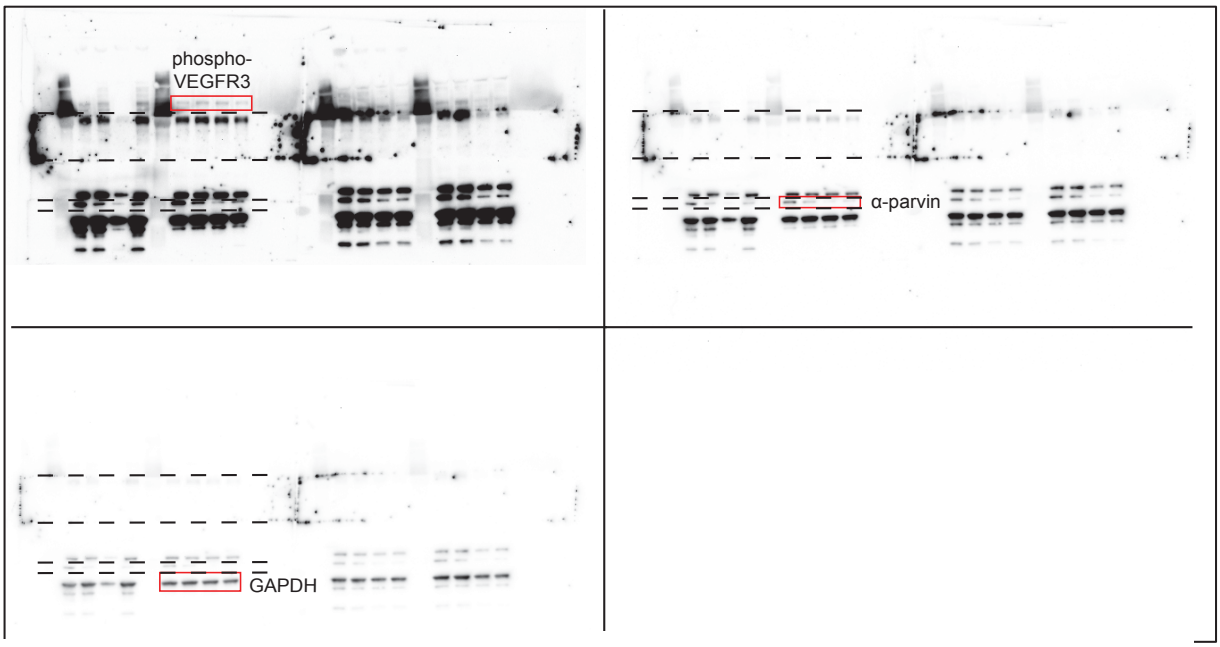

Supplementary Figure 7: Unedited gel images used for Figure 19. Cropped regions used for representative image are indicated by red framing.

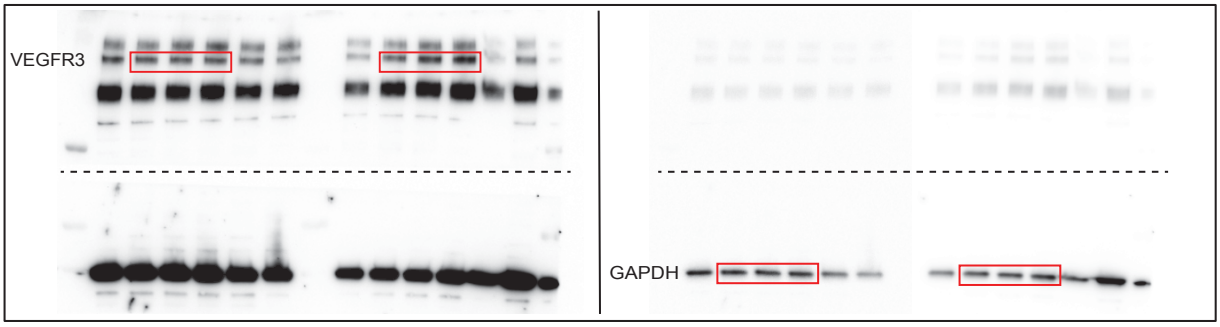

Supplementary Figure 8: Unedited gel images used for Figure 21. Cropped regions used for representative image are indicated by red framing.

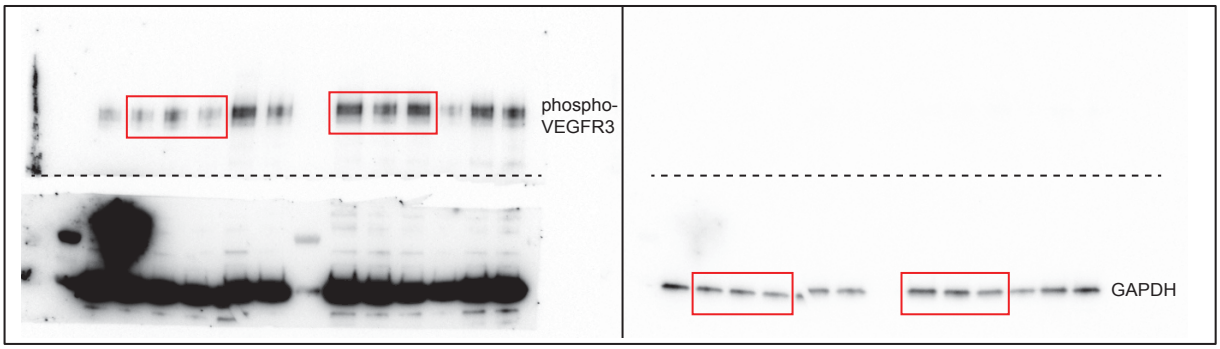

Supplementary Figure 9: Unedited gel images used for Figure 22. Cropped regions used for representative image are indicated by red framing.

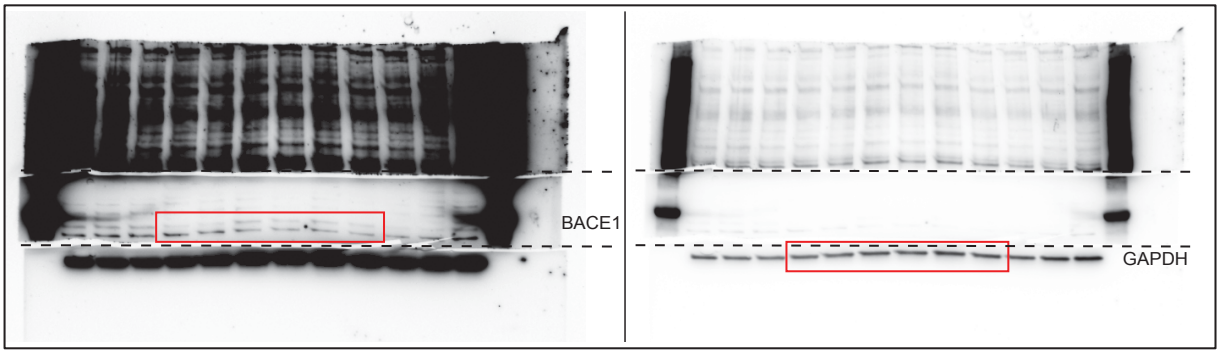

Supplementary Figure 10: Unedited gel images used for Figure 29. Cropped regions used for representative image are indicated by red framing.

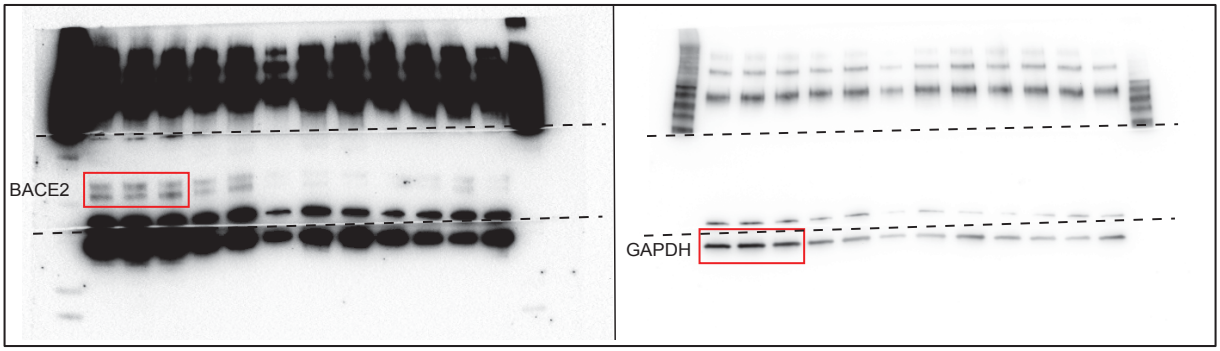

Supplementary Figure 11: Unedited gel images used for Figure 30. Cropped regions used for representative image are indicated by red framing.

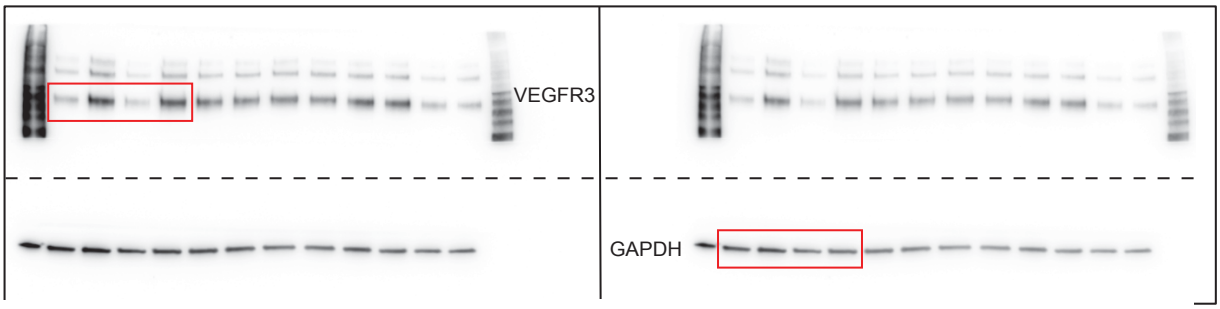

Supplementary Figure 12: Unedited gel images used for Figure 31. Cropped regions used for representative image are indicated by red framing.

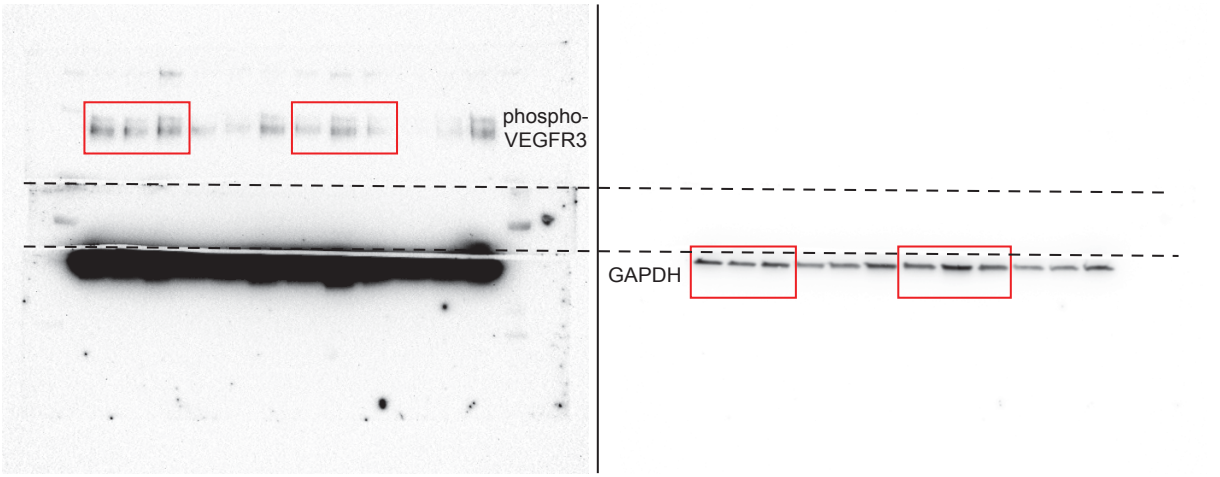

Supplementary Figure 13: Unedited gel images used for Figure 32. Cropped regions used for representative image are indicated by red framing.

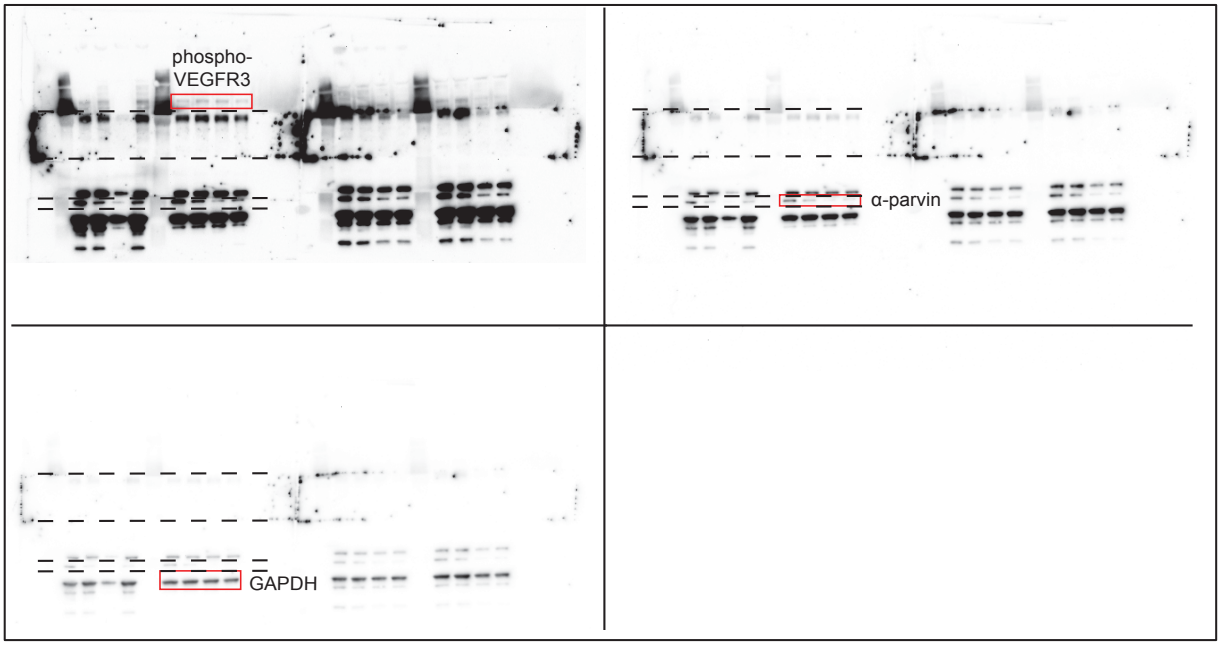

Supplementary Figure 14: Unedited gel images used for Figure 37. Cropped regions used for representative image are indicated by red framing.

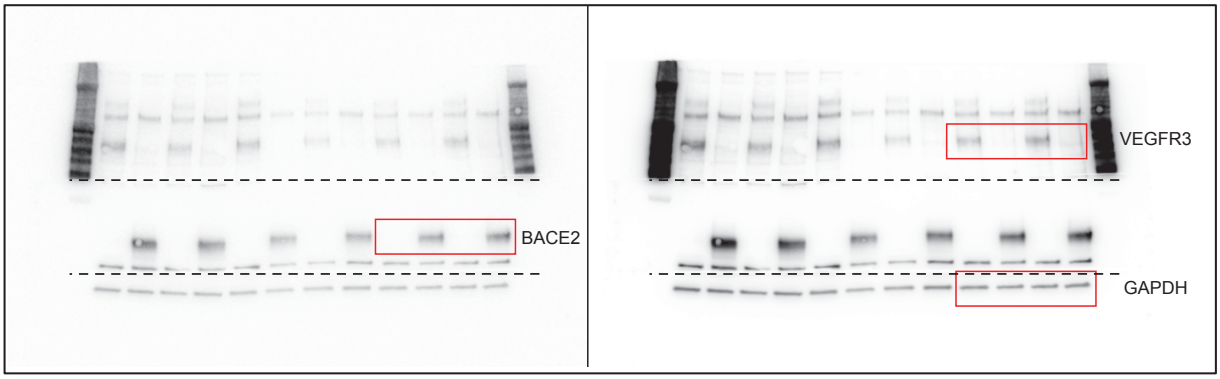

Supplementary Figure 15: Unedited gel images used for Figure 40. Cropped regions used for representative image are indicated by red framing.

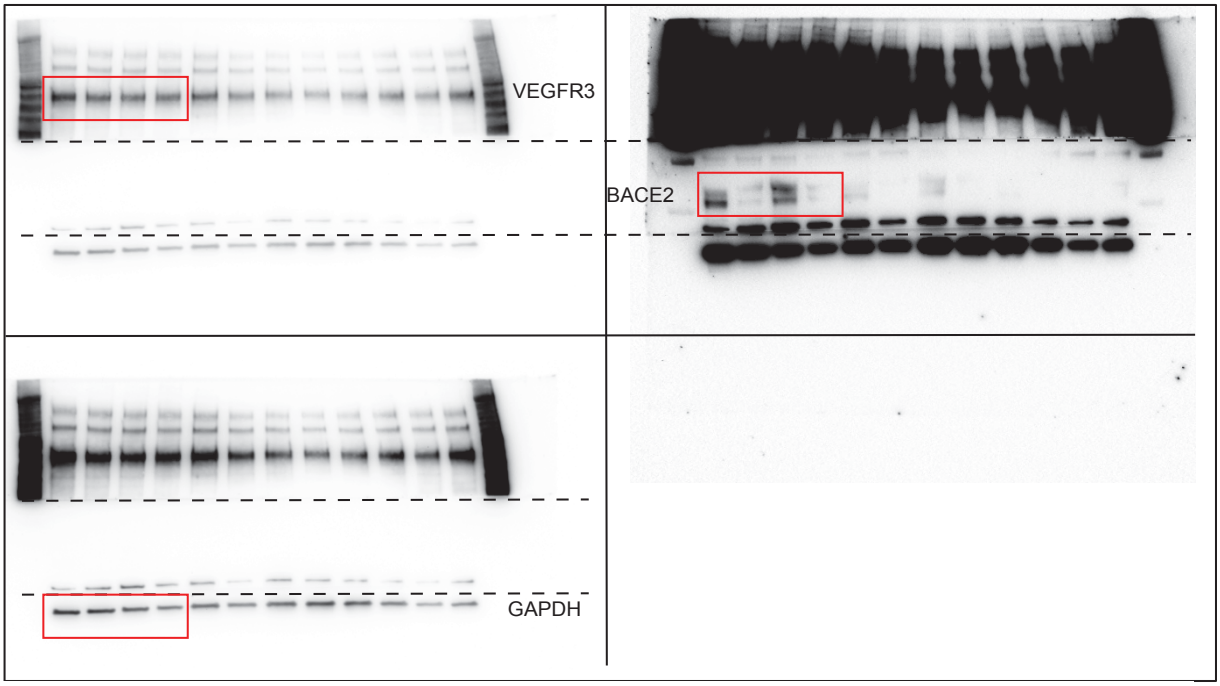

Supplementary Figure 16: Unedited gel images used for Figure 42. Cropped regions used for representative image are indicated by red framing.

Statutory declaration

I hereby declare that I wrote the dissertation “Attenuation of VEGFR3 signaling by intracellular versus extracellular mechanisms” independently and without other resources as indicated in compliance with “Grundsätze zur Sicherung guter wissenschaftlicher Praxis an der Heinrich-Heine Universität Düsseldorf”.

Furthermore, I declare that I did not submit this dissertation, either in full or in part, to any other academic institution and did not absolve any promotion trials before.

Düsseldorf,

_____

Laura Sophie Hilger

Eidesstattliche Erklärung

Ich versichere an Eides Statt, dass die Dissertation „Attenuierung von VEGFR3 Signalwegen durch intrazelluläre versus extrazelluläre Mechanismen” von mir selbstständig und ohne unzulässige fremde Hilfe unter Beachtung der „Grundsätze zur Sicherung guter wissenschaftlicher Praxis an der Heinrich-Heine-Universität Düsseldorf“ erstellt worden ist.

Darüber hinaus versichere ich, dass ich die Dissertation weder in der hier vorgelegten noch in einer ähnlichen Form bei einem anderen Institut eingereicht habe und bisher keine Promotionsversuche unternommen habe.

Düsseldorf,

_____

Laura Sophie Hilger

Danksagung

Abschließend bedanke ich mich bei meinem Doktorvater Ecki für die Möglichkeit, diese Arbeit in seinem Institut anzufertigen. Vielen Dank für die Unterstützung, die fachlichen Anregungen und für die Gelegenheit, mich wissenschaftlich weiterzuentwickeln.

Ich danke Axel für die Übernahme der Aufgabe des Zweitgutachters, sowie für die wissenschaftlichen Anregungen bezüglich meiner Arbeit.

Besonders möchte ich mich bei allen aktuellen und ehemaligen Mitgliedern des Instituts für Stoffwechselphysiologie bedanken, die jeden Tag zu etwas besonderem gemacht haben. Ohne euch und unseren Zusammenhalt wäre diese Zeit nicht halb so produktiv und lehrreich gewesen. Bei Barbara, Silke und Andrea möchte ich mich darüber hinaus auch für die technische Unterstützung bedanken, sowie bei Daniel für jeden erdenklichen Rat. Ich danke Linda für ihr offenes Ohr, für alle aufbauenden Worte und die Hilfe in allen Lebenslagen. Bei Sofia möchte ich mich nicht nur für die Mühe und Zeit bedanken, die sie in mich und meine Weiterentwicklung investiert hat, sondern auch für ihr unermüdliche Freundschaft.

I would like to thank Shayn and all the members of the Department for Biomedical Engineering for hosting me during my research stay at the UVA in Charlottesville. I had a great time in your lab and especially enjoyed every happy hour. In this context, I would also like to thank my roommate Francesca; thank you for the adventurous and inspiring time, for the meals you cooked and all the conversations.

Darüber hinaus möchte ich mich beim IRTG1902 für die Möglichkeit bedanken, ein Teil dieses tollen internationalen Programms zu sein.

Ein besonderer Dank gilt meinen engsten Freunden und ganz besonders meinen Mädels. Für euren uneingeschränkten Rückhalt, eure langjährige Freundschaft und euer Verständnis in dieser so besonderen und teils sehr schweren Zeit, kann ich euch nicht genug danken.

Zuletzt möchte ich mich bei meiner Familie und ganz besonders bei meinen Eltern bedanken. Danke, dass ihr immer an mich glaubt und mich in meinen Plänen unterstützt! Danke für eure unendliche und aufopfernde Hilfe der letzten Jahre. Ihr habt mir gezeigt, dass es immer einen Weg gibt, den es sich zu gehen lohnt.